

ENVIRONMENTAL AND FUNCTIONAL BENEFITS AND TRADE-OFFS OF HOT IN-PLACE RECYCLING TREATMENT TECHNIQUES

FINAL PROJECT REPORT

by

Punit Singhvi
Hasan Ozer
Imad L. Al-Qadi
University of Illinois at Urbana Champaign

for

Center for Highway Pavement Preservation
(CHPP)



In cooperation with US Department of Transportation-Research and Innovative Technology
Administration (RITA)

December 2016

Disclaimer

The contents of this report reflect the views of the authors, who are responsible for the facts and the accuracy of the information presented herein. This document is disseminated under the sponsorship of the U.S. Department of Transportation's University Transportation Centers Program, in the interest of information exchange. The Center for Highway Pavement Preservation (CHPP), the U.S. Government and matching sponsor assume no liability for the contents or use thereof.

Technical Report Documentation Page			
1. Report No. ICT-17-001	2. Government Accession No.	3. Recipient's Catalog No.	
4. Title and Subtitle		5. Report Date	
		6. Performing Organization Code	
7. Author(s) Imad Al-Qadi		8. Performing Organization Report No. UILU-ENG-2017-2001	
9. Performing Organization Name and Address CHPP Center for Highway Pavement Preservation, Tier 1 University Transportation Center Michigan State University, 2857 Jolly Road, Okemos, MI 48864		10. Work Unit No. (TRAI5)	
		11. Contract or Grant No.	
12. Sponsoring Organization Name and Address United States of America Department of Transportation Research and Innovative Technology Administration		13. Type of Report and Period Covered	
		14. Sponsoring Agency Code	
15. Supplementary Notes Report uploaded at http://www.chpp.egr.msu.edu/			
16. Abstract Surface recycling is suitable for pavements with minor cracks limited to 25-50 mm in depth. Hot-in-place recycling (HIR) process includes drying and heating the upper layers, scarifying the soft asphalt, mixing the scarified material with a rejuvenator, if required, and finally placing and compacting the recycled material. Additional asphalt concrete (AC) overlay (OL) or other surface treatment may be required. In some cases, additional aggregate and binder may be added. The HIR performance and its environmental impacts were considered in this study. Three test sites, located in Galesburg and Machesney Park, Illinois, and Dyer, Indiana, were HIR treated and evaluated in-situ and in the lab. Physical and rheological properties of binder recovered from each site were obtained. Interaction plots, combining rut depth from the wheel track test (WTT) and flexibility index (FI) from the Illinois Flexibility Index Test (I-FIT), were in agreement with binder test results. Falling weight deflectometer and roughness measurements were conducted before and after HIR. The environmental assessment showed a difference in energy usage and GHGs of 3.9–17.6% and 1.3–19.2%, respectively, between a HIR process with 38 mm AC overlay and a corresponding traditional 50 mm mill and AC OL for different plant locations. Energy savings from using HIR treatments heavily depend on the surface treatment after HIR, thickness of overlay (if overlay is chosen as the surface treatment), and hauling distances for plant-produced materials needed for overlays. This study will help selecting proper treatment guidelines based on type and condition of pavement, timing of rehabilitation, and construction temperature for the decision-making considering performance, cost, energy, and GHG emission.			
17. Key Words		18. Distribution Statement No restrictions.	
19. Security Classification (of this report) Unclassified.	20. Security Classification (of this page) Unclassified.	21. No. of Pages 68+Appendices	22. Price NA

Table of Contents

CHAPTER 1 - INTRODUCTION.....	1
1.1 BACKGROUND.....	2
1.2 STUDY OBJECTIVE AND SCOPE	6
1.3 RESEARCH APPROACH.....	6
1.4 IMPACT OF RESEARCH.....	8
CHAPTER 2 - LITERATURE REVIEW.....	9
2.1 PAVEMENT PERFORMANCE EVALUATION.....	9
2.2 DESIGN AND PAVEMENT MATERIAL EVALUATION AT BINDER AND MIXTURE LEVELS	9
2.3 LIFE-CYCLE ASSESSMENT FOR PAVEMENT MATERIALS	11
CHAPTER 3 - FIELD INVESTIGATION.....	13
3.1 INTRODUCTION TO PROJECT SITES.....	13
3.1.1 Galesburg, IL	13
3.1.2 Machesney, IL.....	17
3.1.3 Dyer, IN	21
3.2 CONDITION RATING SURVEY (CRS)	25
3.2.1 Galesburg, IL	26
3.2.2 Machesney, IL.....	26
3.2.3 Dyer, IN	26
3.3 FALLING WEIGHT DEFLECTOMETER (FWD).....	27
3.3.1 Galesburg, IL	30
3.3.2 Machesney, IL.....	31
3.3.3 Dyer, IN	34
3.4 INTERNATIONAL ROUGHNESS INDEX (IRI)	35
3.4.1 Galesburg, IL	36
3.4.2 Machesney, IL.....	36
3.5 SUMMARY	39
CHAPTER 4 - LABORATORY INVESTIGATION.....	40
4.1 MIXTURE DESIGN AND VOLUMETRIC CHARACTERISTICS	40
4.1.1 Aggregate Gradation.....	41
4.1.2 Mix Design Volumetrics.....	42
4.1.3 Results and Discussion	42
4.2 BINDER-LEVEL TESTING	43
4.2.1 Performance Grade (PG) Determination	43
4.2.2 Dynamic Shear Rheometer (DSR).....	43
4.2.3 Bending Beam Rheometer (BBR)	44

4.2.4 Frequency Sweep Test	45
4.2.5 Results and Discussion	46
4.3 MIXTURE LEVEL TESTING	47
4.3.1 Illinois Flexibility Index Test (I-FIT)	47
4.3.2 Hamburg Wheel Track Test.....	51
4.3.3 Results and Discussion	52
4.4 FIELD CORES.....	54
4.5 SUMMARY	56
CHAPTER 5 - ENVIRONMENTAL IMPACT ASSESSMENT.....	58
5.1 ENVIRONMENTAL IMPACTS	58
5.2 SCENARIO BASED SUSTAINABILITY ANALYSIS	59
5.3 SUMMARY	60
CHAPTER 6 - SUMMARY, FINDINGS, CONCLUSIONS AND RECOMMENDATIONS	62
6.1 TECHNOLOGY TRANSFER	63
6.2 REFERENCES	64
APPENDIX A: Condition rating survey (CRS) calculation	69
APPENDIX B: Falling weight deflectometer (FWD) deflection basin data	75
APPENDIX C: Extracted gradation of field collected samples.....	91
APPENDIX D: Volumetric details of lab compacted samples.....	96
APPENDIX E: Bending beam rheometer (BBR) summary	99
APPENDIX F.1: I-FIT parameter summary for lab compacted specimens using I-FIT tool.....	100
APPENDIX F.2: I-FIT parameter summary for field core specimens using I-FIT tool.....	101
APPENDIX G: Hamburg wheel track test (HWTT) summary	102

List of Figures

Figure 1-1 Stages showing different in-place recycling techniques throughout the pavement design life (NCHRP Synthesis 421, 2011)	2
Figure 1-2 Construction sequence of HIR	3
Figure 1-3 General arrangement of trains used for (a) surface recycling, (b) repaving, and (c) remixing (Stroup-Gardiner, 2011)	4
Figure 1-4 The experimental program for binders, AC mixtures, and field cores.....	7
Figure 3-1 Image of the project site at Galesburg from Google Earth	13
Figure 3-2 Types of pavement distresses before HIR at Galesburg, IL project site	14
Figure 3-3 HIR construction train showing two heating unit and scarifier followed by compactor	15
Figure 3-4 HIR train showing second heating plate and rejuvenator application (see inset)	15
Figure 3-5 (a) FWD measurement before HIR (b) extraction of cores at Galesburg, IL	16
Figure 3-6 Silo Ridge sections at Machesney Park	17
Figure 3-7 Timberline Hollow section at Machesney Park	18
Figure 3-8 Types of pavement distresses before HIR at Machesney, IL project site	19
Figure 3-9 (a) HIR construction train; (b) compaction; (c) scarification and paver included with the second heating plate; (d) addition of rejuvenator; (e) pavement scarification; and (f) pavement before and after HIR.....	20
Figure 3-10 (a) FWD measurement (b) Extraction of cores at Machesney, IL	21
Figure 3-11 Types of pavement distresses before HIR at Dyer, IL project site	22
Figure 3-12 (a) HIR construction train; (b) scarification, application of rejuvenator followed by laying the mix; and (c) compaction	23
Figure 3-13 (a) FWD measurement and (b) extraction of cores at Dyer, IN.....	24
Figure 3-14 Sampling of recycled asphalt mixture at HIR project site	24
Figure 3-15 Dynatest FWD 8002 trailer	27
Figure 3-16 Deflection basin	28
Figure 3-17 Deflection parameters and their severity for east bound (left) and west bound (right) for the inner lane, Galesburg, IL (Appendix B).....	31
Figure 3-18 Deflection parameters and its severity for east bound (left) and west bound (right) for Section – 4-5-6-7 Machesney Park, IL (Appendix B)	32
Figure 3-19 Deflection parameters for east bound (left) and west bound (right) for Section – 8-9 of Machesney Park, IL (Appendix B).....	33
Figure 3-20 Deflection parameters for east bound (left) and west bound (right) for Section – 15-16-17-18 of Machesney Park, IL (Appendix B)	34
Figure 3-21 Deflection parameters and its severity for east bound (left) and west bound (right) for Dyer, IN (Appendix B).....	35
Figure 3-22 IRI data before filtering (a) and IRI data after filtering (b) with velocity profile	36
Figure 3-23 IRI data for Galesburg before, post-HIR, and post-overlay	36
Figure 3-24 IRI data for different sections of Machesney before, post-HIR, and post-overlay ...	38
Figure 4-1 Centrifuge Extractor (a) and RotoVap (b) for binder extraction.....	41
Figure 4-2 Extracted aggregate gradation.....	42
Figure 4-3 Dynamic shear rheometer	43
Figure 4-4 Bending Beam Rheometer	44

Figure 4-5 Frequency sweep plots for Shear Modulus (a) and Phase angle (b) at 40°C reference temperature	46
Figure 4-6 I-FIT specimen, configuration (a), and geometry of specimen and fixture (b) with an external LVDT (Ozer et. al, 2016).....	48
Figure 4-7 I-FIT specimen fabrication.....	48
Figure 4-8 Load displacement curve from I-FIT fracture test for the test sections	50
Figure 4-9 Comparison of load displacement curve for all test sections	50
Figure 4-10 Hamburg Wheel Track Test equipment with testing molds.....	51
Figure 4-11 From left to right specimens tested by Hamburg: Galesburg Outer Lane, Galesburg Inner Lane, Machesney 15-16, Machesney 17-18, Dyer, respectively.....	51
Figure 4-12 Rut depth as a function of number of wheel passes	52
Figure 4-13 Flexibility index and rutting correlation using balanced mix design approach (Ozer et. al, 2016)	53
Figure 4-14 A comparison of binder and mixture cracking parameters	54
Figure 4-15 Load displacement curve from I-FIT fracture test for field cores of various sections	56
Figure 4-16 Comparison of I-FIT results from field cores and laboratory compacted specimens for test sections	56
Figure 5-1 (a) Energy and (b) GHGs from HIR versus conventional paving by hauling distances	59
Figure 5-2 Scenario analysis for different expected treatment lives for each process using (a) annualized energy and (b) required life for equivalent energy for HIR/OL based on mill/fill.....	60

List of Tables

Table 1-1 Types of in-place recycling used, and types of HIR and degree of in-place recycling used across United States (Stroup-Gardiner, 2011).....	5
Table 3-1 Core Inventory: Eastbound from Henderson to Seminary Street on Freemont.....	16
Table 3-2 Core Inventory: Westbound from Henderson to Seminary Street on Freemont	16
Table 3-3 Machesney Park extracted core locations and size measurements.....	21
Table 3-4 Dyer extracted core location and measurements	24
Table 3-5 Pavement condition assessment as per CRS rating	25
Table 3-6 Non-interstate AC surface CRS calculation model coefficients (Heckel and Ouyang, 2007)	25
Table 3-7 Deflection basin parameters from FWD (Horak and Emery, 2006)	28
Table 3-8 Typical values of normalized area parameter for different pavement structures (Mahoney, et al., 2014)	29
Table 3-9 Typical values for RoC and SCI and its condition (Horak and Emery, 2006).....	30
Table 4-1 Extracted aggregate gradation for different pilot sections (Appendix C)	41
Table 4-2 Volumetric details of recycled AC mixtures sampled from the various tested sections (Detailed volumetric information is provided Appendix D).....	42
Table 4-3 High temperature performance grade based on dynamic shear for field-aged binder installed at various sections	44
Table 4-4 Low temperature binder grade based on stiffness at 60 sec and m – value for different test sections (Appendix E)	45
Table 4-5 Performance Grade and BBR ΔT critical spread based on stiffness and m- value for different sections (Values calculated using data provided in Appendix E).....	45
Table 4-6 Result summary of I-FIT for the various test sections	49
Table 4-7 Hamburg Wheel Track Results (Appendix G)	52
Table 4-8 Summary of $\Delta T_{critical}$ and FI	54
Table 4-9 Result summary of I-FIT for field cores of various sections (Appendix F.2).....	55
Table 5-1 Details for the environmental assessment of HIR versus conventional processes	58

List of Abbreviations

CHPP: Center of Highway Pavement Preservation

MDOT: Michigan Department of Transportation

Acknowledgments

This publication is based on the results of a project sponsored by University Transportation Center, Environmental and Functional Benefits and Trade-offs of Hot In-Place Recycling Treatment Techniques was conducted in cooperation with the Illinois Center for Transportation and the Center for Highway Pavement preservation (CHPP). The IRI measurements and analysis were conducted by Engineering and Research International Inc., Champaign, IL and supported partially by Gallagher Asphalt, Inc. of Illinois.

The contents of this report reflect the view of the authors, who are responsible for the facts and the accuracy of the data presented herein. The contents do not necessarily reflect the official views or policies of the Illinois Center for Transportation. This report does not constitute a standard, specification, or regulation.

Executive Summary

In United States, there are more than four million miles of roadway network and almost three trillion vehicle miles travelled in 2011 alone. The country needs \$101 billion to maintain the roadway infrastructure in its existing condition. However, the current annual investment is just \$91 billion. An estimated \$170 billion of capital investment is required annually for 20 years from 2008 to 2028 to improve the infrastructure as reported in *2013 Report Card for America's Infrastructure*, ASCE. Therefore, in order to improve the condition of pavements, there is an immediate need to find cost-effective methods for pavement preservation.

Today, researchers and professionals are looking for alternative treatment techniques to rehabilitate distressed pavements. The use of in-place recycling techniques can prove to be an economically viable and environmentally sustainable pavement rehabilitation solution. Appropriate implementation of in-place recycling treatments can result in the optimal use of recycled pavement materials without much degradation. This can save costs and environmental related emissions in generating virgin materials and their transportation-related impacts. In-place recycling used the available binder in the recycled material with the addition of suitable rejuvenators or emulsions to reclaim the aged binder properties, eventually saving on binder costs and its related environmental impacts.

The use of hot in-place recycling (HIR) is suitable for pavement distresses limited to the upper few inches with no major structural distresses. The Asphalt Recycling and Reclaiming Association (ARRA) (2014) categorizes HIR into three basic types. Surface recycling is suitable for pavements with minor cracks limited to 25-50 mm in depth. The process includes drying and heating the upper layers, scarifying the soft asphalt, mixing the scarified material with a rejuvenator, if required, and finally spreading and placing the recycled material with the appropriate compaction. Repaving is used when surface recycling is insufficient to restore the pavement condition and an additional asphalt concrete (AC) overlay (OL) of 25-50 mm is required. Remixing is used when the pavement requires significant modification in the physical properties of the existing mix, which includes changes in aggregate gradation, aggregate abrasion, binder content, binder rheology, and mixture volumetric (Stroup-Gardiner, 2011).

As a recycling technique, the economic and environmental benefits of using HIR are often noted. Cost savings may result from the use of less virgin aggregate and asphalt binder, reduced hauling of new and removed materials to and from site, and lower traffic disruption with fewer lane closures (Finalyson et al., 2011). Based on various HIR strategies and existing pavement conditions, Robinette and Epps (2010) found the initial cost savings for using HIR to be up to 25% as compared with conventional overlays. However, for a holistic evaluation of the sustainability of HIR, the performance expectations and environmental impacts from using HIR were considered in this study.

This study investigated the suitability of HIR, as a preservation technique for local roads, by considering pavement performance and environmental impacts based on three test sites. The sites were located in Galesburg and Machesney Park, Illinois, and Dyer, Indiana. Field and laboratory investigations of the Galesburg, Machesney Park, and Dyer projects showed that the sites differed in terms of overall performance. Variation in the material properties was also evident

within these sections. Physical and rheological properties of binder recovered from each site indicated the range of binder performance grades ranged between 40 and 64 and between -34 and -46 for high and low temperature grades, respectively. The balanced mix design approach was useful in evaluating overall mixture performance. The interaction plots combining rut depth from the wheel track test (WTT) and flexibility index (FI) from the Illinois Flexibility Index Test (I-FIT) showed a great variation in mixes expected performance in the field. However, AC mixture test results allowed the prediction of potential cracking and rut resistance of both sites. In addition, the environmental assessment showed a difference in energy usage and GHGs of 3.9–17.6% and 1.3–19.2%, respectively, between a HIR process with 38 mm AC overlay and a corresponding traditional 50 mm mill and AC OL with different plant locations. Some initial energy savings can be expected with HIR treatments which heavily depend on the surface treatment after HIR, thickness of overlay (if overlay is chosen as the surface treatment), and hauling distances for plant-produced materials needed for overlays. A scenario-based analysis was carried out to show the range of expected life for both treatments that could result in similar environmental impact. However, a comprehensive life-cycle assessment (LCA) and cost analysis is recommended utilizing other LCA stages over an expanded analysis period.

This study is useful in the development of selection guidelines based on type and condition of pavement, timing of rehabilitation and construction temperature for the decision-making in order to get the best functional performance as well as reducing the overall energy and GHG emissions using HIR as pavement preservation technique. In addition, the study shows that continuous monitoring of the rehabilitated sections for riding quality (IRI) and distress management can help in developing quantitative performance models.

CHAPTER 1 - INTRODUCTION

According to ASCE Infrastructure Report Card 2013, the road network in United States consists of more than four million miles of roadway network and almost three trillion vehicle kilometers travelled in 2011 alone. As per the report, the country needs \$101 billion to maintain the roadway infrastructure at its existing condition. However, the current annual investment is just \$91 billion. An estimated \$170 billion of capital investment is required annually for 20 years from 2008 to 2028 to improve the infrastructure. Therefore, in order to improve the condition of pavements, there is an immediate need to find cost-effective methods for pavement preservation.

In the past few years, increasing the cost of petroleum products, increasing construction costs, and diminishing state and federal budgets made researchers and professionals look into alternative treatment techniques to rehabilitate distressed pavements. The use of in-place recycling techniques may prove to be an economically viable and environmentally sustainable pavement rehabilitation solution. Appropriate implementation of in-place recycling treatments can result in an optimal use of recycled pavement materials. This can save costs and environmental related emissions in generating virgin materials and their transportation related impacts. In-place recycling used the available binder in the recycled material with the addition of suitable rejuvenators or emulsions to reclaim the aged binder properties, eventually saving on binder costs and its related environmental impacts.

The general classification of in-place recycling techniques consists of the following:

- Hot In-place recycling (HIR)
- Cold In-place recycling (CIR)
- Full Depth Reclamation (FDR)

HIR is a pavement correction measure primarily intended to address surface distresses. The existing surface is softened using heat, followed by scarification of the softened layer and mixing with recycling agents or aggregates as required. The treated layer is compacted followed by an additional asphalt overlay if necessary. The technique is useful to eradicate functional distresses, limited up to the top 25-50 mm (ARRA, 2014). On the other hand, CIR is a rehabilitation measure that rectifies structural distresses generally limited to the depths of 50-100 mm. When the extent of recycling exceeds 100-300 mm, the type of treatment is classified as full depth reclamation (FDR) (ARRA, 2001). In CIR, the materials are recycled and blended in-place without heating the pavement surface. Sometimes virgin aggregates can also be added to meet job specific requirements. The recycled mix is then re-laid and compacted. The schematic shown in Figure 1-1 represents the stages of application for various in-place recycling methods in a pavement design life.

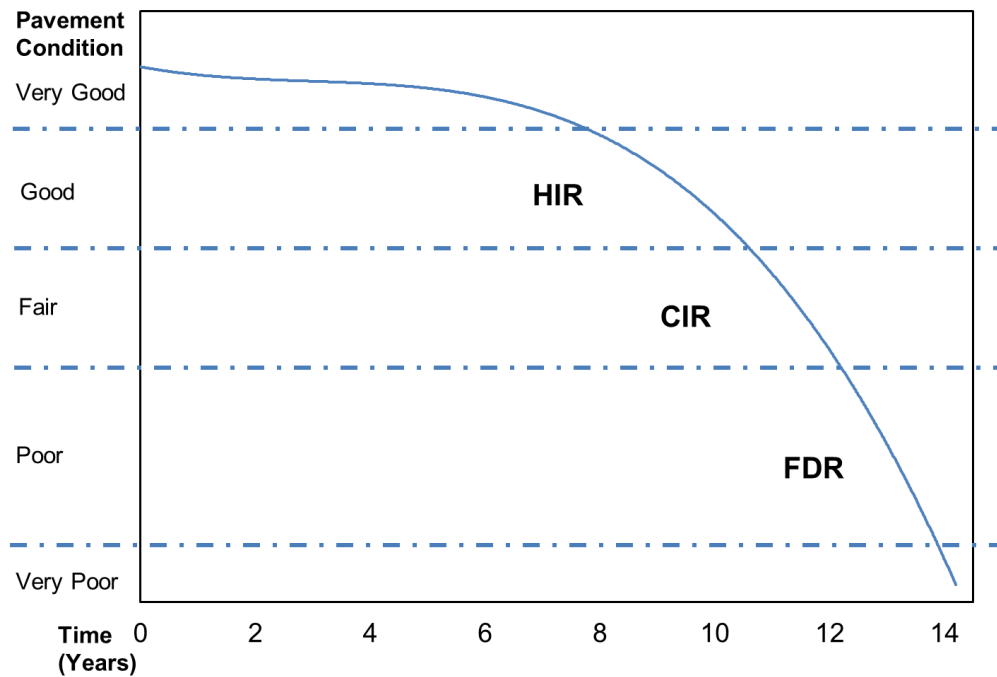


Figure 1-1 Stages showing different in-place recycling techniques throughout the pavement design life (NCHRP Synthesis 421, 2011)

1.1 BACKGROUND

Since the energy crisis of the 1970s, recycling has played a significant role in pavement rehabilitation and preservation strategies of state highway agencies (SHAs) (O’Sullivan 2010). According to a survey conducted by National Asphalt Pavement Association (NAPA), in 2014, the US used approximately 85 million tons of recycled materials in highway construction projects; the Illinois Department of Transportation (IDOT) used approximately 1.64 million tons of that recycled materials in highway construction projects with a value of around \$58 Million (Lippert et.al, 2015). With the increase for materials that needs to be recycled, highway agencies have started looking for alternative technologies and mix designs to accommodate this increase in the recycled pavement supply, which can also reduce the impact on the environment. Local roads constitute a significant portion of the highway system in the United States. Therefore, efficient and proven preventive maintenance techniques for local roads can provide significant contributions to cost and environmental savings.

HIR is a technique, used mainly for preservation of local roads. The process consists of heating and softening of existing AC pavement layers followed by scarification. Figure 1-2 shows the typical construction sequence of HIR. Here, the scarified or softened layers, mixed with virgin asphalt binder or a rejuvenator is laid and compacted as a recycled pavement surface layer. The process can be a single pass, where the restored pavement combined with virgin binder, or in a multi-pass operation, where the recycled material is re-compacted followed by an additional

overlay. The Asphalt Recycling and Reclaiming Association (ARRA) categorizes HIR into three basic types based on the process of application: surfacing recycling, repaving, and remixing.

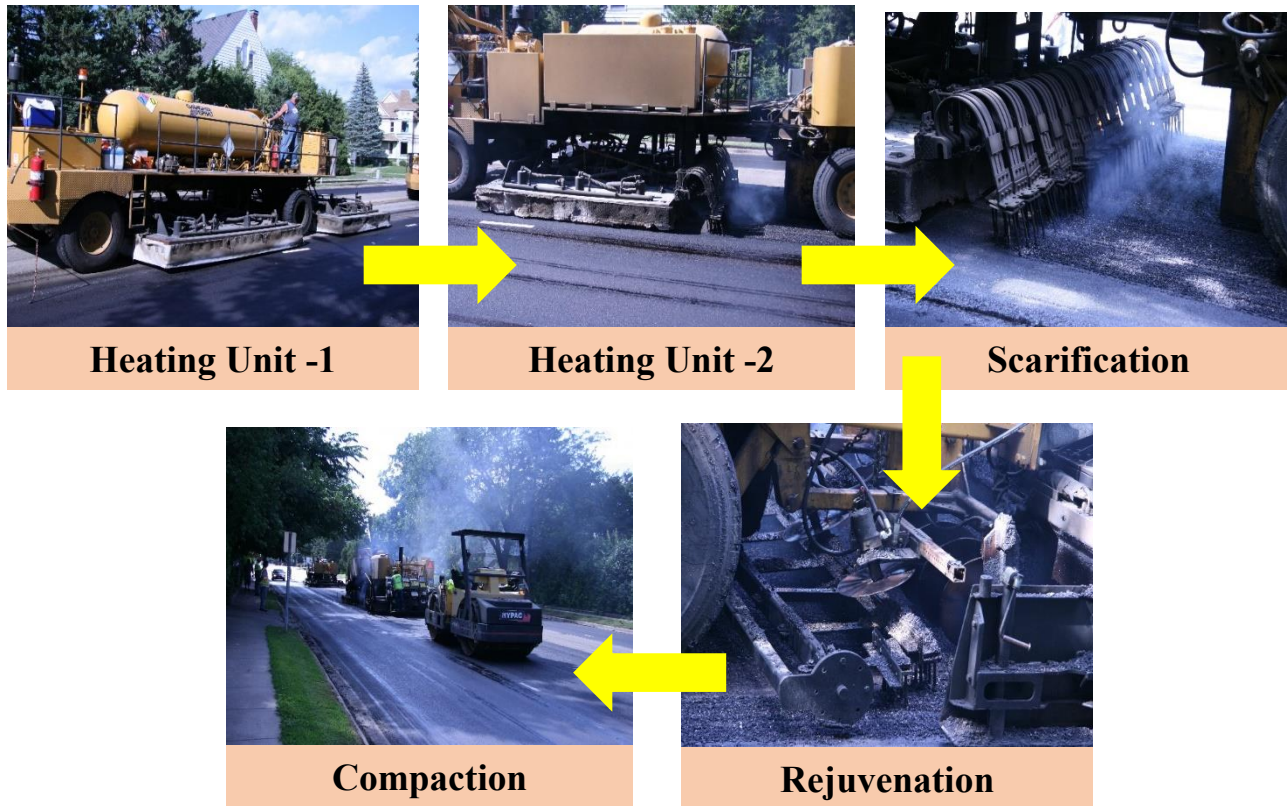


Figure 1-2 Construction sequence of HIR

The use of HIR is suitable where pavement distresses are minimal and limited to the upper few inches with no major structural distresses. Therefore, depending on the severity of distress, different types of HIR processes are implemented for maintaining the pavement structure. According to ARRA, surface recycling is suitable for pavements with minor cracks with depths limited to 25-50 mm. The process includes drying and heating the upper layers followed by scarifying the soft AC, then mixing the scarified material with a rejuvenator, if required, and finally spreading and placing the recycled material with required compaction. Repaving is used when surface recycling fails in restoring the pavement condition. It requires an additional AC overlay of 25-50 mm, in addition to surface recycling. Remixing is used when the pavement requires significant modification in the physical properties of the existing mix to rectify the distresses, which includes change in aggregate gradation, aggregate abrasion, binder content, binder rheology, and mixture volumetric (Stroup-Gardiner, 2011). The schematic shown in Figure 1-3 (a), (b) and (c) represents the difference in each of the HIR methods as mentioned above.

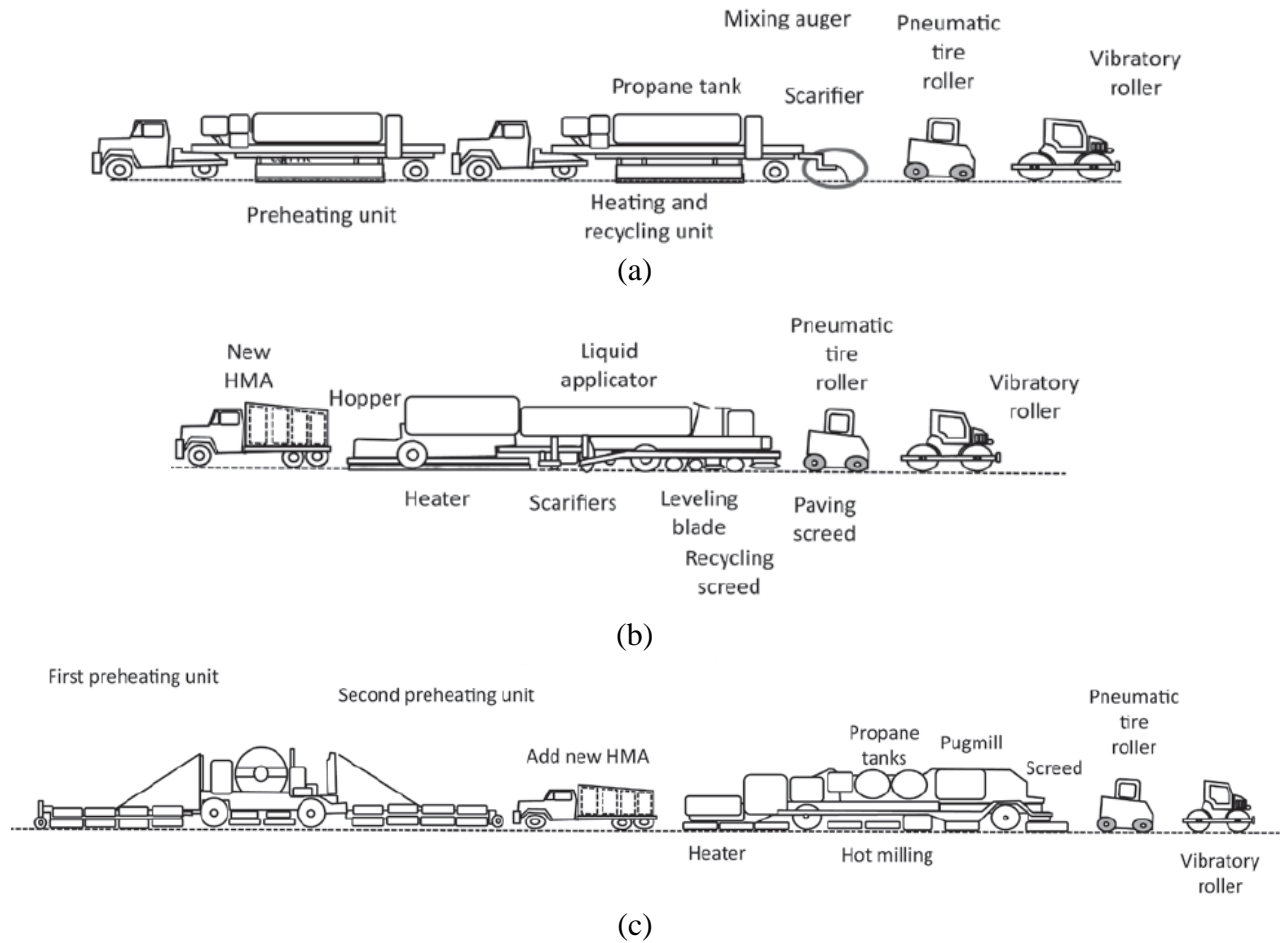


Figure 1-3 General arrangement of trains used for (a) surface recycling, (b) repaving, and (c) remixing (Stroup-Gardiner, 2011)

HIR can minimize energy use, material costs, user delays, improve ride quality, and greenhouse gas (GHG) emissions since it can salvage 100% of the existing pavement with a little addition of asphalt binder or rejuvenator. Even though in-place recycling appears to be a very promising field technique for agencies, there are still uncertainties in terms of recycled pavement performance, quality and reliability of construction and mix design, and its functional and environmental contribution to overall pavement life cycle. In spite of numerous advantages of HIR, this preservation method has a limited use in the industry. This is based on a national survey of contractors having experience with different in-place recycling methods (Stroup-Gardiner, 2011). Survey results are shown in Table 1-1, which includes the type and degree of recycling used across different states.

Table 1-1 Types of in-place recycling used, and types of HIR and degree of in-place recycling used across United States (Stroup-Gardiner, 2011)

	Types of HIPR used		
	Surfacing	Repaving	Remixing
	AR, CA, CO, FL, IL, IA, KS, KY, MT, NC, NE, NV, NY, TX, WY	AR, AZ, CO, FL, KS, KY, MO, NC, TX, WY	AR, AZ, CA, CO, FL, ID, IA, KS, KY, MD, MO, NC, NY, TN, TX, VT, WA, WY

Experience	Types of in-place recycling used		
	HIPR	CIPR	FDR
< 5 yrs	MO, NV	DE, MO, NC, ND, OR, UT	AL, DE, MO, NC, NY, VA, WY
5 to 10 yrs	AZ, GA, IL	IL, WY	AK, CA, CO, GA, IL, IA, MN
> 10 yrs	AR, ON, CO, FL, ID, IA, KS, KY, MD, MY, NC, NE, NY, TX, WA	AZ, CA, CO, CT, ID, IA, KS, MN, MT, NE, NH, NV, NY, RI, SD, VT, WA, WI	CA, CT, ID, MT, ND, NE, NH, NV, SC, SD, TX, UT, VT, WI
No	AK, AL, CT, DC, DE, IN, MN, ND, NH, NJ, OR, RI, SC, SD, TN, UT, VT, WI, WY	AK, AL, AR, DC, FL, GA, IN, KY, NJ, SC, TN, TX	AR, DC, RL, IN, KS, KY, NJ, OR, RI, TN

Lane-mile	Degree of usage of in-place recycling		
	HIPR	CIPR	FDR
< 50	AR, CA, CO, FL, IL, IA, KS, KY, MT, NC, NE, NV, NY, TX, WY	AZ, CA, CO, CT, DE, ID, IL, IN, KS, MN, MT, NE, NH, OR, RI, SD, TN, TX, UT, VT, WA, WY	AL, CO, CT, DE, GA, IL, IN, IA, MN, MO, MT, NH, NY, OR, RI, SD, TN, TX, UT, VA, VT, WI
50 to 100	CO	MO, NE, NY	AK, CA, ID, ND, NE, NV
> 100	KS	IA, NV, WI	CA, SC

In the United States, a number of qualitative performance evaluations for HIR were completed in the past few decades. Attempts were made to quantify the field performance in terms of functional and structural condition of pavements by regular monitoring over the years. Generally, like any other pavement preservation technique, performance varies from section to section depending upon the environmental conditions, time of application and initial pavement condition, type and level of distresses, geometry of the rehabilitated section, type of rejuvenators used, method of HIR used, and also on the type of heating mechanism used in scarifying the pavement. Therefore, it is important for an agency and contractors to make an informed decision as to when HIR should be used as a pavement rehabilitation technique. It is necessary to quantify the effect of various parameters involved in HIR to estimate its performance and optimize the use of depleting natural resources and costs.

To date, each state has its own customized guidelines to carry out HIR and this is attributed to the lack of available performance-based specifications and standard construction guidelines.

Therefore, an extensive research program at the laboratory level is required accompanied with field investigation and assessment to develop standards and specifications for construction.

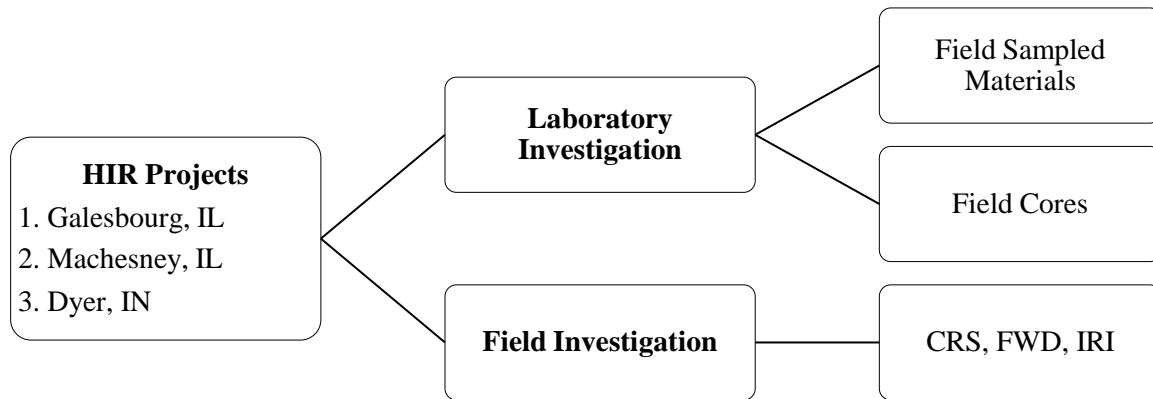
1.2 STUDY OBJECTIVE AND SCOPE

The objective of this project is to quantify the functional and environmental benefits of using HIR by laboratory characterization of mixture and binder of the collected field samples during HIR and assess field performance characteristics of HIR treatment. Three pilot sections were considered in this study: Galesburg and Machesney Park Village in Illinois and Dyer in Indiana. The scope of evaluating functional benefits included laboratory characterization, which consists of mixture- and binder-level tests. Laboratory performance evaluation included Illinois Flexibility Index test (I-FIT) to evaluate cracking potential and Hamburg wheel track test (WTT) to measure rut resistance of the AC mixtures. In addition, recovered binders from the recycled pavements were characterized to determine their viscoelastic modulus properties and performance grades. A field investigation was also conducted to evaluate the pavement structural and functional characteristics at different stages of treatment, i.e., before treatment, after in-place recycling, and post-overlay.

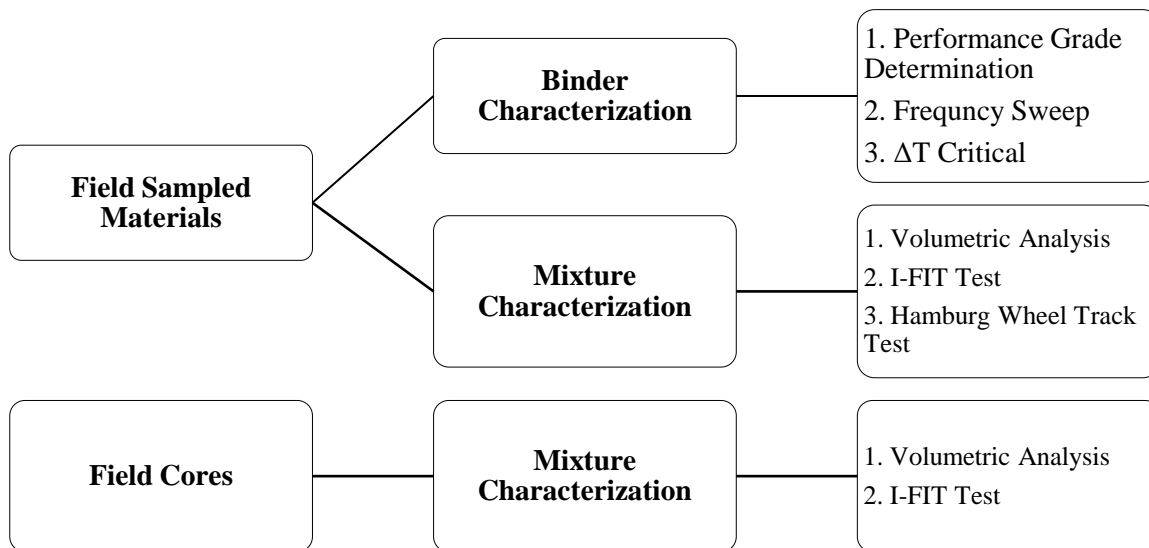
Environmental benefits were addressed by performing life cycle assessment (LCA) between conventional mill and fill to that of HIR treatment. A scenario-based analysis was performed to quantify the environmental impacts of the HIR treatment.

1.3 RESEARCH APPROACH

The research objectives were accomplished by dividing the study into two major sections: Field investigation, including Condition Rating Survey (CRS), Falling Weight Deflectometer (FWD) Analysis and profile prediction of the International Roughness Index (IRI); and laboratory investigation, including binder and mixture characterization. Binder properties were characterized by determination of their Superpave Performance Grade (PG) followed by frequency sweep tests. At mixture level, I-FIT test was used for characterizing cracking related damage resistance and Hamburg wheel track test (WTT) was used to characterize rutting resistance of the AC mixtures. In order to investigate the initial in-situ pavement material performance, field cores collected from the test sites were tested for its cracking performance using I-FIT test. The list of tests conducted in this study is presented in Figure 1-4 (a) and (b).



(a)



(b)

Figure 1-4 The experimental program for binders, AC mixtures, and field cores.

Field evaluation in terms of FWD, IRI and CRS was done for the three project sites, although IRI was an exception for Dyer site in Indiana. Field samples with and without the addition of rejuvenators were collected for Galesbourg, since rejuvenator was added after scarification. In Machesney and Dyer, samples only with rejuvenator were collected since it was added before scarification. Furthermore, for comparison of individual sections, laboratory characterization was performed on materials with rejuvenator. Field cores before the HIR treatment were collected and tested.

1.4 IMPACT OF RESEARCH

In NCHRP Synthesis 421, a survey across the United States was conducted among contractors having experience with different in-place recycling methods (Stroup-Gardiner, 2011). The results based on the survey are shown in Table 1.1, which includes type of recycling and experience across different states.

The survey suggests that HIR is not very common among contractors throughout the country. In addition, the experience with the technique is also limited. It is attributed to lacking adequate specifications and guidelines, because of limited research, field performance data, standard construction procedure, and quality assurance and quality control (QA and QC). Therefore, extensive research is required to characterize laboratory performance and to correlate it with the field performance data. This will enable developing the standard construction procedure and establish guidelines for HIR technique at various levels of QA and QC.

Use of HIR can result in an environmentally sustainable pavement rehabilitation technique by saving the depleting natural resources like virgin aggregates and asphalt binder, reducing GHG emissions caused due to production of aggregates, binder and its transportation, reduction in landfills. The research will allow evaluation of the economic and environmental benefits and trade-offs of using HIR, both qualitatively as well as quantitatively.

A scenario-based study is used to demonstrate the energy and GHGs savings that could be attained using HIR treatment over conventional mill and overlay when similar performance can be achieved. In addition, the economic savings from HIR compared to conventional mill and overlay is presented.

CHAPTER 2 - LITERATURE REVIEW

2.1 PAVEMENT PERFORMANCE EVALUATION

The Ministry of Transportation and the Regional Municipality of Ottawa-Carleton evaluated various projects in HIR and CIR carried out from 1987–1997. Kazmierowski et al. (1999) analyzed pavement performance using roughness, rutting, pavement deflection analysis and crack mitigation, and empirical testing, such as penetration value of asphalt cement, before and after the process. The study showed an increase in binder penetration values from a range of 20-40 to 50-80 after HIR with rejuvenation. Ride condition rating was also improved from average initial value of 6 to 8.5 after HIR. The study suggests that the in-place recycling techniques are advantageous over the conventional rehabilitation techniques. The authors concluded that productivity of the in-place recycling technique used can be maximized by selecting a suitable site depending on the weather conditions, distress type, geometry of the section, material used and initial condition of pavement. For example, HIR can be a good choice for moderate surficial pavement distresses and CIR is suitable for distresses like reflective cracking. In general, it was reported that the efficiency of both methods are maximized during dry and warm weather.

In another study, the Federal Highway Authority's (FHWA) Long-Term Pavement Performance (LTPP) Specific Pavement Studies Category 5 (SPS-5) test sections in Texas were investigated from 1991-2007 (Hong et al. 2011). A comparison was made between an AC with 35% reclaimed asphalt pavements (RAP) pavement section and virgin section (no use of recycled material). The study investigated three parameters: Transverse cracking, rut depth and ride quality. Eight sections with different conditions were investigated out of which four were with 35% RAP and the remaining four were virgin sections. Virgin sections performed better than the recycled sections with respect to transverse cracking whereas in case of rutting potential recycled sections were better. Ride quality showed no statistical difference between recycled and virgin section. Hence, based on this study a well-designed recycled section can perform better and can be used as an alternative to conventional rehabilitation where only virgin materials are used.

Ali et al. (2013) attempted to design HIR pavements using Superpave specifications in Florida. Materials collected from the field were extracted to determine binder grade, content and gradation at various levels of construction including before adding rejuvenator, after adding rejuvenator (excluding mixing), and after mixing with rejuvenator. Binder testing was conducted and the results showed that it was possible to achieve the Superpave specifications for the binder while performing HIR. The volumetric properties were compared to Superpave specifications followed by mixture level testing which included Hamburg WTT and IDT fatigue. The results concluded that HIR mixtures have good rutting performance compared to the conventional mixes used in Florida and the IDT test indicated that the mixtures also have good cracking performance.

2.2 DESIGN AND PAVEMENT MATERIAL EVALUATION AT BINDER AND MIXTURE LEVELS

Shen et.al (2006) studied the effects of rejuvenator on performance-based properties at both binder and mixture level. Viscosity blending charts along with knowledge of the composition of

the rejuvenators were used to identify the optimum level of the rejuvenator needed to achieve the target performance grade (PG) of virgin asphalt binder. The study showed that the use of rejuvenator significantly affects the properties of the AC mixture and the resulting blended binder. Bending Beam Rheometer (BBR) and Dynamic Shear Rheometer (DSR) tests were used at binder level, while Dynamic Stability and Thermal Stress of Refrained Specimen tests were used at mixture level. Blends with 0–14% rejuvenator were tested at binder level and 2.0–7.4% rejuvenator by binder weight was considered optimum. The mixture tests corresponding to these optimum contents were further tested. The results of the study concluded that rejuvenator softens the binder, rutting resistance of the mixture is reduced, and fracture resistance is improved.

In another study, Ali and Bonaquist (2011) evaluated the properties of binder mixed with recycling agents using blending charts. The purpose of the study was to determine the PG after blending, effectiveness of the recycling agents in HIR, and the use of blending charts for recycling agents. It was found that the binder grade was improved from PG 88-10 to PG 76-22 due to the addition of the rejuvenator, and dynamic modulus testing proved that the recycling agents mixed well with existing pavement binder. In addition, the authors concluded that linear blending charts at high, intermediate and low temperatures could be used to estimate the specific quantity of a particular type of recycling agent to be used in the AC mixture. It was recommended that RTFO aging should not be used for the evaluation of blends with recycling agents.

Karlsson et al. (2007) compared a mechanical method (using DSR) with a spectroscopic method (FTIR-ATR), to evaluate the diffusion rate of different binders because of mixing. The changes observed in the rheological properties of the resulting binder were of the order of same magnitude as measured from FTIR-ATR. Hence, it was shown that diffusion in asphalt binder is sufficient to cause a homogeneous blend of binders at the time of recycling. However, blending not only depends on the rate of diffusion but also on factors like mixing method, and compatibility of blending binders.

To determine the range for optimum dosage of rejuvenator, Shen et al. (2007) performed a series of DSR and BBR tests at various rejuvenator contents varying from 0-14% by weight of the binder. Optimum binder was used to evaluate the AC mixture properties using Dynamic Stability test for rutting potential and Thermal Stress of Restrained Specimen Test for fracture properties. The mixture test results indicated that on the one hand, adding rejuvenator improves fracture properties, whereas on the other hand, it decreases the rutting resistance.

In another study (Kunag et al, 2014), the use of composite rejuvenator was compared to common rejuvenators and was shown to be more effective to improve the performance and microstructure of the severely aged asphalt. Composite rejuvenator was prepared by blending the lightweight oil with high amounts of aromatics, which were more polar chemical compounds that dissolve the accumulated asphaltenes. Therefore, composite rejuvenators maintain the colloidal structure of aged asphalt as well as restore its microstructure.

Different rejuvenator sources at different dosage rate were used to evaluate the engineering properties of recycled AC mixtures (Im et al., 2014). Mixtures with different recycled aggregate contents were used in this study and the effect of three different types of rejuvenators were used to evaluate performance. Properties in terms of dynamic modulus, moisture damage, rutting

resistance, and cracking resistance were evaluated. The results indicated that the mixtures had improved cracking resistance compared to unrejuvenated mixtures, irrespective of the rejuvenator used. It also showed reduced moisture susceptibility and improved rutting resistance. However, AC performance based on the type of rejuvenator did not show any trend since the rejuvenator addition was not based on optimum dosage; instead the dosages used were recommended by the manufacturer.

Temperature of mixing and compaction are among the factors affecting construction quality of HIR treated pavements. Pavement temperatures fluctuate during construction because of wind, weather, or rain. Hence, it is necessary to maintain the desired mixing and compaction temperature to achieve target performance by regulating the temperature within the specified limits. Mallick et al. (1997) used finite element modelling along with an experimental study to see the effect of heating on HIR. The extent of rejuvenation is dependent on time of mixing, viscosity of rejuvenator, and temperature. Rejuvenation decreases across the film thickness with a minimum closest to the surface of aggregate. A higher temperature and longer mixing time results in higher rejuvenation up to a specific point along the film thickness. There exists a limit of rejuvenation for the aged binder based on film thickness. In addition, once the temperature falls below mixing temperature, the extent of rejuvenation becomes constant and the remaining thickness of the binder film acts as “black rock”.

Zaumanis et al. (2013) conducted a mixture level evaluation of nine different types of rejuvenators. The effect of rejuvenator on creep compliance, tensile strength, and fracture energy was evaluated. This study used the Penetration Index (PI), which is an indicator of oxidative hardening and cracking and is reported to be more representative of field oxidation. PI can be calculated by measuring the penetration results at two temperatures by using equation developed by Pfeiffer and Van Doormaal (see Equation below); this study used 4°C and 25°C.

$$PI = \frac{120 - 500 \times A}{1 + 50 \times A} \quad (2-1)$$

$$A = \frac{\log(\text{penetration at } T1) - \log(\text{penetration at } T2)}{T1 - T2}$$

The aforementioned studies showed that the extent of blending of the recycled materials during HIR affects its performance. Hence, more work is needed to identify the proper rejuvenator type and optimized dosage that needs to be used in HIR treatments.

2.3 LIFE-CYCLE ASSESSMENT FOR PAVEMENT MATERIALS

Miliutenko et al. (2013) compared the Global Warming Potential (GWP) and Cumulative Energy Demand (CED) of using RAP in recycling and reuse. The recycling of AC refers to the use of RAP in new AC mixes, where the old asphalt binder performs a similar function as that of the original binder. However, in case of reuse, the RAP is used as fill, base course or as foundation material where the binder is not considered to perform equivalent to the original binder. Recycling was further classified as in-plant and in-place recycling and their relative impacts

were also compared. The outcome of the study showed that recycling, both in-place and in-plant, resulted in net savings in GWP and CED. The reuse resulted in greater reduction in GWP and HIR was slightly better than in-plant recycling in terms of GWP and CED.

Different types of pavement preservation and rehabilitation techniques were evaluated based on the energy usage and its greenhouse gas (GHG) emissions (Galehouse, 2010.). Life extension by each of the preservation techniques was assumed to calculate the annualized energy use and GHG emissions for construction, rehabilitation and preservation processes for comparison. The results of the study showed that HIR had lesser energy consumption and GHG emissions compared to an overlay.

Detailed life cycle assessment (LCA) of the HIR treatment is still limited. The impact of HIR on the various stages of the LCA is needed to quantify the benefits of HIR on GHG and GWP.

CHAPTER 3 - FIELD INVESTIGATION

3.1 INTRODUCTION TO PROJECT SITES

Three project sites from Illinois and Indiana were evaluated. The sites were located in Galesburg, IL, Machesney, IL, and Dyer, IN. The sites are introduced in details in the following sections along with the activities conducted at these sites required to carry out the field as well as laboratory testing.

3.1.1 Galesburg, IL

The HIR project at City of Galesburg was the first field project among the three projects. The length of the project is 1530 m straight alignment from West to East. The project limits stretched across Fremont Street from East of Henderson to Seminary Street and is a residential road. The corridor is a four-lane with two lanes in each direction. The project had surface recycling of the first one inch of the existing AC surface for the entire corridor followed by an overlay of 38 mm thickness. Figure 3-1 shows the corridor.

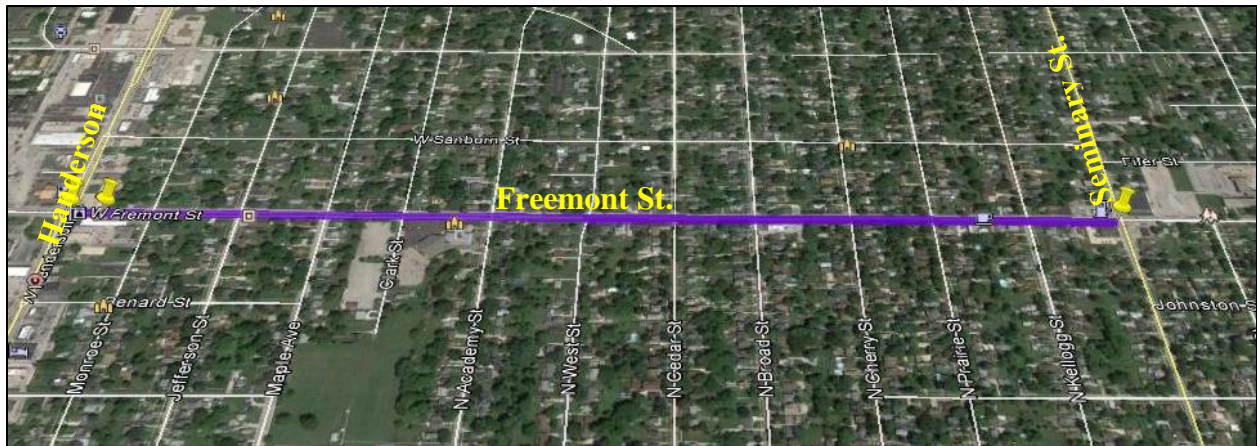


Figure 3-1 Image of the project site at Galesburg from Google Earth

The pavement structure at Galesburg consists primarily of brick as base layer with AC overlays. There was a stretch within the project limit with rigid pavement as the base layer. The condition of the pavement was poor with severe distresses (as shown in Figure 3-2). Edge cracking was common in the entire stretch, transverse cracks were prominent, and some longitudinal cracks of more than 30 m were common on the outer lanes. Fatigue cracking and shoving were limited. The intersections had block cracking. Minor fresh patch work was conducted prior to recycling to ensure sufficient material during HIR. Figure 3-2 shows the condition of the pavement before the HIR.



Edge Cracking



Longitudinal Cracking



Transverse and Longitudinal Cracking



Block Cracking



Block Cracking at Intersections



Patching

Figure 3-2 Types of pavement distresses before HIR at Galesburg, IL project site

The HIR construction train was made of two portable propane fired heating units and a compactor (Figure 3-3). The first heating unit comprised of two propane heaters, which consumed 5678 liters/day of propane and 95 liters/day of diesel. The second heating unit included the asphalt scarifying attachment and paver (Figure 3-3). It has one propane heater and consumed 1893 liters/day of propane and 189 liters/day of diesel. Rejuvenator application is included with the second unit (Figure 3-4). A Kendex rejuvenator was applied at a rate of 2.3 liters/min (0.16 liters/m²). Approximately top 25-50 mm of the pavement was scarified. The final

construction phase involved constructing a 38 mm overlay on top of the HIR treated layer. The speed of the HIR train was around 4.6 m/min.

The construction sequence for HIR at Galesburg was as follows:

- Heating of the pavement surface by Heating Unit – 1.
- Further heating of the pavement using Heating Unit – 2.
- Pavement scarification with a scarifier attached to Heating Unit – 2.
- Spraying of rejuvenator on the scarified pavement material.
- Mixing of the rejuvenated material with mixing augers attached to the Heating Unit – 2.
- Laying of the mixed material as a newly recycled surface followed by compaction using the compactor.



Figure 3-3 HIR construction train showing two heating unit and scarifier followed by compactor



Figure 3-4 HIR train showing second heating plate and rejuvenator application (see inset)

Field evaluation of the treated layers was conducted by measuring IRI, conducting FWD, and testing of field cores. IRI was calculated for all longitudinal profiles before and after HIR, the FWD was conducted every 61 m and cores were taken every 244 m. 24 cores were extracted and sample materials with and without rejuvenator were collected at the time of HIR for laboratory evaluation. Roughness was measured for existing pavements and after HIR to study the improvement in pavement performance. FWD was conducted for existing pavement, post-HIR, and post-overlay. Tables 3-1 and 3-2 show the inventory of the collect field cores.



Figure 3-5 (a) FWD measurement before HIR (b) extraction of cores at Galesburg, IL

Table 3-1 Core Inventory: Eastbound from Henderson to Seminary Street on Freemont

East Bound							
Inner Lane				Outer Lane			
No.	Location (m)	Thickness (mm)	Diameter (mm)	No.	Location (m)	Thickness (mm)	Diameter (mm)
1	123.4	73	150	1	121.9	80	150
2	369.1	97	150	2	368.8	87	150
3	611.7	74	150	3	609.6	139	150
4	855.6	116	150	4	853.4	200	150
5	1097.6	83	150	5	1097.3	106	150
6	1341.4	106	150	6	1341.1	101	150

Table 3-2 Core Inventory: Westbound from Henderson to Seminary Street on Freemont

West Bound							
Inner Lane				Outer Lane			
No.	Location (m)	Thickness (mm)	Diameter (mm)	No.	Location (m)	Thickness (mm)	Diameter (mm)
1	120.7	163	150	1	117.3	58	150
2	364.2	84	150	2	365.8	97	150

3	609.0	136	150	3	609.6	87	150
4	853.1	113	150	4	853.4	64	150
5	1096.7	72	150	5	1097.3	69	150
6	1342.3	68	150	6	1341.1	69	150

3.1.2 Machesney, IL

The Village of Machesney Park was the second field project evaluated. It consisted of two sites: Silo Ridge and Timberlyne Hollow. Each one of the sites consists of three road sections. The Silo Ridge sections are 1-2, 2-3 and 4-5-6-7 while sections for Timberlyne Hollow are 8-9, 15-16 and 17-18. Figures 3-6 and 3-7 show different sections from the project location.



Figure 3-6 Silo Ridge sections at Machesney Park





Figure 3-7 Timberline Hollow section at Machesney Park

The pavement structure consists of compacted sub-base with multiple lifts of AC layers. Pavement condition was similar for all of the section in this site. Distresses observed in both sites consisted of block cracking (low and medium), raveling, potholes, longitudinal cracking and transverse cracking. Fatigue cracking was limited due to less traffic. Settlements were observed also but more severe in the Silo Ridge sections compared to the other site. Pavements in both sites show clear signs of aging and oxidization. Figure 3-8 shows distress types found in Machesney.

In addition, many patches (small and large) were observed in both sites. A few of these patches were old and most of them were new indicating that they were placed to have sufficient material for the HIR construction. Another observation was the presence of localized old overlay. This was observed in the cores taken from overlaid section.



Old Patch



New Patch



Block Cracking



Raveling



Longitudinal Cracking



Localized Overlay

Figure 3-8 Types of pavement distresses before HIR at Machesney, IL project site

The HIR construction train was made of two portable heating units (Figure 3-9 (a)) and a compactor (Figure 3-9 (b)) following the heating units. The second unit included asphalt scarifying attachment and paver (Figure 3-9 (c) and 3-9 (e)). Rejuvenator application is also included with the second unit but was applied before scarification (Figure 3-9 (d)).

Approximately 25-50 mm of the top of the pavement was scarified. The pavement before and after compaction is shown in Figure 3-9 (f). The final construction phase involved constructing a 38 mm overlay on top of the HIR layer. The construction sequence for HIR at Machesney was as follows:

- Heating of the pavement surface by Heating Unit – 1.
- Further heating of the pavement using Heating Unit – 2.
- Spraying of rejuvenator on the heated pavement surface.
- Pavement with rejuvenator was scarified with a scarifier attached to Heating Unit – 2.
- Mixing of the rejuvenated material with mixing augers attached to the Heating Unit – 2.
- Laying of the mixed material as a newly recycled surface followed by compaction using the compactor.



(a)



(b)



(c)



(d)



(e)



(f)

Figure 3-9 (a) HIR construction train; (b) compaction; (c) scarification and paver included with the second heating plate; (d) addition of rejuvenator; (e) pavement scarification; and (f) pavement before and after HIR

The field investigations conducted were similar to those in Galesburg. The FWD measurement and core extraction process are shown in Figure 3-10. Table 3-3 shows the extracted core locations and dimensions. Twenty-one cores were extracted and materials with rejuvenator were collected at the time of HIR for laboratory evaluation. Roughness was measured for existing pavements and after HIR to study the improvement in pavement performance due to HIR process. FWD was measured for existing pavement, post-HIR, and after overlay only for sections 4-7, 8-9, and 15-18.



Figure 3-10 (a) FWD measurement (b) Extraction of cores at Machesney, IL

Table 3-3 Machesney Park extracted core locations and size measurements

Section	Core Location (m)	Thickness (mm)	Diameter (mm)
1-2	184.7	48	150
	367.0	68	150
2-1	365.5	85	150
2-3	122.8	44	150
	243.8	73	150
3-2	304.2	83	150
4-5-6-7	124.7	79	150
	304.8	40	150
	489.2	40	150
	610.5	70	150
	671.2	62	150
7-6-5-4	671.2	45	150
8-9	129.8	66.5	150
	249.6	50.8	150
15-16	505.1	44.9	150
	545.6	49	150
	609.9	45	150
16-17	671.5	45	150
17-18	976.0	53	150
	1045.5	51	150
	1097.6	53	150

3.1.3 Dyer, IN

The HIR project at Dyer, Indiana was the third field project evaluated. The length of the project was around 1646 m. The section was a two lane residential road with rolling terrain. The project

included surface recycling of the first 25-50 mm of the existing AC surface with an additional overlay of 38 mm.

The pavement structure was a conventional AC pavement. It comprises of a compacted subgrade, a layer of asphalt treated base, and multiple AC overlays. The pavement had severe fatigue cracking along the wheel paths. Excessive fatigue cracking resulted in potholes, which were patched along the stretch. Block cracking was also observed in some parts of the section. The lane on the eastbound direction had several long patches of more than 30 m and were in extremely bad condition. These patches were recently placed to provide sufficient material for HIR. Figure 3-11 shows variety of distresses at the site.



Fatigue cracking along wheel path



Severe Fatigue Cracking



Block Cracking



Pot Hole



Patching



Transverse and Longitudinal Cracking

Figure 3-11 Types of pavement distresses before HIR at Dyer, IL project site

The construction sequence for HIR at Dyer was as follows:

- Heating of the pavement surface by Heating Unit – 1.
- Further heating of the pavement using Heating Unit – 2.
- Spraying of rejuvenator on the heated pavement surface.
- Pavement with rejuvenator was scarified with a scarifier attached to Heating Unit – 2.
- Mixing of the rejuvenated material with mixing augers attached to the Heating Unit – 2.
- Laying of the mixed material as a newly recycled surface followed by compaction using the compactor.

The construction details were similar to those at the Machesney Park site (Figure 3-12). Figure 3-13 shows the FWD measurement and core extraction process. However, at this site no roughness was measured. Table 3-4 presents the extracted core locations and dimensions. Fourteen cores were extracted and recycled mix with rejuvenator were collected at the time of HIR for laboratory evaluation as seen in Figure 3-14. FWD was measured for existing pavement, post-HIR, and post-overlay.

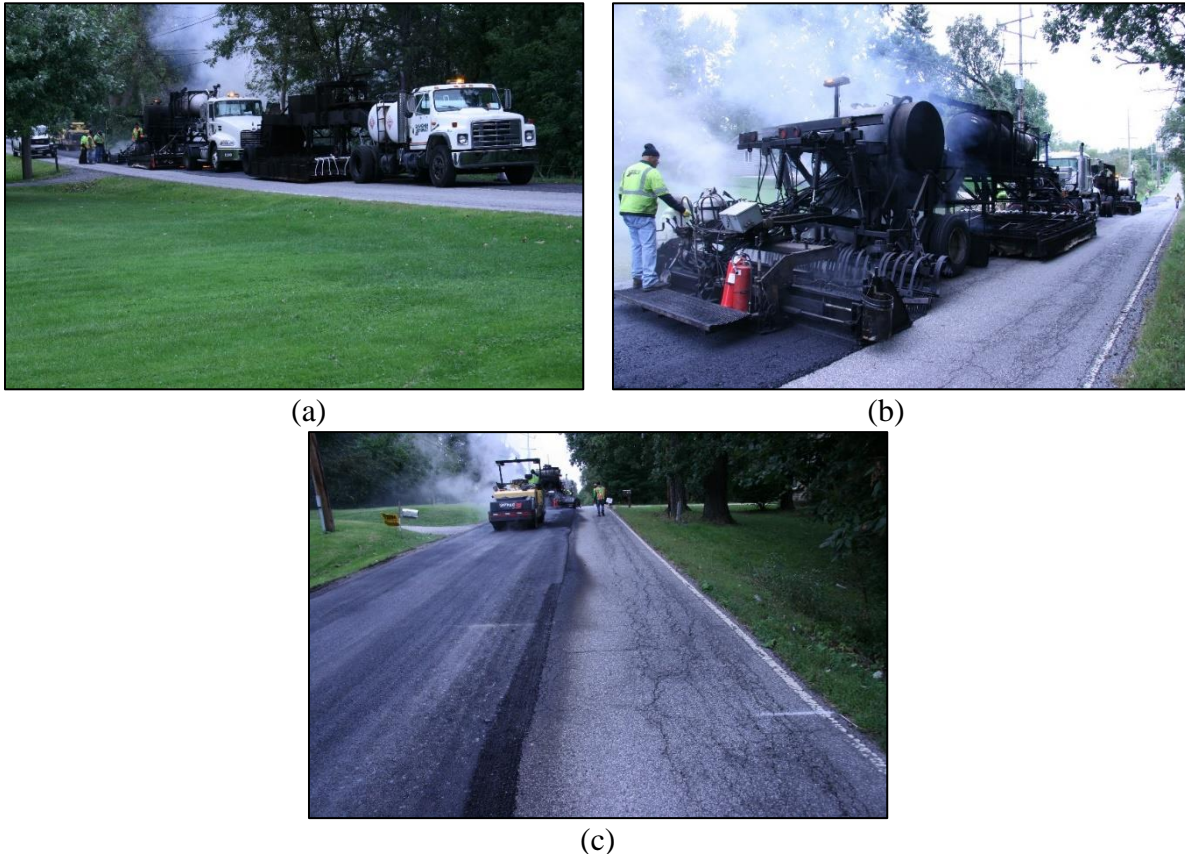


Figure 3-12 (a) HIR construction train; (b) scarification, application of rejuvenator followed by laying the mix; and (c) compaction



(a)



(b)

Figure 3-13 (a) FWD measurement and (b) extraction of cores at Dyer, IN



Figure 3-14 Sampling of recycled asphalt mixture at HIR project site

Table 3-4 Dyer extracted core location and measurements

East Bound				West Bound			
Core No.	Location (m)	Thickness (mm)	Diameter (mm)	Core No.	Location (m)	Thickness (mm)	Diameter (mm)
1	670.9	145	150	1	670.0	149.5	150
2	856.2	138	150	2	853.4	157.7	150
3	1097.6	137.8	150	3	1097.3	126.4	150
4	1340.2	120	150	4	1340.8	138.3	150
5	1585.6	196.4	150	5	1582.5	169	150
6	1894.3	125	150	6	1889.2	148.4	150
7	2134.2	125.2	150	7	2133.6	109	150

3.2 CONDITION RATING SURVEY (CRS)

Existing pavement condition had been assessed before HIR was evaluated using the IDOT's Condition Rating Survey (CRS) method. The evaluation was based on the CRS calculated as per research report FHWA-ICT-07-012 (Heckel and Ouyang, 2007). This report is an updated version of CRS obtained from Chapter 53 – Pavement Rehabilitation of Bureau of Design and Environmental Manual. The equation used to calculate the value of CRS is the following:

$$CRS = Intercept - x * IRI - y * Rutting - z * Faulting - a * A - b * B - c * C \dots \quad (3-1)$$

where:

- Intercept is the starting point for calculation
- x,y and z are coefficients for the sensor data (as applicable)
- IRI, Rutting and Faulting are the values of sensor data
- a,b,c...are the coefficients for the distresses
- A,B,C.....are the severity values of distresses recorded by the raters

As per Chapter 53– Pavement Rehabilitation of Bureau of Design and Environmental Manual, the CRS value is defined as poor, fair, satisfactory and excellent based on the rating obtained. Table 3-5 shows the criteria for condition of the pavement as per CRS values.

Table 3-5 Pavement condition assessment as per CRS rating

Pavement Condition	CRS Rating
Poor	1.0 to 4.5
Fair	4.6 to 6.0
Satisfactory	6.1 to 7.5
Excellent	7.6 to 9.0

The CRS Model varies for Interstates and Non-Interstate roads. In addition, it also depends on the pavement structure. All the pavements in this study were considered as non-interstate sections. Hence, coefficients corresponding to only non-interstate type were used and are presented in Table 3-6.

Table 3-6 Non-interstate AC surface CRS calculation model coefficients (Heckel and Ouyang, 2007)

Distress	ACPLT**	ACP**	AC/JPCP**	AC/CRCP**	AC/BBO**
Intercept	9	9	9	9.182	9
IRI	-0.004	-0.002	-0.002	-0.001	-0.002
Rut	-0.3 if >= 0.25*	-1.403	-0.43	-1.068	-0.998
L		-0.236	-0.203	-0.207	
M	-0.574	-0.271	-0.21	-0.209	-0.204
O	-0.305	-0.378	-0.444	-0.483	-0.485
P			-0.036		

Q		-0.199	-0.175	-0.184	-0.25
R		-0.088	-0.063		-0.113
S	-0.286	-0.252	-0.237	-0.29	-0.123
T	-0.409	-0.208	-0.176	-0.178	-0.182
U		-0.146	-0.61	-0.604	
V		-0.253	-0.114		
W	-1.531	-0.311	-0.316	-0.264	-0.283
X			-0.074		

* 0.3 CRS point are deducted from the CRS value if rutting is greater than or equal to 0.25 as measured by the sensors on the van.

**ACPLT is Asphalt Concrete Pavement – Low Type

**ACP is Asphalt Concrete Pavement – High Type

**AC/JPCP is Asphalt Overlays of Jointed Plain Concrete Pavement-No reinforcement

**AC/CRCP is Asphalt Overlays of Continuously Reinforced Concrete Pavement

**AC/BBO is Asphalt Overlays of Brick, Block or Other type

3.2.1 Galesburg, IL

The pavement system at Galesburg consists of a brick base with multiple AC overlays of asphalt. The section was identified as AC/BBO for calculation of model coefficients based on the information retrieved from field cores. The section was severely distressed with longitudinal cracking, transverse cracking, block cracking, frequent patching and edge cracking. Based on the field survey data collected, the severity level for each distress type was input in the model (equation 3-1) for the CRS calculation. Since the CRS value is dependent on the individual rater, a minimum and maximum value of severity was assigned for each distress type to get the range of CRS instead of a unique CRS. The CRS for Galesburg, IL ranged from 2.2 to 4.2. The condition of the pavement is considered poor as per the values in Table 3-5. The details of calculations are provided in Appendix A. Two years after the rehabilitation of Galesburg section, the CRS ranged from 5.9 to 7.3.

3.2.2 Machesney, IL

The pavement at Machesney Park Village, IL was a conventional flexible pavement. Based on the details extracted from field core information, the section was categorized under ACP for calculation of model coefficients. The section was highly oxidized with a high degree of raveling. Longitudinal cracking was common along with severe block cracking. A combination of old and new patches suggested that the pavement had distress related problems in the past as well. Fatigue cracking was categorized as moderate to severe. The range of the CRS calculation using the model varied from 1.1 to 3.7. This section was also categorized as poor per the values given in Table 6. The details of calculations are provided in Appendix A. Two years after the rehabilitation of Machesney section, the CRS ranged from 8.4 to 8.7.

3.2.3 Dyer, IN

The pavement section at Dyer was also a conventional flexible pavement. The section had severe fatigue cracking observed along the wheel paths, stretches up to a length of more than 30 m were patched, and block cracking was common. Overall, the section was highly distressed. Rutting and roughness were not measured for this site. Therefore, rutting and IRI effect were not

considered in the evaluation of CRS. Hence, the CRS obtained would be greater than the actual value (including rutting as well as IRI). The range of CRS was from 1.6 to 3.7. This suggested that the section was also in poor condition. Details of the calculations are provided in Appendix A. Two years after the rehabilitation of Dyer section, the CRS ranged from 5.2 to 7.1.

3.3 FALLING WEIGHT DEFLECTOMETER (FWD)

FWD is a non-destructive technique used to evaluate the structural capacity of the pavement layers. The FWD trailer consists of a specially designed rubber spring system, which produces half-sine shaped, single-impact load with a duration ranging between 25-30 secs. The impact load is thought to simulate a moving wheel load of up to 120 kN. The range of the peak load varies from 7 kN to 120 kN. Seven seismic sensors are usually mounted in movable holders along a 2.4 m long bar for deflection measurements. Typical testing takes 40 secs to obtain one measurement. The testing procedure usually applied is in accordance with ASTM specifications D-4694 and AASHTO T256.

The equipment used in this study is a Dynatest 8002 FWD (Figure 3-15). The system consists of four main components:

- A Dynatest 8002 FWD
- The FwdWin field data collection program
- A Dynatest 9000 System Processor
- A computer system



Figure 3-15 Dynatest FWD 8002 trailer

A deflection basin formed under the applied load and back calculation method is used to predict the moduli of the pavement layers. Layer thicknesses, obtained from either the field core data or from construction data provided by the agency, were used to improve the back calculation prediction accuracy of the pavement layer moduli. However, back calculated moduli may not be reliable if the layer thicknesses are less than 75 mm. In addition, incomplete information about pavement layer thicknesses and its underlying structural details, can produce misleading backcalculated moduli. Deflection basin obtained from FWD testing also yields some useful parameters that can be used to predict the pavement behavior (Horak, 1987). There are numerous parameters which can be derived from the deflection basin of FWD and are listed in Table 3-7,

along with their respected applications and their relation to specific pavement behavior. Figure 3-16 shows a typical deflection basin resulted from FWD testing.

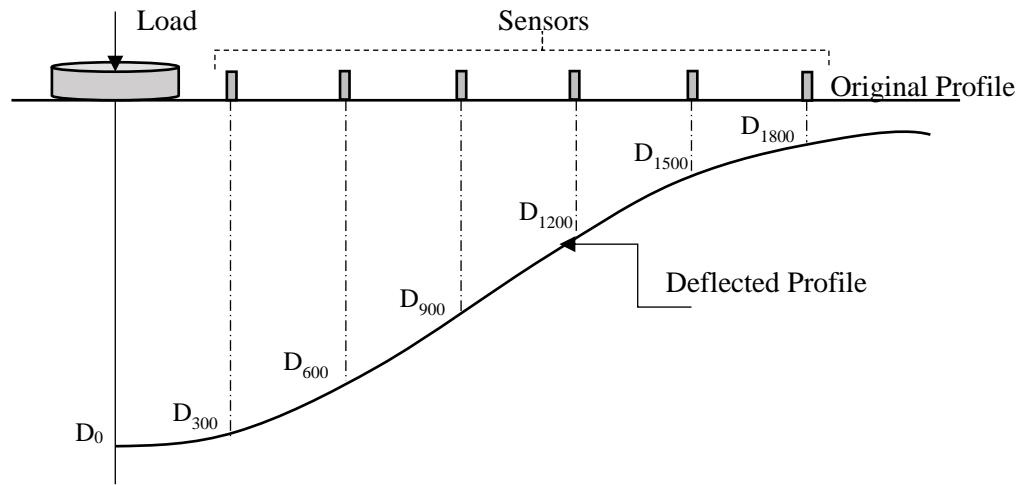


Figure 3-16 Deflection basin

Table 3-7 Deflection basin parameters from FWD (Horak and Emery, 2006)

S. No.	Parameter	Formula	Units	Structural Indicator
1	Maximum Deflection	D ₀ as measured	mm	Gives an indication of all structural layers with about 70% contribution by the subgrade
2	Radius of Curvature	$R_oC = L^2 / [2D_0(1 - D_0/D_{200})]$ Where L=127mm in the Dehlen curvature meter and 200mm for the FWD	m	Gives an indication of the structural condition of the surfacing and base condition
3	Area	$A = 150[1 + 2(D_{300}/D_0) + 2(D_{600}/D_0) + D_{900}/D_0]$	mm	Indicates the response of the whole pavement structure
4	Spreadability	$S = \{[(D_0 + D_{300} + D_{600} + D_{900})/5]100\} / D_0$, Where D ₃₀₀ , D ₆₀₀ , D ₉₀₀ spaced at 300mm		Indicates the response of the whole pavement structure. Ratio of surface layer to support layer strengths
5	Shape Factors	F1=(D ₀ -D ₆₀₀)/D ₃₀₀ F2=(D ₃₀₀ -D ₉₀₀)/D ₆₀₀		The F2 shape factor provides better correlations with subgrade moduli while F1 provides weak correlations

6	Surface Curvature Index	$SCI = D_0 - D_{300}$	mm	Gives an indication of primarily the base layer structural condition. Indicates the strength of upper portion of pavement
7	Base Curvature Index	$BCI = D_{600} - D_{900}$	mm	Provides strength information on the lower structural layers including subgrade
8	Base Damage Index	$BDI = D_{300} - D_{600}$	mm	Provides information on the sub-base and probably selected layer structural condition
9	Slope of Deflection	$SD = \tan^{-1}(D_0 - D_{600})/600$		Weak correlations observed

The purpose of the study is to quantify the impacts of HIR at different stages of construction. Therefore, only selected parameters (highlighted in Table 3-7) were selected for further analysis in this study. The selected parameters for further analysis are area parameter, radius of curvature, and surface curvature index. These parameters were selected as they represent either the behavior of the upper layers (because of using HIR) or the entire pavement structure.

The area parameter (A) is calculated as normalized area of the deflection basin between the deflection measured at the center of the applied load and the deflection measured at sensor located at 900 mm from the center. It is calculated as per the equation presented in Table 3-7 and is expressed in the units of length. Lower values of area suggest that the pavement structure is similar to the underlying subgrade material (Mahoney, et al., 2014). Typical values of area for various pavement structures are presented in Table 3-8.

Table 3-8 Typical values of normalized area parameter for different pavement structures (Mahoney, et al., 2014)

Pavement Structure	Area Parameter (mm)*
PCC pavement Range	600 – 825
“Sound” PCC	725 – 800
Thick AC (225 mm of AC)	> 675
Medium AC (125 mm of AC)	575
Thin AC (50 mm AC)	425
Chip sealed flexible pavement	375 – 425
Weak chip sealed flexible pavement	300 – 375

Radius of curvature (RoC) is a parameter that provides information on the structural condition of the surface and base condition. Typical range of RoC values is given in Table 3-9

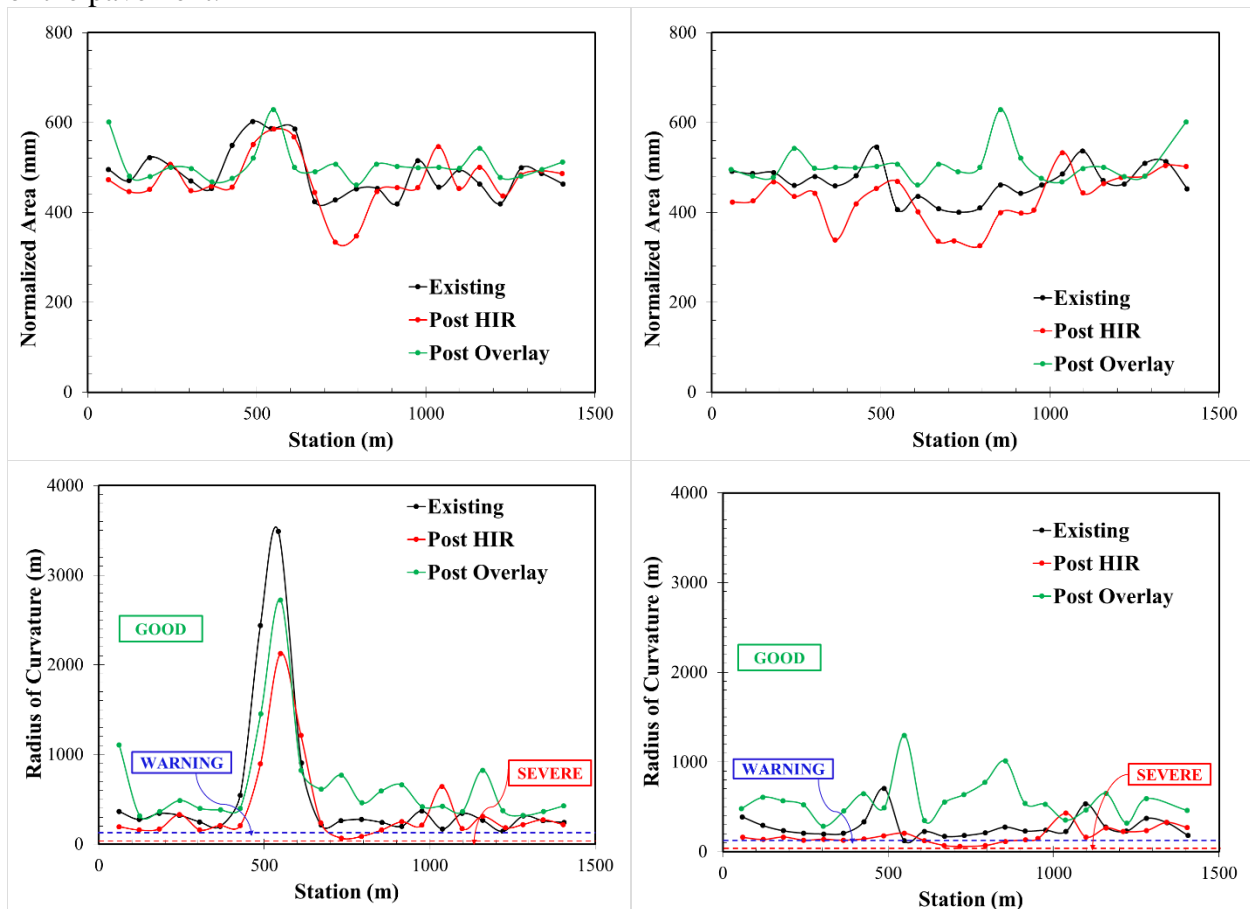
Surface curvature index (SCI) is another parameter that provides information on the strength of the upper layers of the pavement structure. It is calculated as shown in Table 3-7 and is expressed in the unit of length. Typical range of SCI is presented in Table 3-9.

Table 3-9 Typical values for RoC and SCI and its condition (Horak and Emery, 2006)

Condition	RoC (m)	SCI (mm)
Sound	> 120	< 0.15
Warning	40 – 120	0.15 – 0.50
Severe	< 40	> 0.50

3.3.1 Galesburg, IL

The variation of the selected parameters from deflection basins resulting from FWD testing is shown in Figures 3-17. The values indicate a reduction in the structural capacity post-HIR whereas after the overlay application it shows improvement as compared to the initial condition of the pavement.



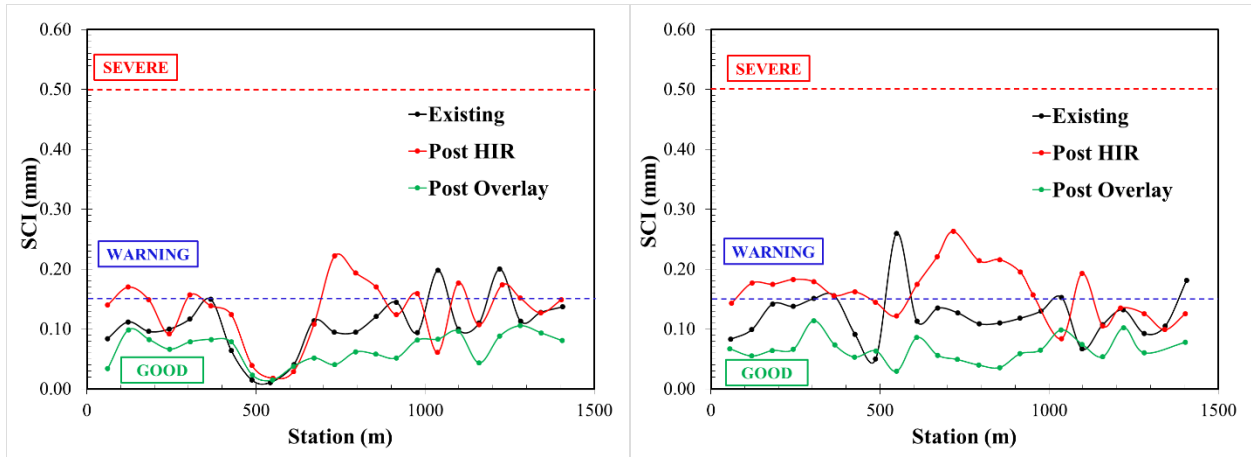
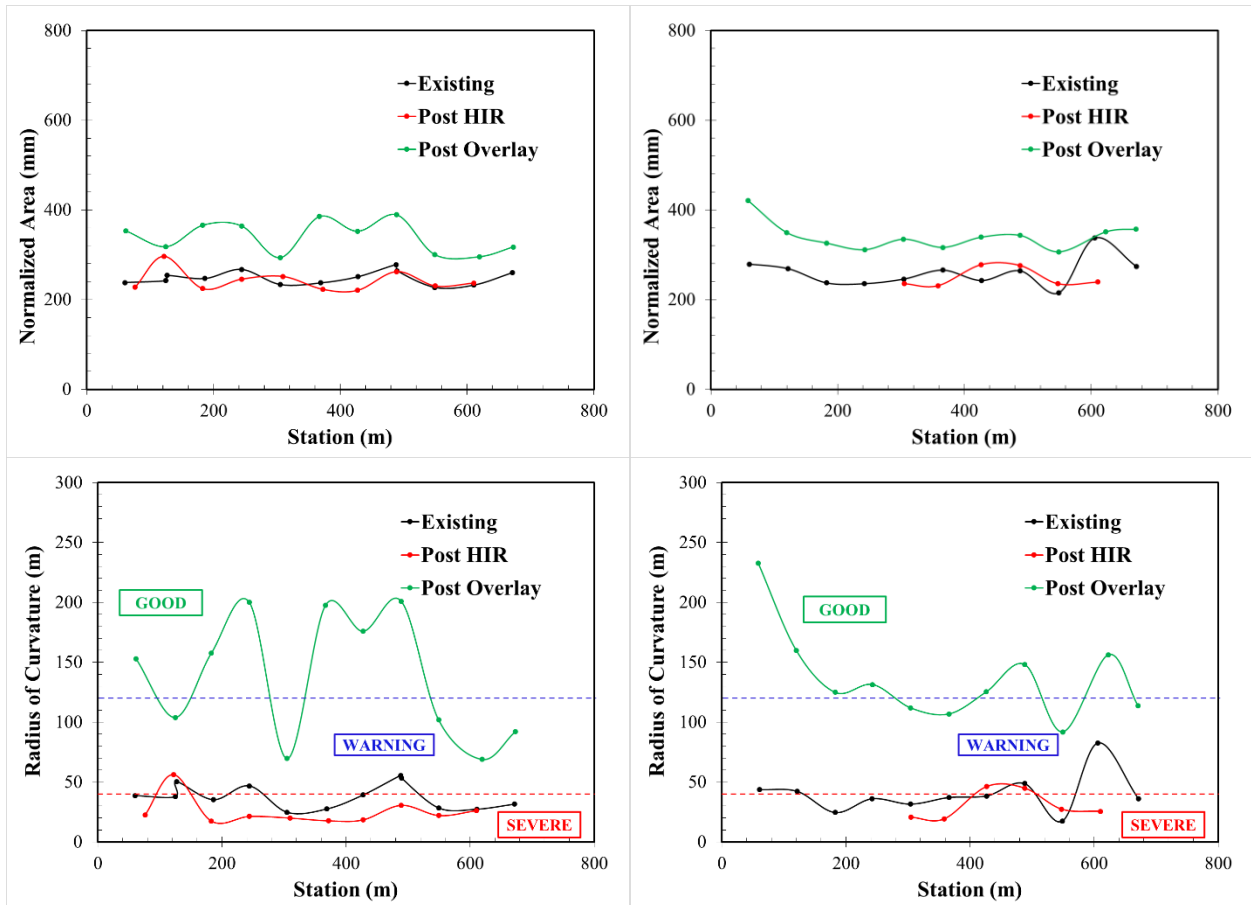


Figure 3-17 Deflection parameters and their severity for east bound (left) and west bound (right) for the inner lane, Galesburg, IL (Appendix B)

3.3.2 Machesney, IL

The variation of the selected parameters from deflection basins as a result of FWD testing is shown in Figures 3-18 through 3-20. The values indicate a reduction in the structural capacity post-HIR whereas after the overlay application, it shows improvement as compared to the initial condition of the pavement.



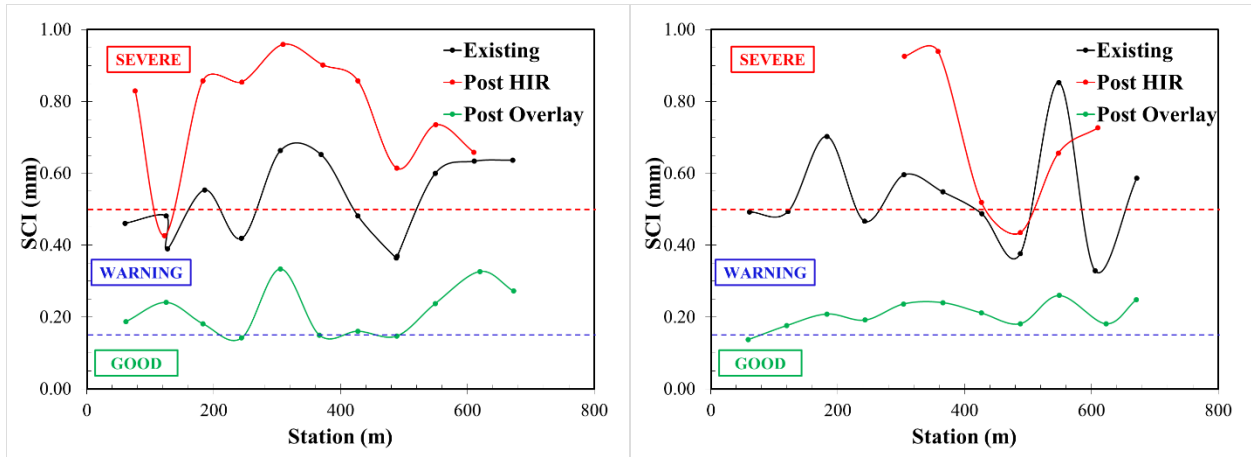
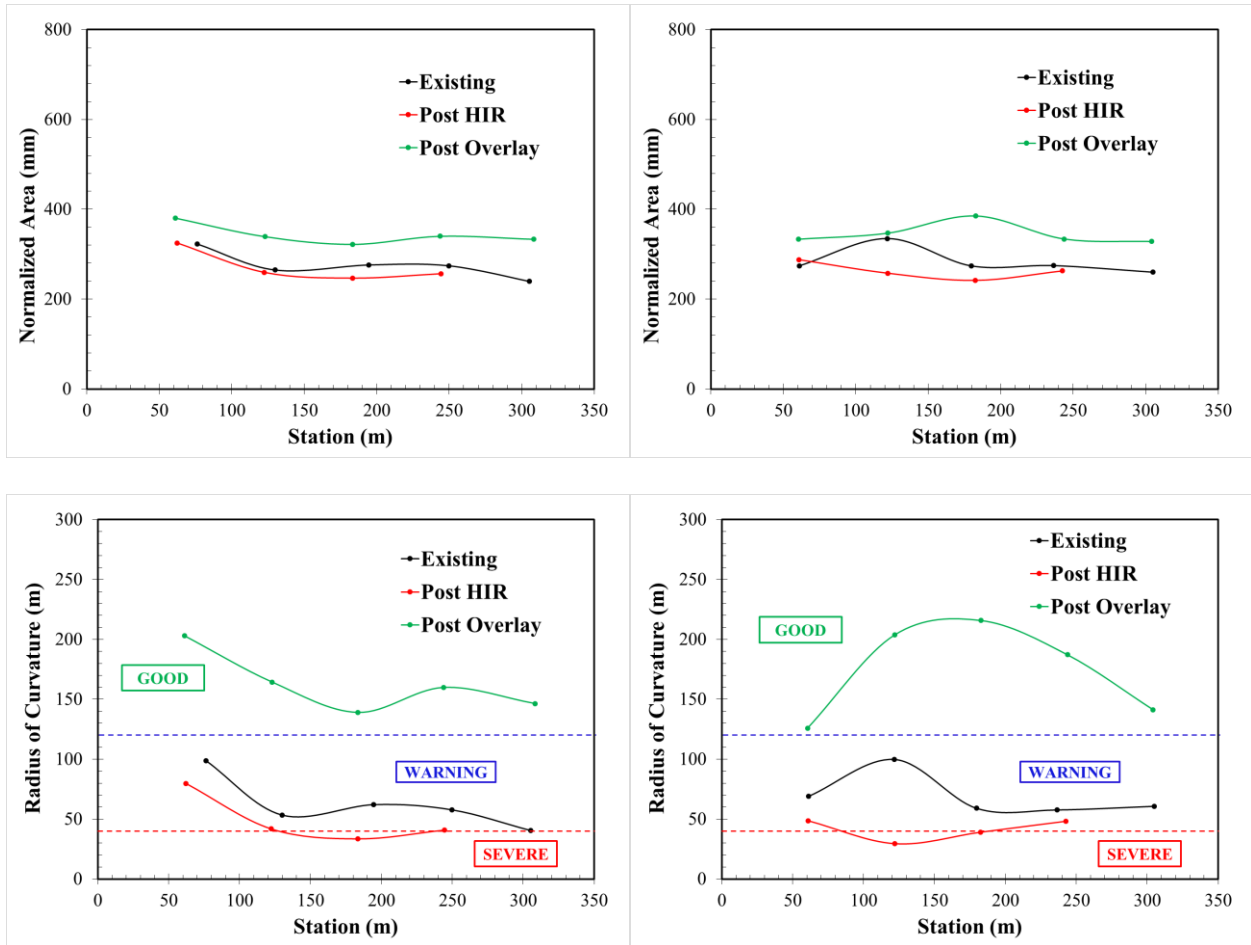


Figure 3-18 Deflection parameters and its severity for east bound (left) and west bound (right) for Section – 4-5-6-7 Machesney Park, IL (Appendix B)



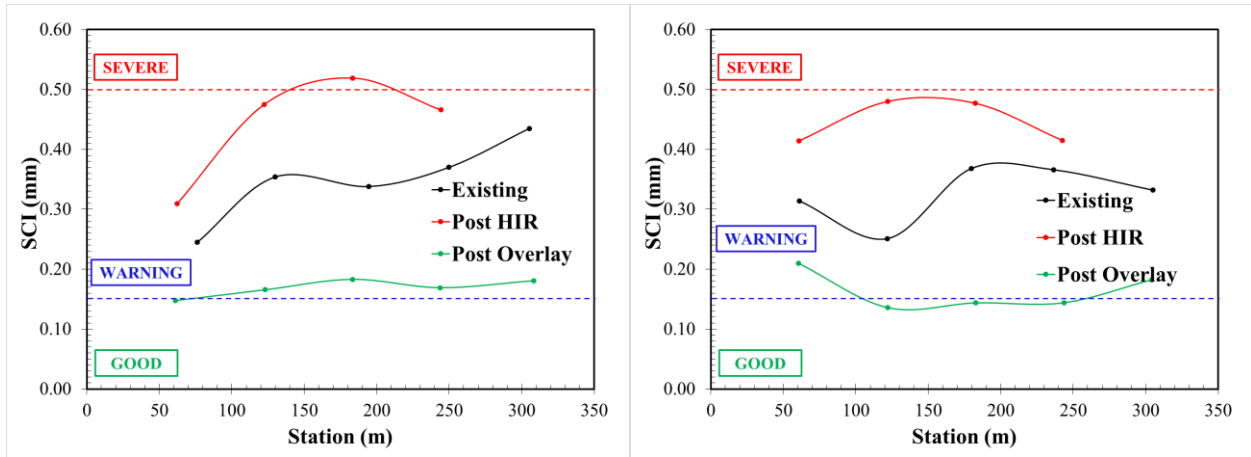
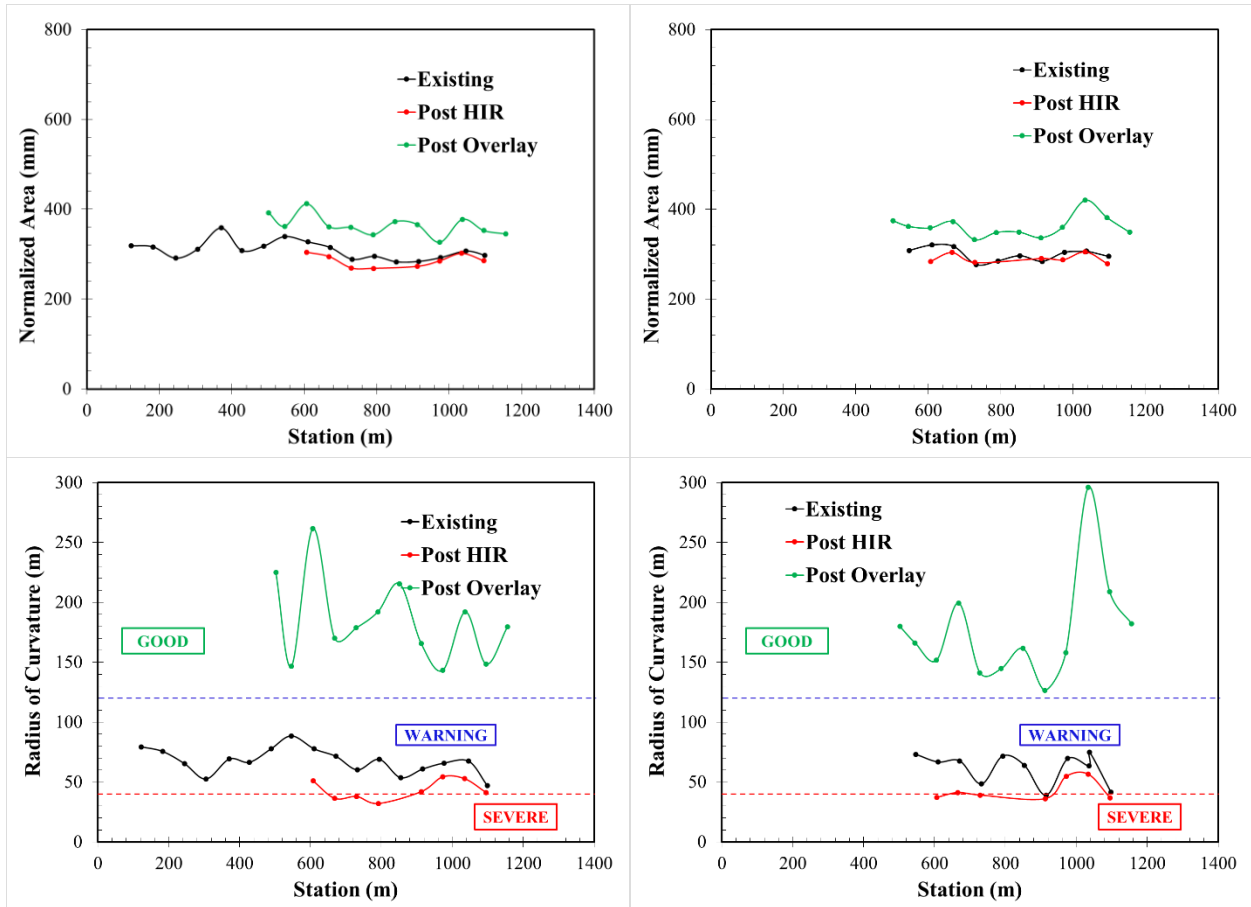


Figure 3-19 Deflection parameters for east bound (left) and west bound (right) for Section – 8-9 of Machesney Park, IL (Appendix B)



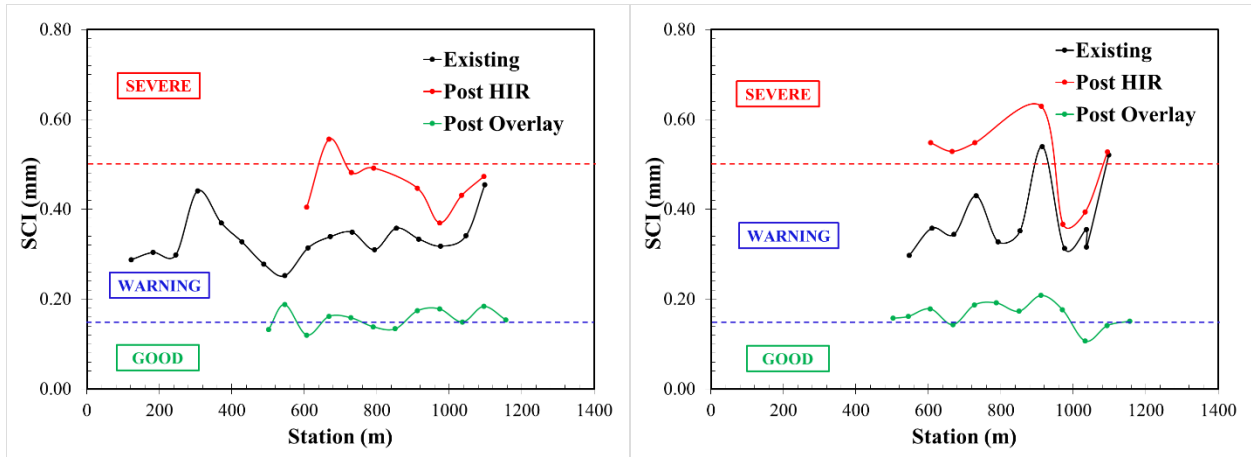
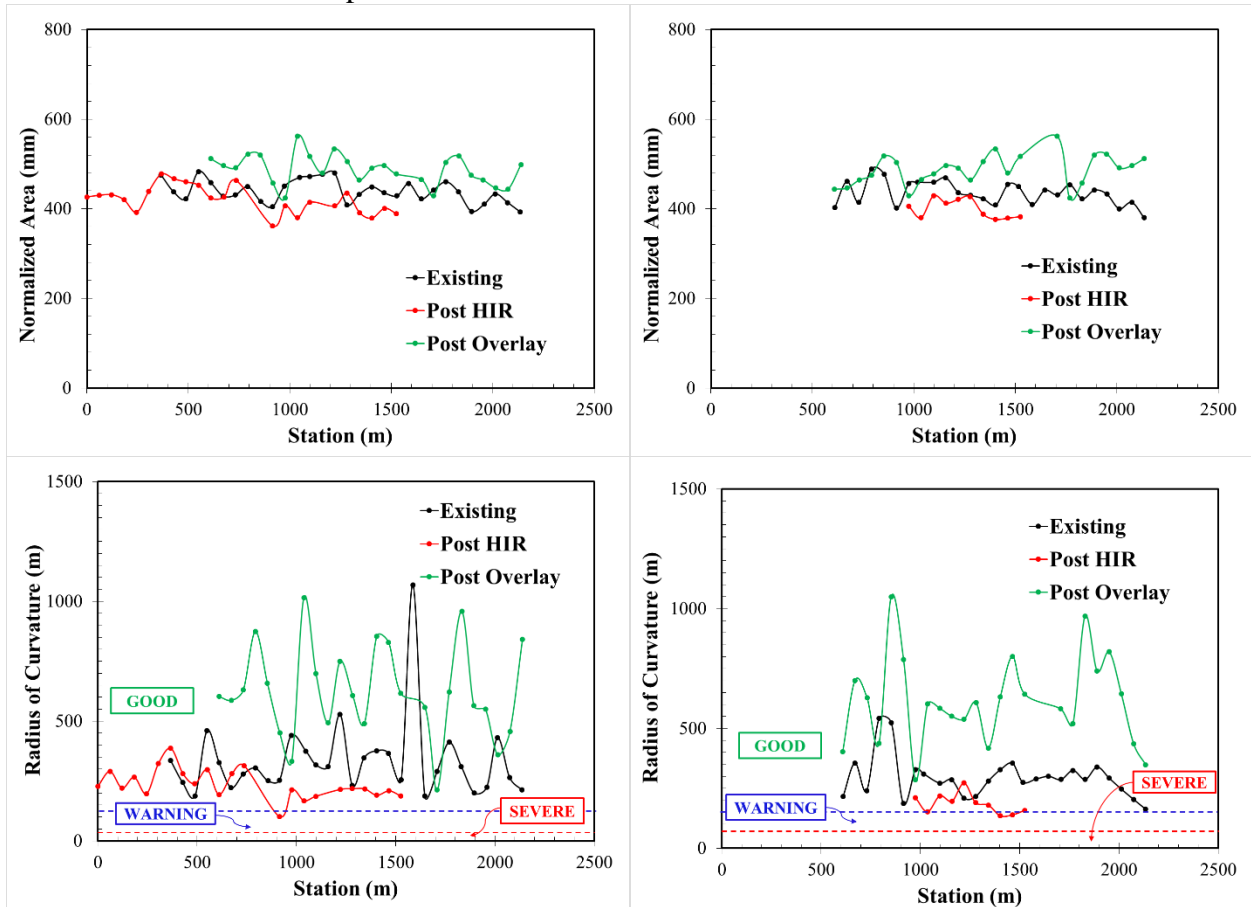


Figure 3-20 Deflection parameters for east bound (left) and west bound (right) for Section – 15-16-17-18 of Machesney Park, IL (Appendix B)

3.3.3 Dyer, IN

The variation of the selected parameters from deflection basins resulted from FWD testing for the Dyer section is shown in Figure 3-21. The values indicate a reduction in the structural capacity post-HIR whereas after the overlay application it shows improvement as compared to the initial condition of the pavement.



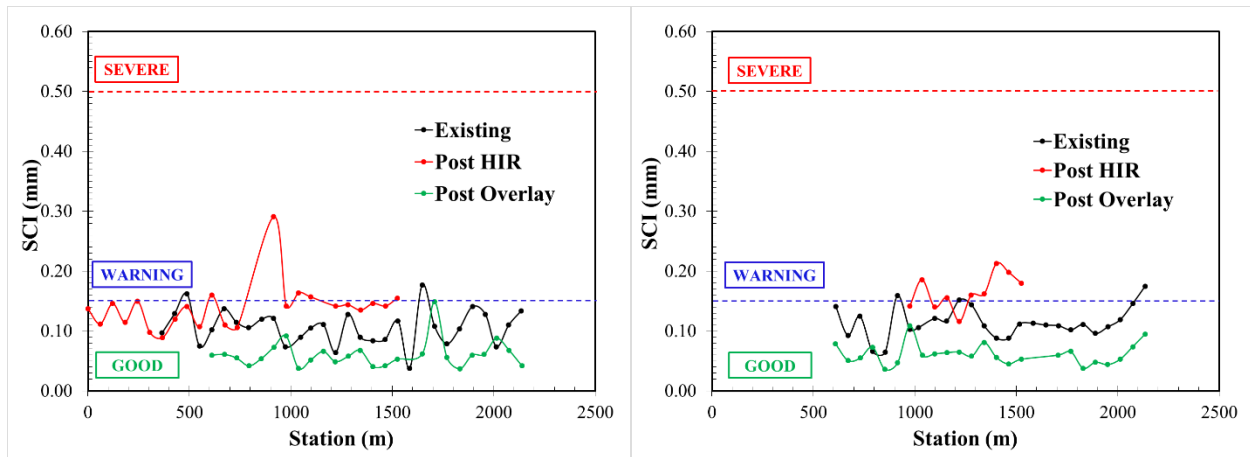


Figure 3-21 Deflection parameters and its severity for east bound (left) and west bound (right) for Dyer, IN (Appendix B)

3.4 INTERNATIONAL ROUGHNESS INDEX (IRI)

IRI is a measure of roughness commonly used in project- and network-level condition assessment of pavements. It is measured in m/km. IRI measurements were conducted as per ASTM E1926-08(2015). IRI measurements for speeds lower than 24 km/hr should be avoided since it results in instant jumps in IRI because of braking effect. Therefore, IRI measurements for the sites located in residential areas posed some challenges in this study.

Roughness was measured for Galesburg and Machesney and the units reported are in/mi. The measurement was performed before HIR (BH), post-HIR (AH) and post-overlay (AO). The post-overlay condition was two years after the rehabilitation. The data was collected every 0.3 m interval. The data presented is averaged at every 7.6 m. This allows obtaining a representative IRI for the section and at the same time to remove the unrealistic peaks occurring from sudden breaks and slow down. Furthermore, the data was filtered for speed lower than 24 km/hr. In addition, the significantly high IRI values were considered as outliers and filtered out. This eliminated the unusual IRI readings occurring in the analysis. Figure 3-22 illustrates the original data and filtered data. The filtered results for the individual sites are discussed in the section below.

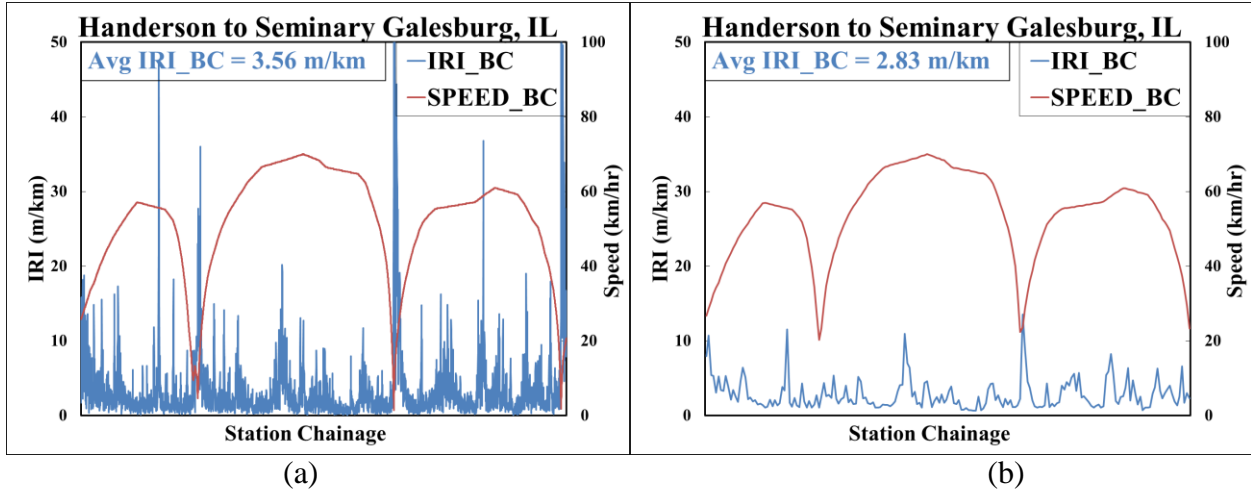


Figure 3-22 IRI data before filtering (a) and IRI data after filtering (b) with velocity profile

3.4.1 Galesburg, IL

Figure 3-23 shows eastbound (Handerson to Seminary) and westbound (Seminary to Handerson) IRI in m/km. The results show that HIR improves IRI compared to existing condition but it is still higher as compared to a newly constructed pavement. Initial IRI is about 2.68 m/km and is improved to around 2.05 m/km.

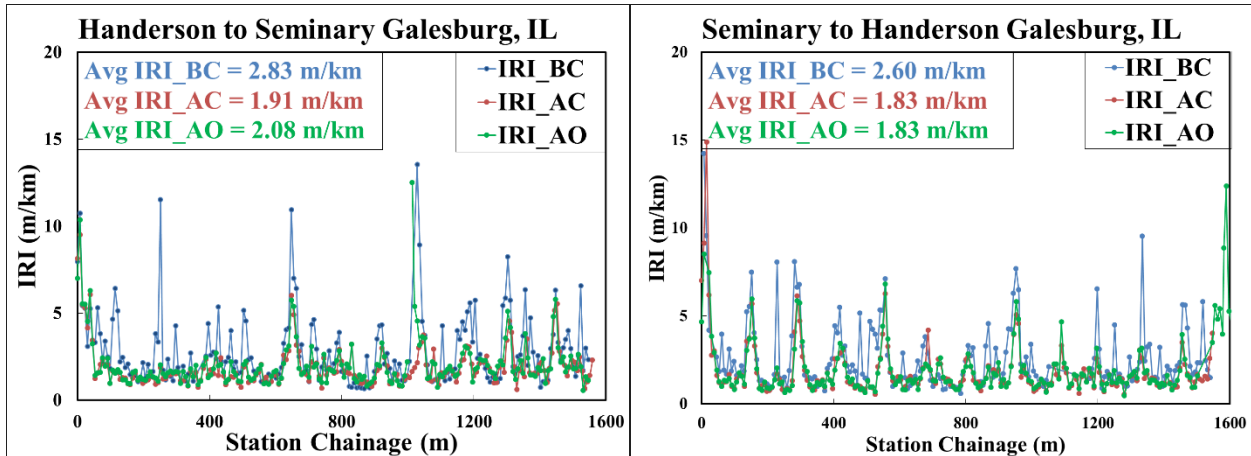
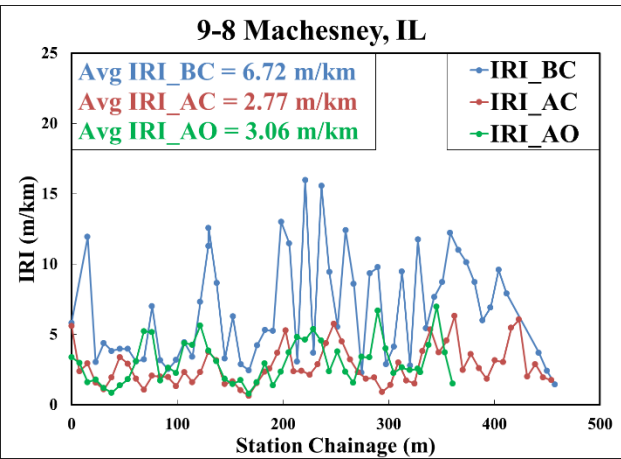
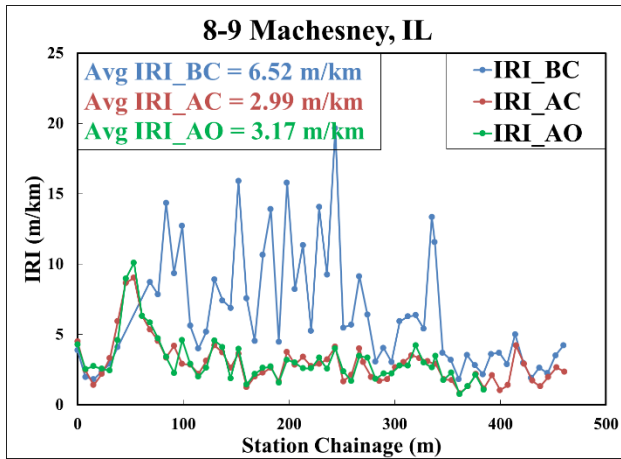
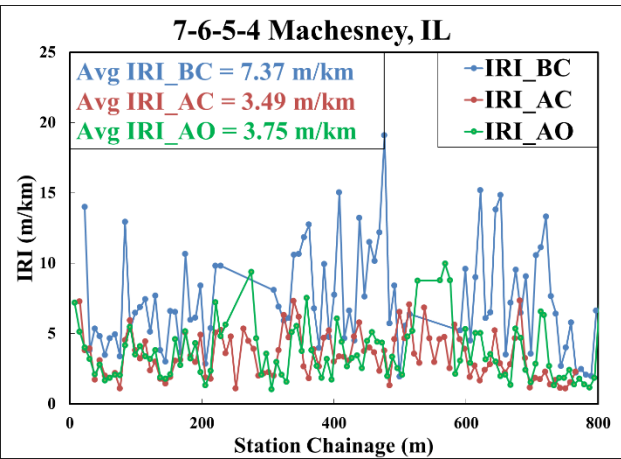
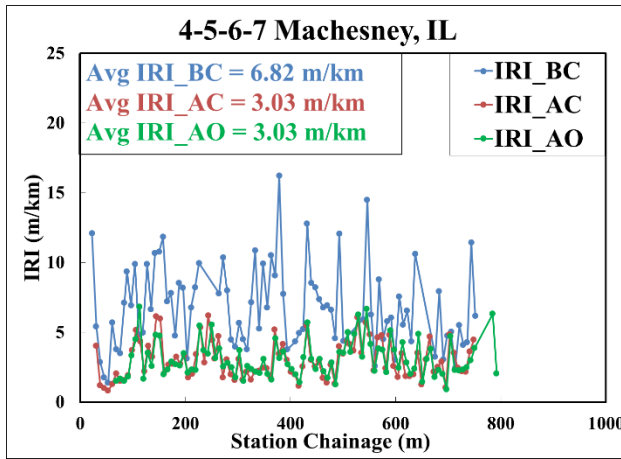
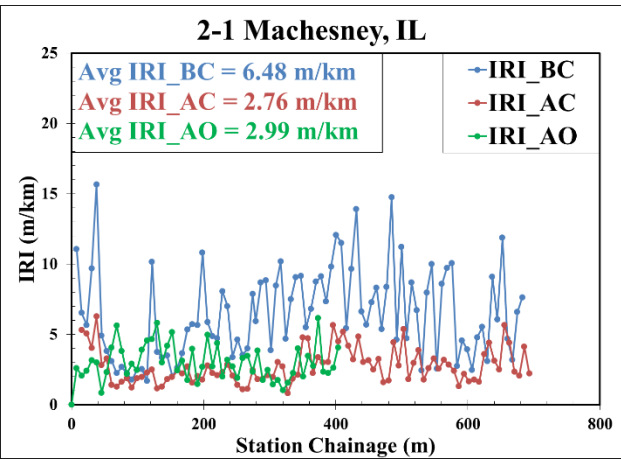
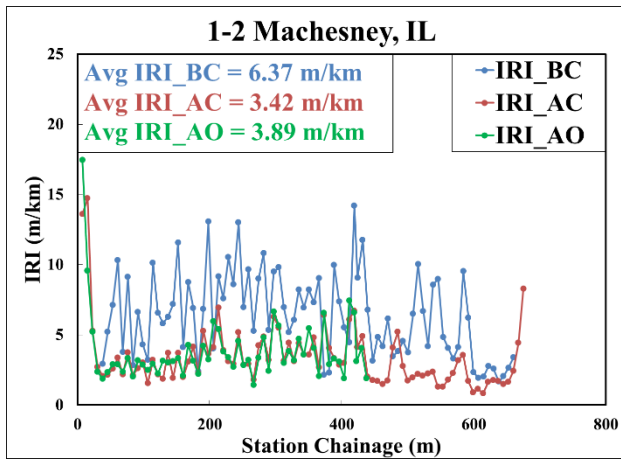


Figure 3-23 IRI data for Galesburg before, post-HIR, and post-overlay

3.4.2 Machesney, IL

Figure 3-24 shows IRI in in/mi for different sections of Machesney. The results show that HIR improves IRI as compared with existing conditions; but it is still higher compared to a newly constructed pavement. The section was extremely rough before the HIR as it can be seen from Figure 3-24. Machesney was divided into smaller sections and the IRIs ranged from 4.96 – 7.35 m/km from the initial condition to 2.64–3.75 m/km after the HIR.



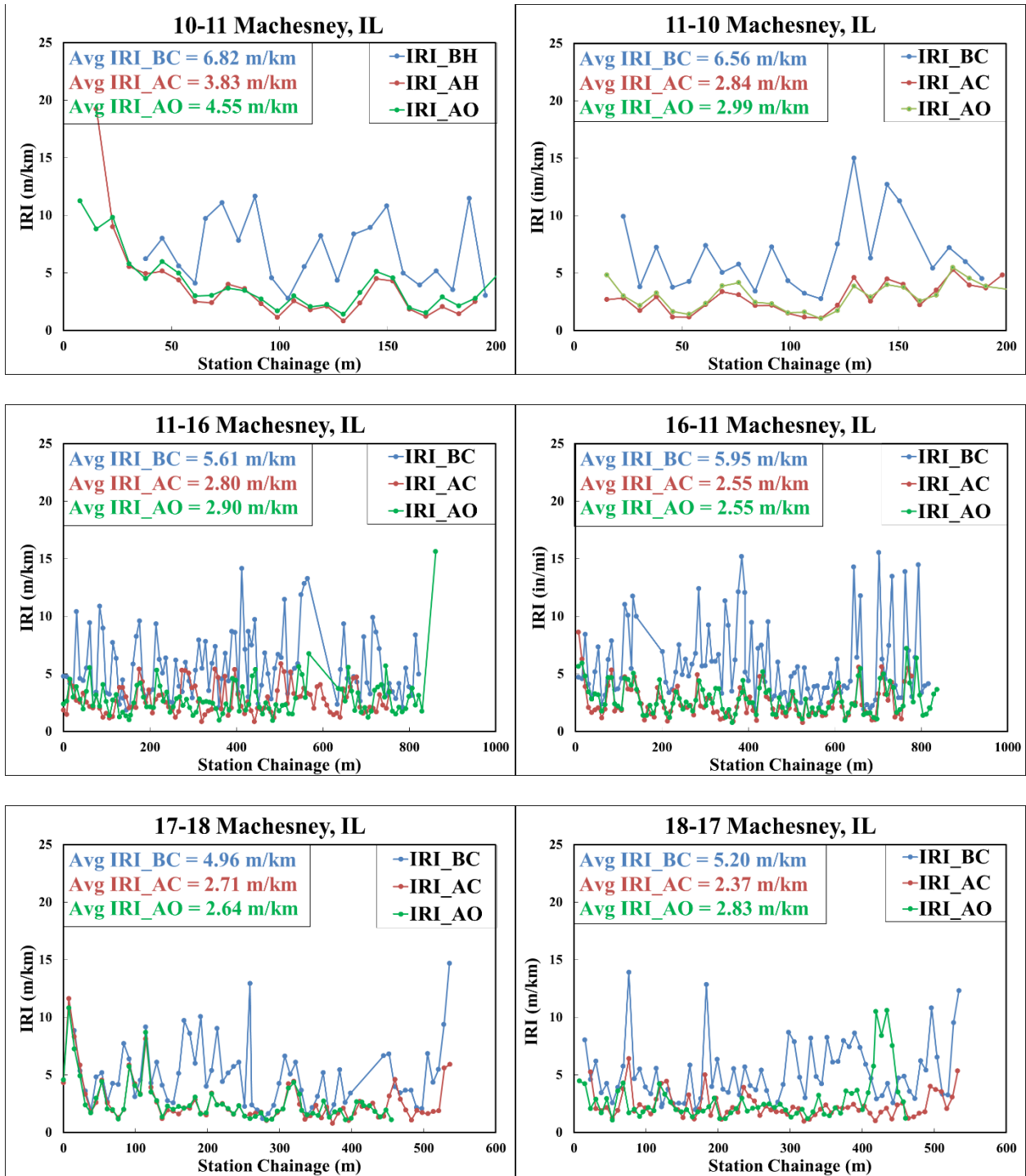


Figure 3-24 IRI data for different sections of Machesney before, post-HIR, and post-overlay

3.5 SUMMARY

In this chapter, the three sites, evaluated in this thesis, were introduced. Each project details, construction, and field tests were presented. Two different HIR trains were used in the sites for heating, scarifying, and paving. HIR treated layers were overlaid as part of a separate contract took place in the following weeks after HIR application.

According to the visual survey and CRS calculations, the three sites were considered to be in poor condition prior to the HIR treatment. The deflection basin parameters yielded very useful information. The area parameter categorized the pavement structure of Galesburg and Dyer into medium AC while Machesney into thin AC as per Table 3-8. The results were verified with the field core data. FWD parameters RoC and SCI showed that overlay application improved the structural capacity of the upper layer of the pavement. The improvement was significant in case of Machesney Park while it was marginal in case of Galesburg and Dyer. Hence, repaving was the appropriate selection. Roughness measurements showed significant improvements of around 30-100% from the initial condition to post-HIR condition. This should be followed by periodic long-term monitoring to evaluate the change in IRI over the years. The final values of IRI were still higher those of the newly built conventional pavements. The average IRI values for Galesburg improved from roughly 2.68 m/km to about 2.05 m/km while for Machesney the improvement was roughly from 6.31 m/km to 2.78 m/km.

CHAPTER 4 - LABORATORY INVESTIGATION

Laboratory characterization at both AC mixture and binder levels was conducted to understand the properties of the recycled AC mixture. Samples collected from test sites before and during the HIR treatment was used for various laboratory tests. Mixture volumetric studies were carried out based on material extraction and volumetric analysis. The materials were extracted using centrifuge extractor and RotoVap extraction device to check aggregate gradation and recovered binder. The recovered binder was further used for binder-level testing.

4.1 MIXTURE DESIGN AND VOLUMETRIC CHARACTERISTICS

It is important to have accurate mixture design parameters such as voids in mineral aggregates (VMA), voids filled with asphalt (VFA), air voids (AV), N-Design and total asphalt content in the design of AC mixtures. In order to obtain these parameters for field-sampled loose materials, RotoVap in combination with a centrifuge extractor were used to extract the asphalt binder and determine its content.

To establish the AC mixture design, splitting and quartering of the field-sampled materials were done using ASTM C702 specification. Superpave mix design was used in the study. Mix design trials were performed to obtain the target air voids of 4% for a specimen height of 115 mm using a Superpave gyratory compactor. The resultant number of gyrations were selected as the N-Design for the AC mixes. Two samples measuring roughly 1500 g of material were split and quartered for the calculation of theoretical maximum specific gravity (G_{mm}) as per ASTM D2041/ AASHTO T209. The specification used to measure the bulk specific gravity (G_{sb}) of the mix was ASTM D2726/ AASHTO T166. The compacted AC test specimens had $7 \pm 0.5\%$ target air voids.

Binder was extracted using a combination of centrifuge extraction (ASTM D2172/ AASHTO T164) followed by solvent extraction (ASTM D1856/ AASHTO T319) using a RotoVap as shown in Figure 4-1. The extracted binder was used for characterizing binder properties as per the tests mentioned in the following section. The extracted material was sieved to identify the AC mix aggregate gradation in accordance with ASTM D5444/ AASHTO T30 and detailed calculation is presented in Appendix C.



(a)



(b)

Figure 4-1 Centrifuge Extractor (a) and RotoVap (b) for binder extraction

4.1.1 Aggregate Gradation

Aggregate forms the major part of the total AC mixture composition. It is approximately 85% by volume and around 95% by weight in the AC mixture. Hence, aggregate properties and gradation play an important role in AC mixture performance. Samples used to determine G_{mm} were extracted to obtain the aggregate gradation. Figure 4-2 shows aggregate gradation of the sampled material. Table 4-1 shows the extracted aggregate gradation and Nominal Maximum Aggregate Size (NMAS) for each section (marked as blue).

Table 4-1 Extracted aggregate gradation for different pilot sections (Appendix C)

Sieve Size	Sections				
	Galesburg Outer Lane	Galesburg Inner Lane	Machesney 15-16	Machesney 17-18	Dyer
1" (25 mm)	100.0	100.0	100.0	100.0	100.0
3/4" (19.5 mm)	100.0	100.0	96.6	89.5	100.0
1/2" (12.5 mm)	99.6	99.2	79.9	72.4	100.0
3/8" (9.5 mm)	92.9	91.2	70.8	62.4	95.1
#4 (4.75 mm)	58.0	56.8	40.2	35.5	58.3
#8 (2.36 mm)	35.2	35.2	23.7	23.4	41.3
#16 (1.18 mm)	26.9	28.1	17.3	19.9	32.9
#30 (600 μ m)	21.3	23.2	13.1	16.4	26.1
#50 (300 μ m)	12.9	14.6	9.1	8.5	16.4
#100 (150 μ m)	7.9	9.0	7.0	5.2	10.4
#200 (75 μ m)	5.8	6.6	5.4	3.9	7.3

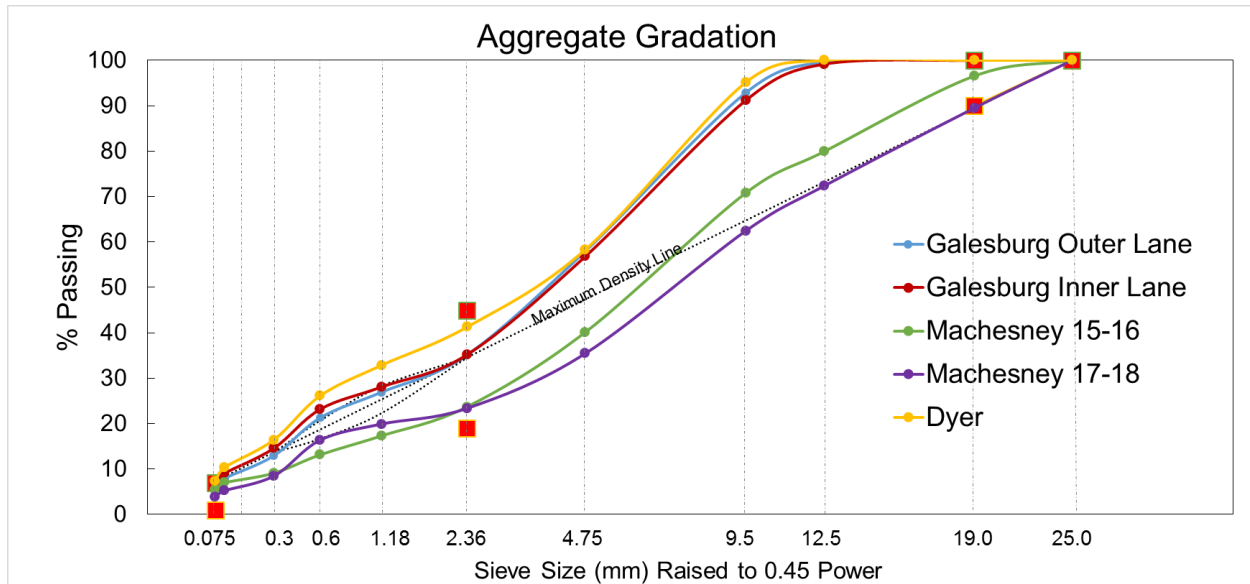


Figure 4-2 Extracted aggregate gradation

4.1.2 Mix Design Volumetrics

The extraction results gave the binder content for the materials obtained from the various sections as shown in Table 4-2.

Table 4-2 Volumetric details of recycled AC mixtures sampled from the various tested sections (Detailed volumetric information is provided Appendix D)

Sections	% AC	NMAS (mm)	G _{mm}	G _{mb}	% Air Voids	Height Compacted (mm)	No. of Gyrations
Galesburg Outer Lane	5.00	9.5	2.522	2.432	3.6	115.00	28
Galesburg Inner Lane	5.21	9.5	2.505	2.397	4.3	114.87	17
Machesney 15-16	4.78	19.5	2.558	2.476	3.2	115.00	150
Machesney 17-18	4.15	25	2.547	2.464	3.2	115.00	182
Dyer	5.48	9.5	2.516	2.409	4.2	114.98	62

4.1.3 Results and Discussion

The aggregate gradation for the AC mixes is classified as well graded. The gradation result for Galesburg and Dyer were close to each other; with the NMA S is 9.5 mm. The HIR samples (with rejuvenators) showed a total binder of 5% for Galesburg outer lane and 5.48% for Dyer. Machesney had coarser gradation than the other two sites with lower binder content of the order of 4.15% and 4.78% for sections 17-18 and 15-16, respectively. The NMA S for Machesney was 19.5 mm and 25.4 mm for the 15-16 and 17-18 sections, respectively.

4.2 BINDER-LEVEL TESTING

Binders were recovered through extraction and were used for Superpave PG determination as well as their time and temperature dependent modulus properties using the frequency sweep tests.

4.2.1 Performance Grade (PG) Determination

Binder characterization for the extracted binders was done using DSR and BBR for PG determination and frequency sweep test using DSR to develop the master curves for complex modulus and the phase angle. The test results of the extracted binders from various HIR sections are presented in the following sections.

4.2.2 Dynamic Shear Rheometer (DSR)

Tests in accordance with ASTM D7175/ AASHTO T315 specification for DSR was used for high temperature grade determination for the unaged binder. The recovered binder was obtained after short-term aging (heated during mixing and construction), but it was rejuvenated at the same time. Therefore, to identify the binder grade, RTFO aging criteria was used to determine the binder grade. ASTM D6373 was used as a reference to determine the PG grade. A parallel plate of diameter 25 mm at 1 mm gap was used and the test was performed at a frequency of 10 rad/s and a strain rate of 12%. The test setup is shown in Figure 4-3. The results of PG for the various test sections are presented in Table 4-3 using dynamic shear criteria.



Figure 4-3 Dynamic shear rheometer

Table 4-3 High temperature performance grade based on dynamic shear for field-aged binder installed at various sections

Section	Sample ID	Dynamic Shear (in Pa)							
		>2200 Pa							
Temperature (in °C)		40	46	52	58	64	70	76	82
Galesburg Outer Lane	S1			4962	2220	1011			
	S2			5138	2371	1074			
Galesburg Inner Lane	S1			14360	6516	2936	1334		
	S2				6025	2741	1282		
Machesney 15-16	S1		1329						
	S2		1404						
Machesney 17-18	S1		5260	2562	1258				
	S2			2484	1273				
Dyer	S1					18200	8032	3730	1798
	S2						7462	3577	1714

4.2.3 Bending Beam Rheometer (BBR)

Bending Beam Rheometer (BBR) was used to determine the low temperature grade as per ASTM D6648/ AASHTO T313 guidelines (Figure 4-4). A beam measuring 127 x 6.35 x 12.7 mm was loaded at a test load of 980 mN and was loaded for 240 sec. The stiffness and m-value were obtained at 60 sec and used in the analyses. Table 4-4 shows the summary of results from BBR test. The binder grade obtained from the DSR and BBR results are presented in Table 4-5.



Figure 4-4 Bending Beam Rheometer

Table 4-4 Low temperature binder grade based on stiffness at 60 sec and m – value for different test sections (Appendix E)

Section	Temperature (°C)	Stiffness @ 60 s(MPa)	m-Value
Galesburg Outer Lane	-30	169.3	0.337
	-36	317.0	0.300
Galesburg Inner Lane	-24	131.7	0.335
	-30	258.3	0.290
Machesney 15-16	-36	78.7	0.365
	-38	254.7	0.315
Machesney 17-18	-36	162.3	0.323
	-40	184.5	0.216
Dyer	-18	129.0	0.307
	-24	259.0	0.267

$\Delta T_{critical}$ spread, a parameter obtained from BBR, is used to evaluate brittleness of the asphalt binder. The following equation was used to calculate the critical spread:

$$BBR \Delta T_{critical} = PG_{(Stiffness)} - PG_{(Creep)} \quad (4-1)$$

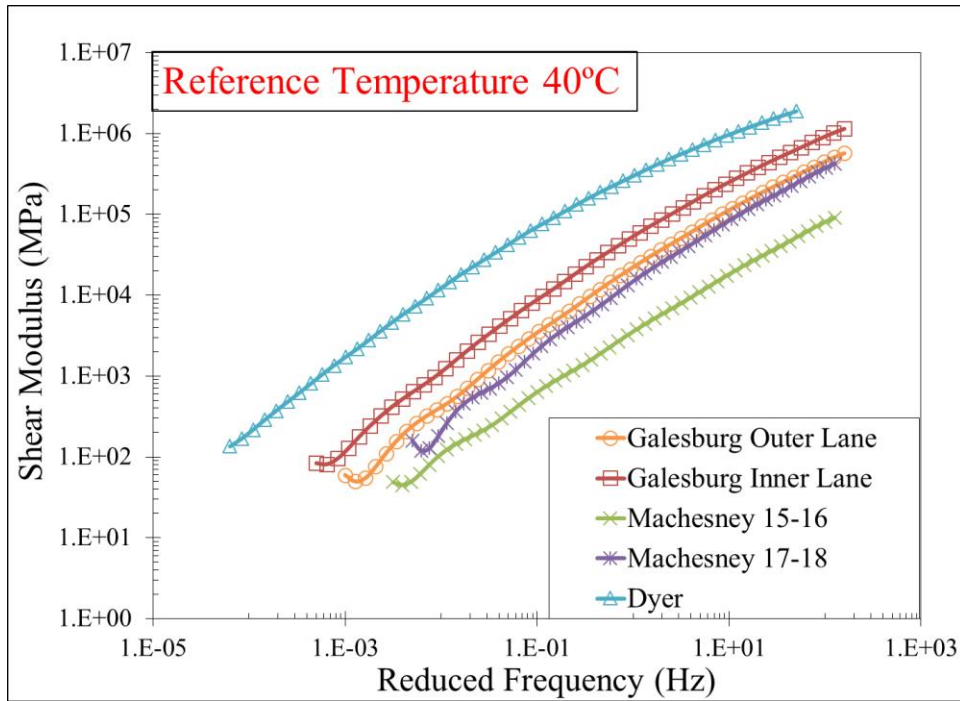
The binders with a value of $\Delta T_{critical}$ less than -5°C are expected to behave as brittle and may the AC mix used that binder may experience pavement thermal cracking. The values of $\Delta T_{critical}$ were calculated and are presented in the Table 4-5.

Table 4-5 Performance Grade and BBR ΔT critical spread based on stiffness and m- value for different sections (Values calculated using data provided in Appendix E)

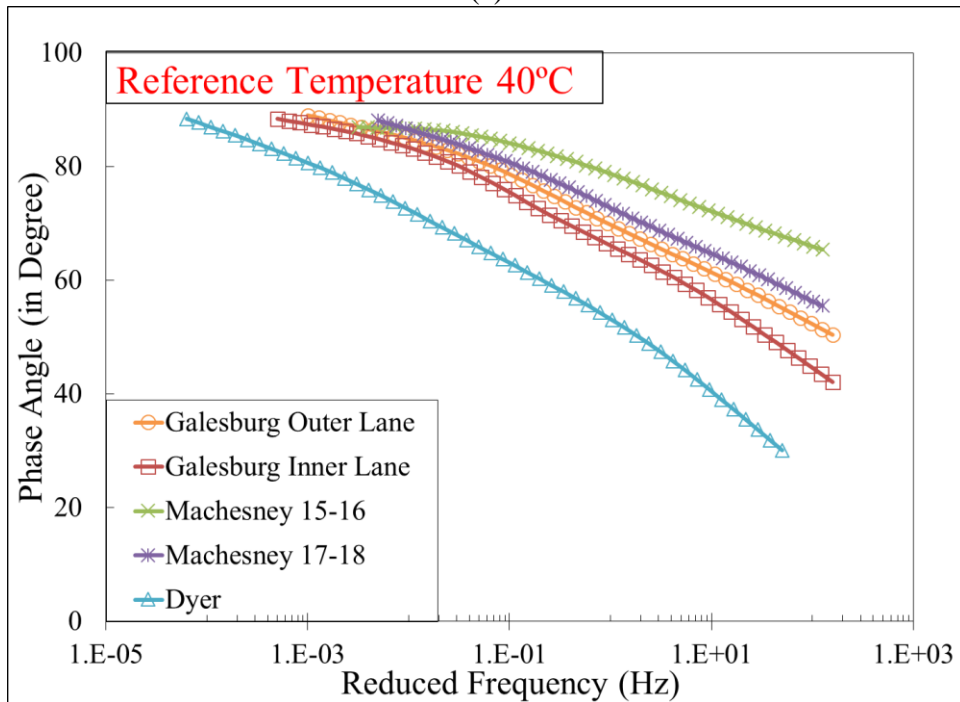
Section	Performance Grade	$\Delta T_{critical}$ Spread (°C)	PG (Stiffness)	PG (m-Value)
Galesburg Outer Lane	PG 58-40	0.5	-35.3	-35.8
Galesburg Inner Lane	PG 64-34	-3.3	-32.0	-28.7
Machesney 15-16	PG 40-46	-0.1	-38.5	-38.6
Machesney 17-18	PG 52-46	-23.8	-60.8	-36.9
Dyer	PG 76-28	-6.7	-25.9	-19.1

4.2.4 Frequency Sweep Test

Time and temperature dependency of the extracted binder was determined using a frequency sweep test ranging from 0.16 to 16 Hz over various temperatures ranging from 30°C up to 88°C at constant strain of 4% using the DSR. Master curves were generated for shear modulus and the phase angle at a reference temperature of 40°C with reduced frequency. Two replicates corresponding to each section were tested. Figure 4-5 shows various plots obtained from different sections with reduced frequency (logarithmic scale) in x-axis, and shear modulus (logarithmic scale) and phase angle (linear scale) on y-axis.



(a)



(b)

Figure 4-5 Frequency sweep plots for Shear Modulus (a) and Phase angle (b) at 40°C reference temperature

4.2.5 Results and Discussion

Binder testing showed that Machesney 15-16 section had the softest binder after rejuvenation while the binder for Dyer was the stiffest among all. Even within the individual sites, Galesburg

inner and outer lanes differed by one PG grade both at high and low temperatures, which suggests variability in rejuvenation application, existing material in the pavement prior to recycling and/or the variation in degree of heating for pavement scarification. The binder grades achieved after milling and rejuvenation had a wide spectrum with some binders ranging from PG 40-46 to PG 76-28. Since treatment design and construction did not differ among the section, such differences in the material properties would have implications on the pavement performance of the rehabilitated sections. The frequency sweep analysis followed the trend of PG grade obtained, with Machesney 15-16 being the softest with highest phase angles at specific frequency and Dyer being the stiffest showing lowest phase angles at the same frequency. A clear distinction between the AC mixes with respect to binder shear modulus and phase angles plotted against reduced frequency can be derived from Figure 4-5.

4.3 MIXTURE LEVEL TESTING

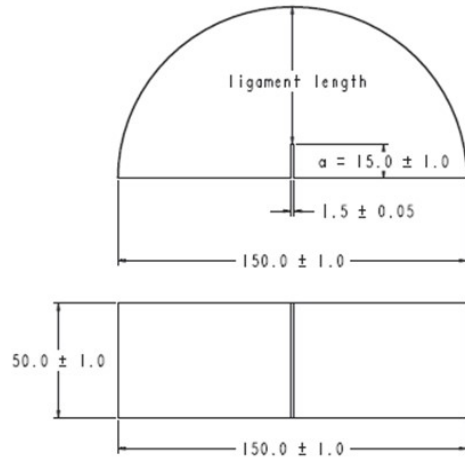
Asphalt concrete mixture is a heterogeneous material composed of binder, aggregates and air voids. A mixture performance is therefore extremely dependent on these parameters. Performance can be improved by fine-tuning these parameters to obtain a good performing mix resisting permanent deformation and cracking. This section evaluates the performance of the recycled AC mixture and compacted on the sites. Illinois Flexibility Index test (I-FIT) and Hamburg WTT were used to characterize the low temperature cracking potential and rut resistance for the various test mixtures, respectively. The results obtained from these tests will allow for further improvement of the AC mix, to achieve desired performance, by modifying volumetric properties or selecting a different rejuvenator.

4.3.1 Illinois Flexibility Index Test (I-FIT)

The Illinois Flexibility Index Test (I-FIT) was used to determine the fracture energy and flexibility index (FI) of AC mixtures obtained from different sites. The I-FIT is a load line displacement controlled test with a monotonic load applied along the vertical diameter of the specimen at a displacement rate of 50 mm/min at 25°C. Fracture energy is defined as the area under the load displacement curve normalized by the area of crack propagation. The test was conducted in an environmental chamber using a custom-designed semi-circle beam (SCB) fixture that was placed in a servo-hydraulic asphalt-testing machine as shown in Figure 4-6. Load cells with capacity of 97.8 kN was used for this test to measure the fracture load. The I-FIT fracture test was conducted at an intermediate temperature based on the standard protocols developed recently in ICT study R27-128, “Testing Protocols to Ensure Performance of High Asphalt Binder Replacement Mixes Using RAP and RAS.” (Al-Qadi et al., 2015)



(a)



*All the dimensions are in millimeters

(b)

Figure 4-6 I-FIT specimen, configuration (a), and geometry of specimen and fixture (b) with an external LVDT (Ozer et. al, 2016)

The I-FIT specimens were fabricated from 150 mm diameter gyratory-compacted specimens. The test pills were compacted at 150°C. Two slices of thickness 50 mm were cut from the middle of the specimen as illustrated in Figure 4-7. The slices were further halved and notched to produce four test specimens per 180 mm high gyratory-compacted specimen. Specimens were dried after fabrication for 24 hrs using an electric fan. Dried specimens that were tested at 25°C were conditioned in an environmental chamber until reaching the targeted temperature. Temperature was monitored using a thermocouple embedded in a dummy specimen.

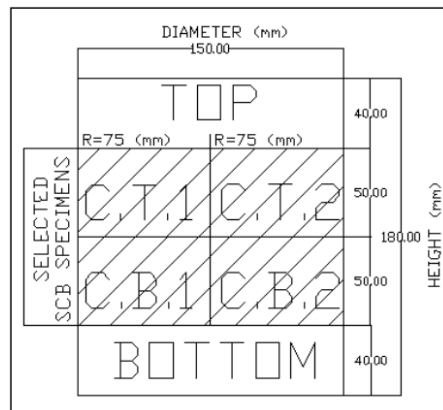


Figure 4-7 I-FIT specimen fabrication

The I-FIT parameters including fracture energy, peak load, the slope of the post-peak curve, and the slope's intercept with the x-axis were measured (Ozer et. al, 2015). In addition, the FI was calculated to understand the change in flexibility with different sections. The FI was calculated using the following equation:

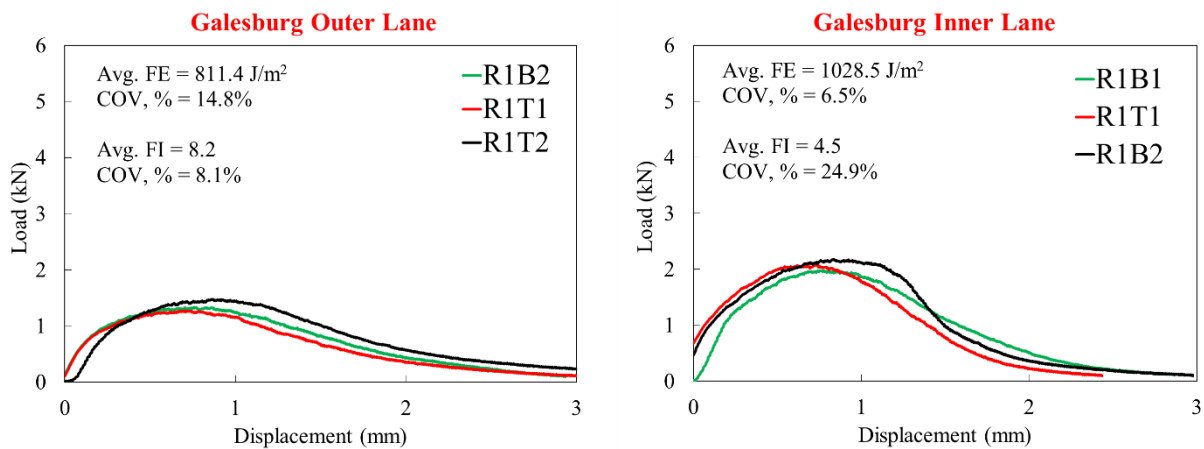
$$FI = A \times G_f / abs(m) \quad (4-2)$$

where G_f is fracture energy and reported in J/m^2 and m is slope of the post-peak curve of inflection point and reported as kN/mm . Coefficient A is a unit conversion factor and scaling coefficient. A is 0.01 in this study (Ozer et. al, 2015).

In this study, the I-FIT was conducted under the condition of short-term aging, where the AC mixtures were aged only during the production of the mix, and fabricated specimens were tested at $25^\circ C$. Figure 4-8 shows the load displacement curve from testing specimens fabricated from sections of Galesburg, Machesney, and Dyer, respectively. The I-FIT parameters, including fracture energy, peak load, the slope of the post-peak curve, and the slope intercept with the x-axis, were measured and are presented in Table 16. In addition, the FI was calculated to understand the change in flexibility for the various sections. The calculations are included in the Appendix F.1. Figure 4-9 compares the load displacement curves from different test sections.

Table 4-6 Result summary of I-FIT for the various test sections

Section	Fracture Energy (J/m^2)		Flexibility Index	
	Average	COV, %	Average	COV, %
Galesburg Inner Lane	1028.5	6.5	4.5	24.9
Galesburg Outer Lane	811.4	14.8	8.2	8.1
Machesney 15-16	360.6	8.8	4.1	7.7
Machesney 17-18	960.0	21.1	0.6	18.6
Dyer	1042.4	8.8	0.3	30.2



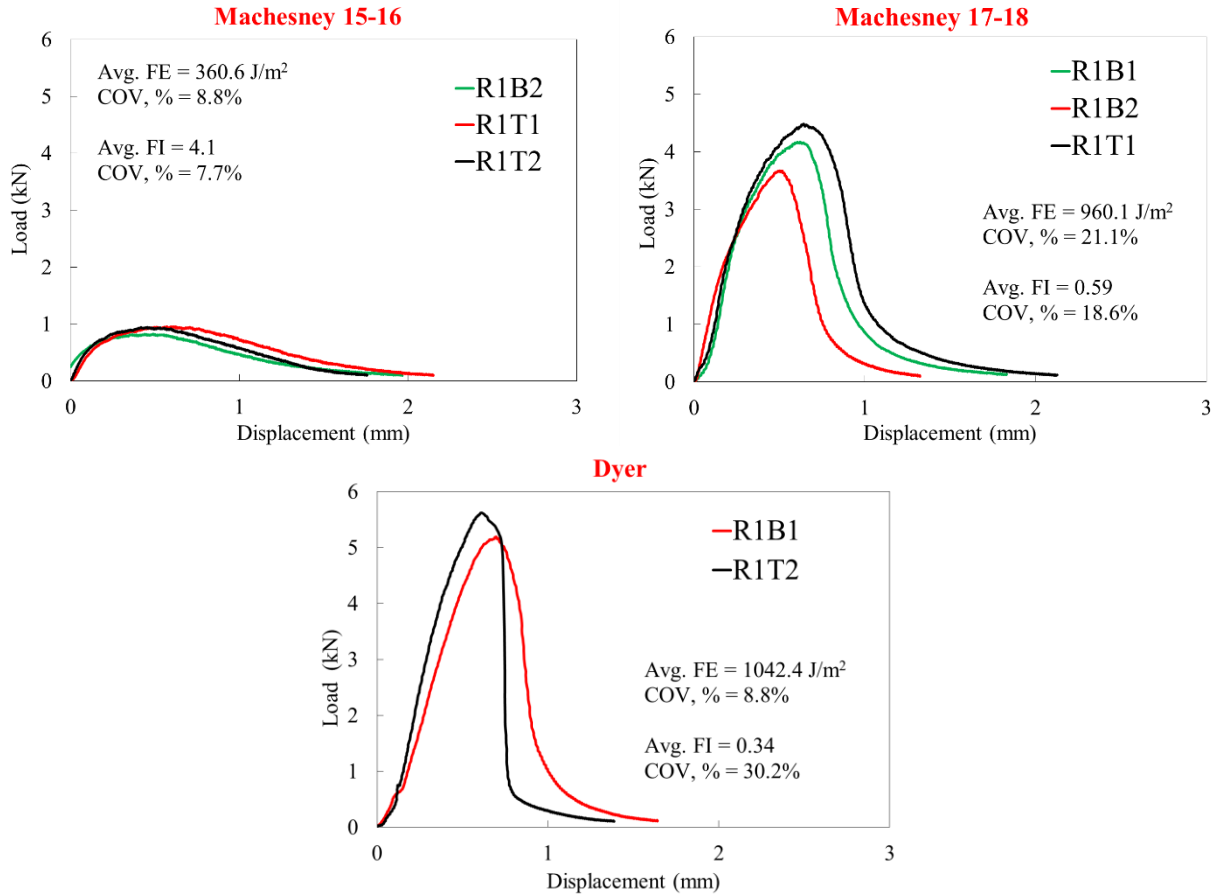


Figure 4-8 Load displacement curve from I-FIT fracture test for the test sections

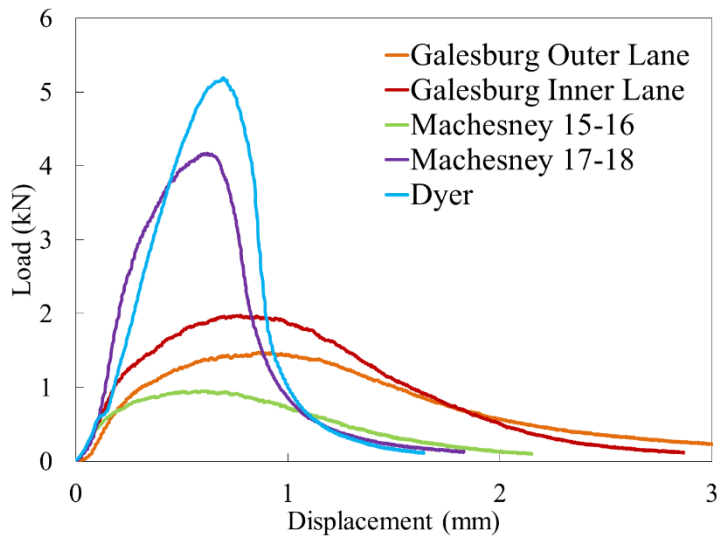


Figure 4-9 Comparison of load displacement curve for all test sections

4.3.2 Hamburg Wheel Track Test

The Hamburg wheel track test (WTT), performed as per AASHTO T324, was utilized to predict rutting potential of the field collected AC mixtures. The WTT is an electrically powered and is designed to run a 203.2 mm diameter, 47.0 mm wide steel wheel over the tested specimen. The apparatus has two wheels to accommodate testing two pairs of specimens at a time. Each wheel has a load of 705 ± 4.5 N, and passes about 52 ± 2 passes per minute across the specimen at a speed of 0.305 m/sec. Figure 4-10 shows the Hamburg WTT specimen mold and apparatus. Samples were tested while being submerged in water bath that had a temperature of 50°C. Twenty thousand passes were applied to the specimens and the failure criteria was based on the number of wheel passes corresponding to the 12.5 mm rut depth or depth of rut at 20000 passes, whichever is less. The rutting performance was evaluated with the final rut depth caused by the movement of the wheels on the specimens after a specific number of passes. The WTT system records the displacement at 11 locations on the specimen for each wheel pass. Permanent deformation curves were plotted using the data exported from the WTT system to characterize the rutting performance by showing the rut depth with respect to the increased number of wheel passes.

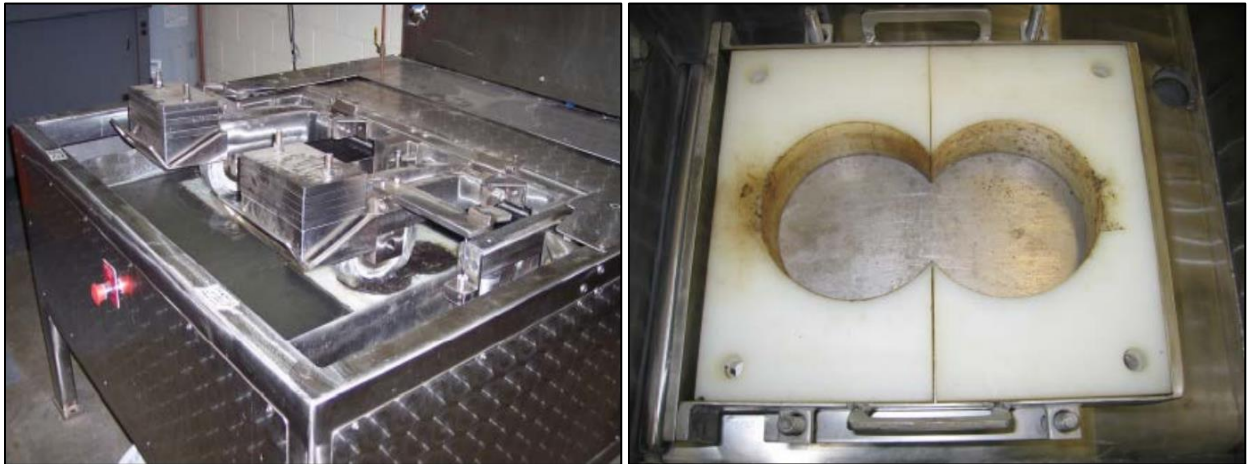


Figure 4-10 Hamburg Wheel Track Test equipment with testing molds

Figure 4-11 shows the specimens from the wheel track test and Table 4-7 shows rut depth corresponding to the wheel passes. Figure 4-12 illustrates the comparison of rutting potential for different sections over the entire period of the test.



Figure 4-11 From left to right specimens tested by Hamburg: Galesburg Outer Lane, Galesburg Inner Lane, Machesney 15-16, Machesney 17-18, Dyer, respectively

Table 4-7 Hamburg Wheel Track Results (Appendix G)

Section	Rut Depth (mm)	No. of Passes
Galesburg Outer Lane	12.5	11420
Galesburg Inner Lane	12.3	20000
Machesney 15-16	12.5	19840
Machesney 17-18	4.5	20000
Dyer	1.7	20000

* 1 in = 25.4 mm

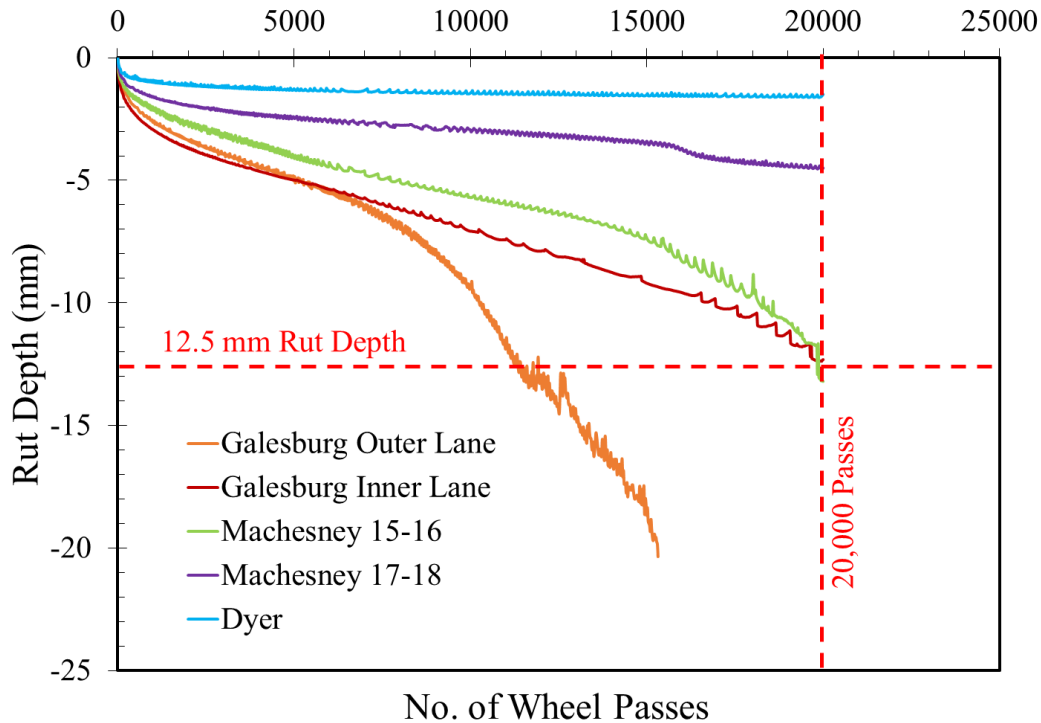


Figure 4-12 Rut depth as a function of number of wheel passes

4.3.3 Results and Discussion

Flexibility Index (FI) and Fracture Energy (FE) were calculated and FI was used as an indicator for potential cracking related damage. The value of the FI for Galesburg outer lane was highest and was lowest for Dyer, with a value of 8.2 and 0.34, respectively. Higher index value suggests better low temperature cracking resistance. However, the FE values showed highest value for Dyer and the lowest for Machesney 15-16 having respective averaged values of 1042.4 J/m² and 360.6 J/m².

The rutting potential was measured using the rut depth corresponding to 20,000 wheel passes or 0.5 in (12.5 mm) whichever reached first in a Hamburg WTT. Not all the sections passed the 20,000 cycle criteria: some of them failed at the rut depth criterion before achieving 20,000 passes. The results showed Dyer as the most rut resistant whereas Galesburg outer lane was the least.

To compare the overall AC mixture performance, balanced mix design approach was used to compare the tested sections (Ozer, et. al, 2016). The sections were plotted with rut depth in x-axis corresponding to 10,000 passes and FI on y-axis; the 10,000 passes criterion was used to have a fair comparison among mixtures as one of the samples failed around 10,000 passes . Figure 4-13 shows the interaction of FI with rut depth. The interaction plot shows that AC characteristics vary from very stiff and brittle (Dyer and Machesney AC mixes) to relatively flexible and less stiff (indicating less rutting resistance). When preliminary thresholds proposed by Al-Qadi et al. (2015) are considered, all of AC mixes except Galesburg (outer lane) failed. However, the preliminary thresholds were developed considering conventional surface overlays with N70 and N90 AC mixture designs. When AC mixes for low volume and local roads are considered and/or field aged, these thresholds may be lowered. The very low FI values for Dyer and Machesney 17-18 AC mixes suggest that these mixes would perform poorly in the field.

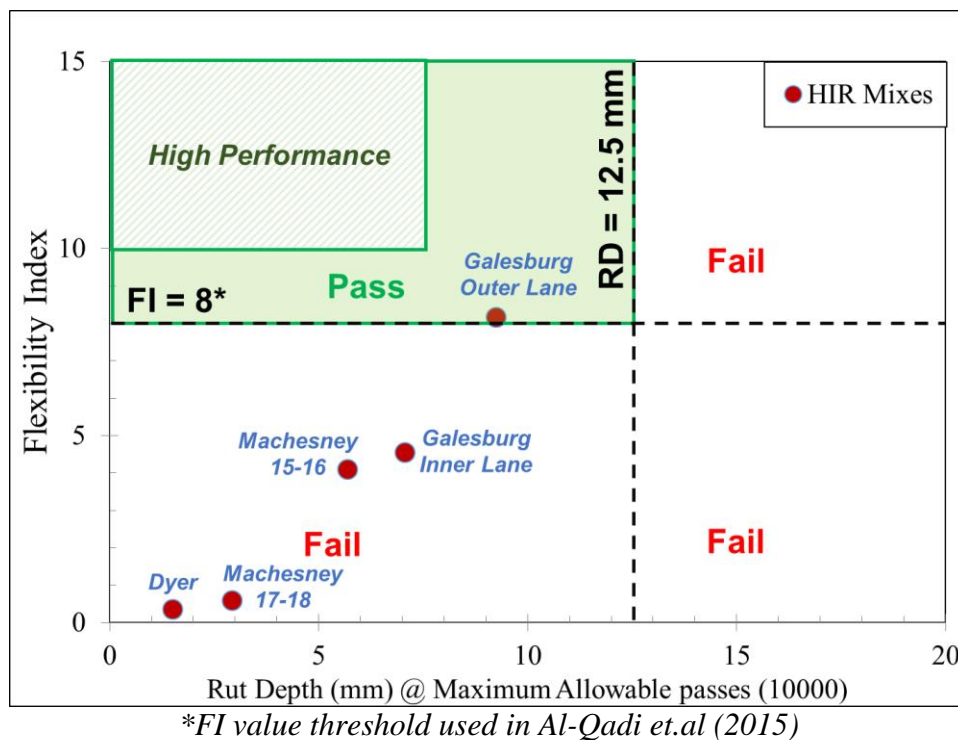


Figure 4-13 Flexibility index and rutting correlation using balanced mix design approach (Ozer et. al, 2016)

FI and $\Delta T_{critical}$ were used to see a correlation between AC mixture and binder-level cracking performance. A plot between FI and $\Delta T_{critical}$ was drawn as shown in Figure 4-14. Higher the $\Delta T_{critical}$, higher was the brittleness of binder; hence, AC pavement is prone to thermal cracking. There was no clear distinction among the AC mixes with $\Delta T_{critical}$ higher than -5°C ; such as Galesburg and Machesney 15-16 sections. On the other hand, it distinguished the AC mixes well with values than 5°C (9°F); such as for Dyer and Machesney 17-18 sections. Similar observations were derived from the balanced mix design approach as seen in Figure 4-13 and the values are presented in Table 4-8.

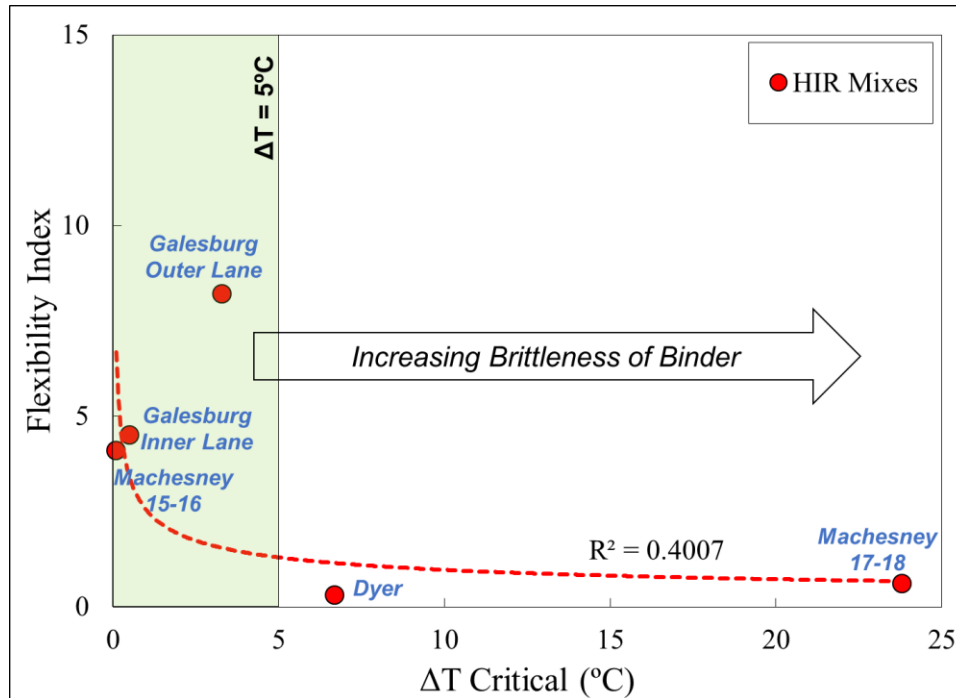


Figure 4-14 A comparison of binder and mixture cracking parameters

Table 4-8 Summary of $\Delta T_{\text{critical}}$ and FI

Section	Grade	$\Delta T_{\text{critical}}$	Spread (°C)	FI
Galesburg Inner Lane	PG 58-40		0.5	4.5
Galesburg Outer Lane	PG 64-34		-3.3	8.2
Machesney 15-16	PG 40-46		-0.1	4.1
Machesney 17-18	PG 52-46		-23.8	0.6
Dyer	PG 76-28		-6.7	0.3

4.4 FIELD CORES

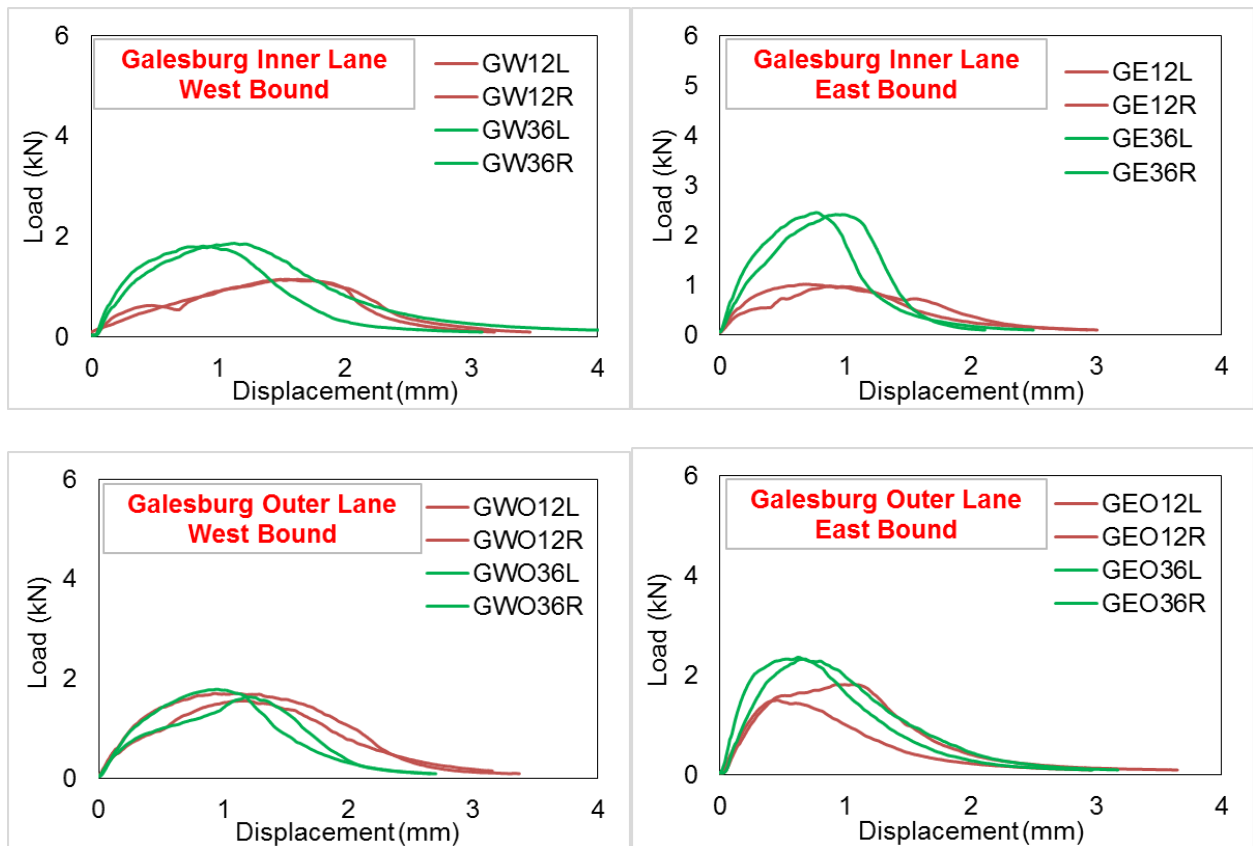
Field cores were collected from each of the project site before applying HIR treatment. The field cores represent the initial conditions of the pavement. To characterize the field cores, top lift of the field cores was cut and prepared to perform I-FIT test to evaluate its cracking potential before HIR. The thickness of the field cores for the top lift varied significantly between cores and was lower than the thickness required as per the specification. The volumetric details of the field cores with thickness is presented in Appendix F.2.

The results of I-FIT test from the field cores is summarized in Table 4-9 and the load displacement curves for the three test sites is shown in Figure 4-15. The results showed high variability within the same section. In addition, field cores showed variability in thickness within the same section. The range of the calculated FI values clearly indicates that all test sections required attention to address potential cracking damage. On comparison, after HIR treatment, some sections showed slight improvement with respect to AC cracking potential, while others did not show any significant improvement. Fracture energy values showed reduction after HIR;

this can be attributed to the addition of the rejuvenators. Figure 4-16 shows comparison of cracking parameters obtained from I-FIT test of field cores and laboratory compacted specimens of HIR treated AC mixes.

Table 4-9 Result summary of I-FIT for field cores of various sections (Appendix F.2)

Section	Fracture Energy (J/m^2)		Flexibility Index	
	Average	COV, %	Average	COV, %
Galesburg Inner Lane West Bound	1543.2	15.4	6.2	51.4
Galesburg Outer Lane West Bound	1450.6	4.6	3.8	4.8
Galesburg Inner Lane East Bound	1225.7	2.3	1.7	2.3
Galesburg Outer Lane East Bound	1475.1	1.9	4.6	8.2
Machesney 15-16	1323.5	23.0	1.1	31
Machesney 17-18	1837.5	15.3	2.8	64.1
Dyer West Bound	1201.7	11.0	3.6	5.6
Dyer East Bound	1189.6	19.9	1.0	26.4



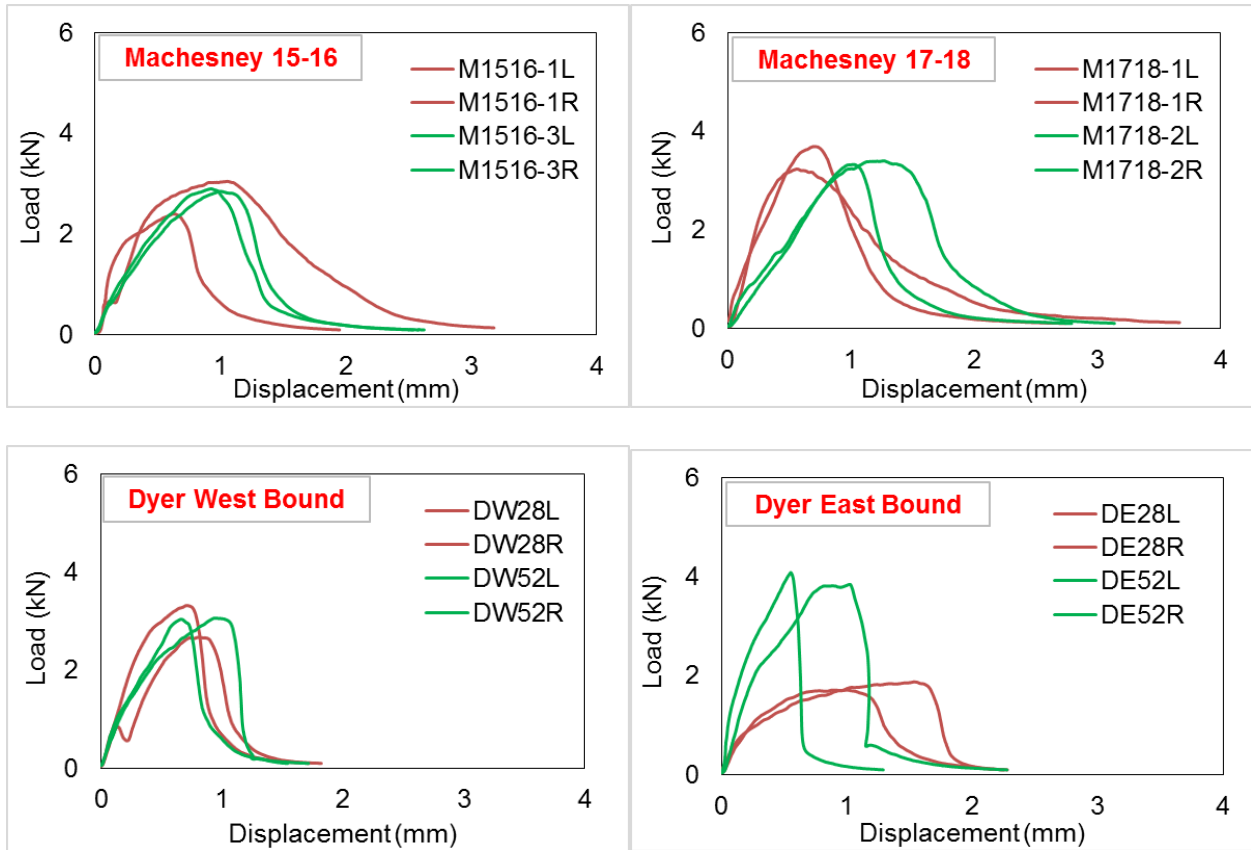


Figure 4-15 Load displacement curve from I-FIT fracture test for field cores of various sections

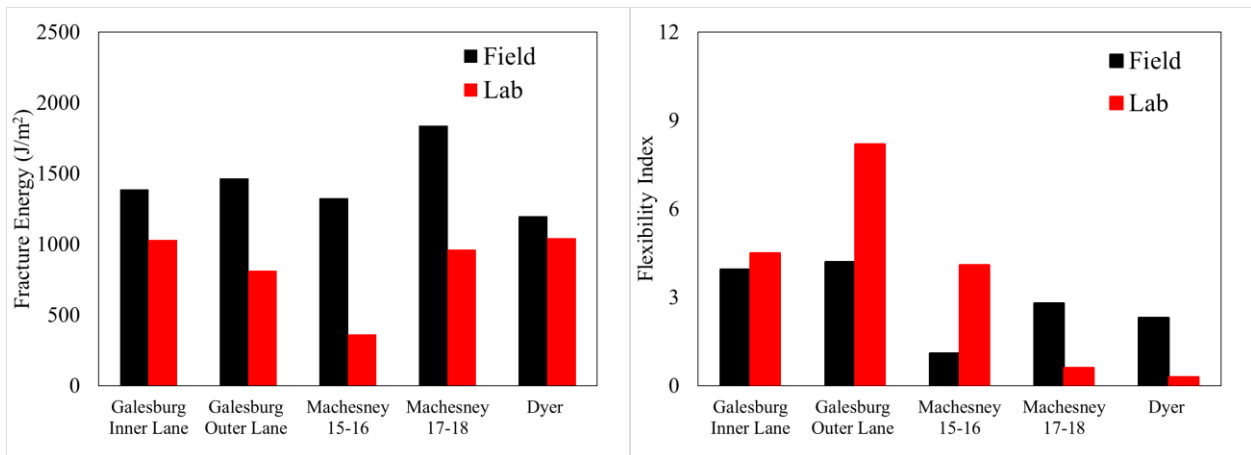


Figure 4-16 Comparison of I-FIT results from field cores and laboratory compacted specimens for test sections

4.5 SUMMARY

To summarize, laboratory testing was divided into binder and AC mixture testing. The results from the binder testing showed clear distinction among different sections as observed from the

PG determination and frequency sweep test results. After treatment, the section at Dyer was the stiffest section; its binder grade is PG 76-28 and the complex modulus master curves also reflected the stiff behavior. While, the binder of Machesney 15-16 section behaved the softest; its grade is PG 40-46 and the complex modulus master curve supported that.

At the AC mixture level, same trends were observed from I-FIT test results. WTT also showed similar trends with some exceptions. Machesney 17-18 sections had extremely low $\Delta T_{\text{critical}}$ of -23.8°C. Although the binder grade is soft (PG 52-46), the AC was very stiff. The balanced mix design approach showed Galesburg outer lane to be the best performing section and Dyer as the worst performing section among all the sections. These observations are in agreement with the trend obtained from the binder $\Delta T_{\text{critical}}$ and AC mixture FI values.

Most of the sections were susceptible to cracking initially (Galesburg and Machesney) and showed an improvement after HIR as compared to other sections (Dyer). There was a consistent reduction in the fracture energy in all sections, which may be due to the softening effect of rejuvenators.

CHAPTER 5 - ENVIRONMENTAL IMPACT ASSESSMENT

5.1 ENVIRONMENTAL IMPACTS

In addition to performance-based analyses of using HIR, an environmental assessment was also conducted for HIR. In this study, a HIR repaving process with 38 mm scarification and 38 mm AC OL was compared with a conventional 50 mm mill and 50 mm AC overlay for a one-lane-km section (3.6 m lane). The same 30% RAP overlay was used for both cases. A summary of relevant items used for the environmental analysis is shown in Table 5-1.

Table 5-1 Details for the environmental assessment of HIR versus conventional processes

Process	Item	Amount (per lane-km)	Unit	Notes
38 mm HIR	Propane fuel ¹	2073	liters	For heater scarifier units 1 and 2
	Diesel fuel ¹	36	liters	For heater scarifier units 1 and 2
	Rejuvenator ²	660	liters	Assume same as asphalt binder; transport ⁴ 160 km to site
50 mm mill	Diesel fuel ¹	28	liters	For milling machine; transport ⁴ 40/160 km off-site
38/50 mm OL	Asphalt binder ²	13/18	ton	Transport ⁴ 100 km to plant
	Virgin aggregate ¹	223/298	ton	Transport ⁴ 40 km to plant
	RAP ³	98/129	ton	Assume from stockpile at plant
	Plant operations ³	333/443	ton	Transport ⁴ mix 40/160 km to site
	Diesel fuel ¹	175/237	liters	For paver and three rollers

**Environmental impact data from ¹default processes from US-Ecoinvent 2.2 database (2009), ²Illinois processes in Yang (2014), ³ Illinois processes by Yang et al. (2015), and ⁴Illinois processes by Kang (2013)*

The construction information for HIR is based on the Galesburg project, where the train speed was approximately 4.6 m/min and the rejuvenator was applied at a rate of 0.16 liters/m². The construction information for the traditional mill and fill process is representative for that of a typical 30% RAP mix used in Illinois with equipment fuel usage from literature (Skolnak et al., 2013). As the hauling distance of materials on-site and off-site varies widely by project, scenarios for an AC plant located 40 km and 160 km from the project site were considered. The per-unit energy and GHG emissions data for producing materials and operating equipment and trucks were taken from various sources, as referenced in Table 5-1.

The environmental impact results for HIR and their corresponding conventional paving alternatives with various hauling distances (i.e., 40 and 160 km) are shown in Figure 5-1, separated

by activity type as well as material production (including mixing and raw material transportation) and equipment operation (including transportation of millings off-site). Robinette and Epps (2010) found comparable energy values for HIR repaving and conventional AC equivalent to 370 and 434 GJ/lane-km, respectively.

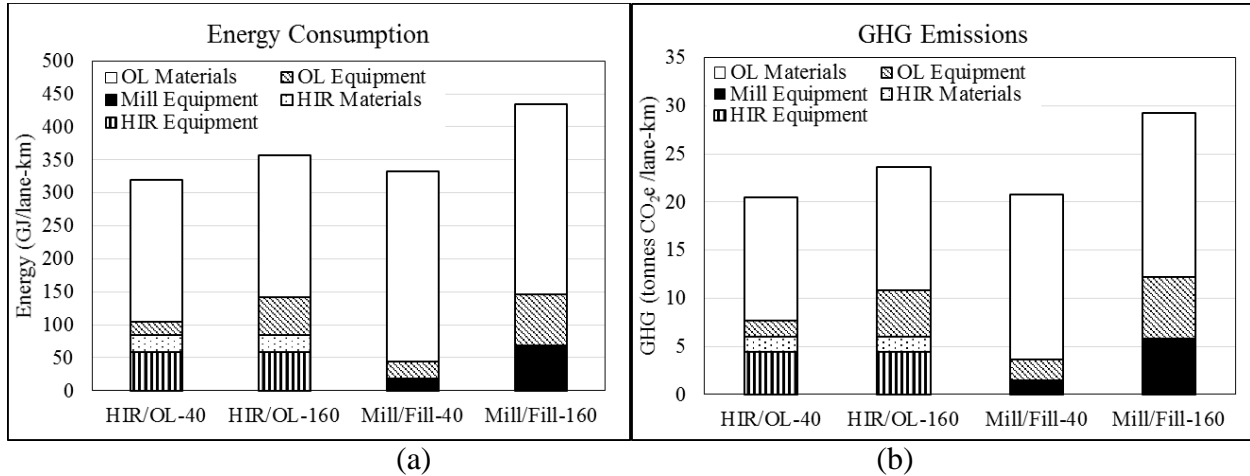


Figure 5-1 (a) Energy and (b) GHGs from HIR versus conventional paving by hauling distances

Overall, the HIR/OL processes showed a savings of 3.9% in energy and 1.3% in GHGs when the haul distance was 40 km and a savings of 17.6% energy and 19.2% in GHGs when the haul distance was 160 km. The overlay materials contribute the most environmental burdens for both processes due to the amount of virgin materials produced and mixed. For the HIR process, the overlay contributed 74–77% and 70–74% to overall energy consumption and GHG, respectively. These values are similar to those in another study which found that HMA production was responsible for 68.5–71.2% of GHGs in HIR (ECRPD, 2010). Similarly, the energy and GHGs attributed to the overlay for conventional paving in Figure 5-1 were found to be 84–95% and 80–93%, respectively.

5.2 SCENARIO BASED SUSTAINABILITY ANALYSIS

While an initial environmental assessment may favor using HIR over conventional paving processes, a life-cycle approach requires that future performance, maintenance, use, and end-of-life of the pavement be considered. As a full LCA is out of scope, a scenario analysis based on expected treatment life is used. The expected treatment life of a thin dense-graded AC OL is typically 7–15 years, while that of HIR repaving with a thin HMA OL is 5–12 years (Peshkin et al., 2011). Annualizing energy consumption over a range of expected treatment lives for both processes produces the relationships in Figure 5-2.

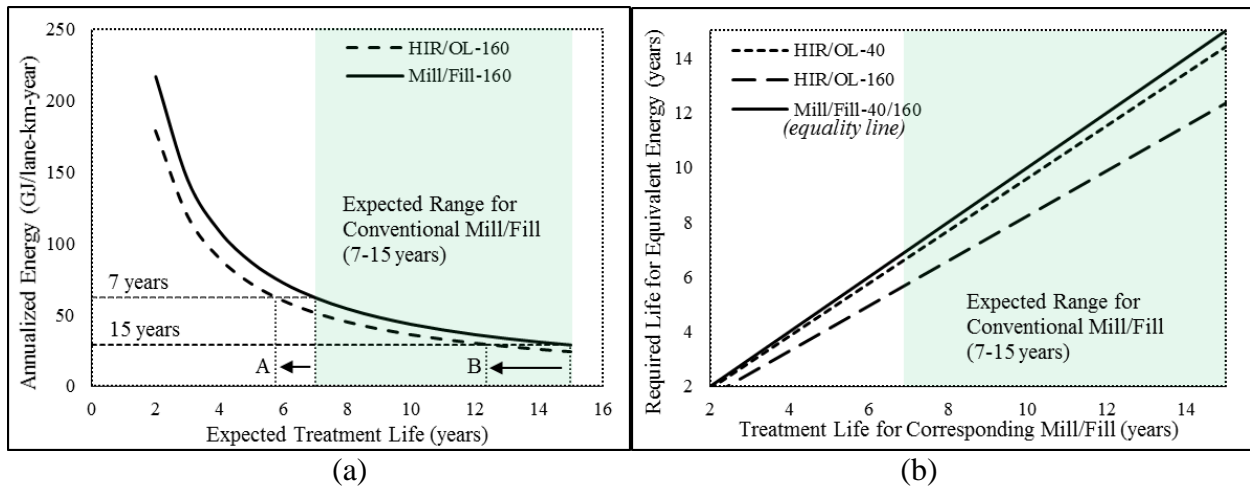


Figure 5-2 Scenario analysis for different expected treatment lives for each process using (a) annualized energy and (b) required life for equivalent energy for HIR/OL based on mill/fill

In Figure 5-2(a), the energy is annualized by expected treatment life for the 160 km hauling case. Arrow A shows that HIR/OL-160 can have a reduced treatment life of down to 5.8 years and still have the same annualized energy consumption as a poor-performing Mill/Fill-160 with a life of 7 years. On the other hand, Arrow B shows that an HIR/OL-160 would need a minimum treatment life of 12.4 years to match a well-performing Mill/Fill-160 of 15 years for the same annualized energy consumption; the HIR/OL would need to perform beyond what is typically expected, indicating that it may be more effective to use Mill/Fill when the pavement is expected to perform very well. Figure 5-2(b) summarizes the treatment life tradeoffs for both HIR/OL hauling cases as compared to their respective Mill/Fill cases. Overall, the treatment life to offset the energy savings from HIR is reduced by less than 1 year for the 40 km case, but increases with higher hauling distance. Greater distances increase the energy consumption for Mill/Fill more than that for HIR/OL due to transportation of millings off-site and plant mixes on-site.

For the two sites examined in this study, the Machesney Park site exhibited severe existing pavement conditions and poor AC mixture characteristics. This implied that the expected HIR treatment life might be in the lower range, potentially offsetting some of the pavement's life-cycle energy and GHGs savings. The Galesburg site exhibited more favorable conditions that indicated an expected HIR treatment life in the higher range and a greater possibility of life-cycle savings. The performance of the pavements will greatly affect the overall life-cycle environmental impacts due to additional maintenance or rehabilitation tasks as well as extra vehicle fuel consumption due to deteriorating pavement conditions.

5.3 SUMMARY

The environmental assessment showed a difference in energy usage and GHGs of 3.9–17.6% and 1.3–19.2%, respectively, between a HIR process with 38 mm AC overlay and a corresponding traditional 50 mm mill and AC OL for different plant locations. Some initial energy savings can be expected with HIR treatments which heavily depend on the surface treatment after HIR, thickness of overlay (if overlay is chosen as the surface treatment), and hauling distances for plant-produced materials needed for overlays. A scenario-based analysis was carried out to determine

the range of expected life for both treatments that could result in similar environmental impact. It was shown that for a 160 km hauling distance, HIR/OL with 5.8 years of expected treatment life could perform equivalent to a poorly performing Mill/Fill with an expected life of 7 years. While the same HIR/OL treatment, has to outperform its capacity to 12.4 years compared to a good performing Mill/Fill treatment that can last for 15 years. However, in order to draw concrete conclusions, a comprehensive LCA and cost analysis is required, including other life-cycle stages, over an expanded analysis period.

CHAPTER 6 - SUMMARY, FINDINGS, CONCLUSIONS AND RECOMMENDATIONS

The study comprises field performance evaluation, laboratory investigation, and environmental impact assessment of three test sections from Illinois and Indiana. FWD, IRI, and visual surveys were conducted as part of the field evaluation at different levels of construction including existing condition prior to HIR, post-HIR and post-overlay. In addition, to complement the field study, laboratory characterization at binder as well as AC mixture levels was undertaken. The scope of laboratory investigation included the collected samples mixed with rejuvenator.

Summary of the findings from field evaluation and laboratory investigation are listed below:

- Initial pavement condition before HIR for all the sections were rated poor according to CRS calculations.
- Findings from deflection basin parameters using FWD measurements showed a consistent trend with all the sections, reduction in pavement structural capacity from the initial condition after HIR and an increase after overlay application.
- The area parameter in general showed that Dyer and Galesburg sections had relatively higher structural capacity as compared to Machesney section.
- IRI was improved significantly compared to the initial condition in all the sections. However, continuous monitoring is required to assess long-term improvement.
- Preliminary laboratory characterization at binder level indicated Dyer section had the stiffest binder followed by Galesburg and Machesney sections based on the results from PG determination and frequency sweep analysis.
- The FI value of the AC mixes showed that Galesburg section performed best considering potential cracking followed by Machesney and Dyer.
- Dyer section showed the highest resistance to rutting followed by Machesney and Galesburg.
- Even though Machesney section had the softest binder, its rutting resistance was better than Galesburg section, which can be attributed to possibly its lower binder content and coarser gradation.
- Balanced mix design approach was used to compare overall performance of the AC mixture combining potential rut and cracking resistance. According to this approach, The Galesburg section showed the best performance followed by Machesney and the worst being Dyer.
- Results from binder and AC mixture parameters for cracking, $\Delta T_{critical}$ and FI, respectively, were in agreement with the balanced mix design approach results.
- The environmental assessment showed a difference in energy usage and GHGs of 3.9–17.6% and 1.3–19.2%, respectively, between a HIR process with 38 mm AC OL and a corresponding traditional 50 mm mill and AC OL with different plant locations.
- Scenario-based analysis shows that the HIR treatments heavily depends on the surface treatment after HIR, thickness of overlay (if overlay is chosen as the surface treatment), and hauling distances for plant-produced materials needed for overlays.

The following conclusions were made based on this study:

- HIR treatment, using proper type and dosage of rejuvenator can reduce the cracking potential of AC mixes.

- FWD measurements and IRI calculations showed that HIR with OL can improve the structural capacity of the pavement and its smoothness.
- Sustainability of HIR depends highly on factors like initial pavement condition, applied surface treatment after HIR, thickness of overlay (in case of overlay application in HIR), and hauling distances.

Recommendations for future work are summarized as follows:

- Continuous monitoring of the rehabilitated sections for riding quality (IRI) and deteriorating conditions needs to be undertaken to establish quantitative field performance models.
- Rheological and chemical characterization for different types of rejuvenators is required to ensure compatibility with AC and to define optimal dosage requirements.
-
- Development of treatment selection guidelines based on type and condition of pavement, timing of rehabilitation. and construction temperature. Performance, economic, and sustainability parameters should be considered

6.1 TECHNOLOGY TRANSFER

1. Singhvi, P., Ozer, H., and Al-Qadi, I.L., “Impact of Rejuvenators on the Binder Rheological Characterization of Hot In-Place Recycled Mixtures”. Airfield and Highway Pavement Conference, 2017: Philadelphia. (*Presentation*).
2. Ozer, H., Singhvi, P., Al-Qadi, I.L., Abuawad, I., and Satish G.K., “Field Performance and Laboratory Characterization for Prediction of Overall Pavement Performance of Hot In-Place Recycled Mixtures”. Transportation Research Board, Washington D.C. 2017. (*Submitted*).
3. Singhvi, P., Ozer, H., and Al-Qadi, I.L., “Performance Evaluation and Environmental Assessment of Hot In-Place Recycled Asphalt Pavement”. Poster Presentation at National Pavement Preservation Conference, Nashville, TN. October 11-14, 2016. (*Submitted*).
4. Singhvi, P., “Laboratory Characterization and Field Performance of Hot In-Place Recycled mixtures”. Masters’ Thesis. University of Illinois at Urbana Champaign. May 2016.
5. Singhvi, P., Abuawad, I., Yang, R., Ozer, H., and Al-Qadi, I.L., “A Sustainability Evaluation of Hot In-place Asphalt Recycling Technique”. Eighth International Conference on Maintenance and Rehabilitation of Pavements, Singapore, July 27-29, 2016.
6. Singhvi, P., Abuawad, I., Coenen, A., Ozer, H., and Al-Qadi, I.L., “Field Investigation and Laboratory Performance Characterization of Hot In-Place Recycled Asphalt Mixtures.” Airfield and Highway Pavement Conference, Miami, Florida, June 2015. (*Presentation*).
7. Singhvi, P., Abuawad, I., Ozer, H., and Al-Qadi, I.L., “Laboratory Performance Characterization and Field Evaluation of Hot In-Place Recycled Asphalt Mixtures.” Mid-SURE Symposium, 2015: Michigan State University, East Lansing, Michigan. (*Presentation and Poster Presentation*).

6.2 REFERENCES

- Al-Qadi, I. L., Ozer, H., Lambros, J., El-Khatib, A., Singhvi, P., Khan, T., Perez, J.R., and B. Doll (2015). Testing Protocols to Ensure Performance of High Asphalt Binder Replacement Mixes Using RAP and RAS. Report No. FHWA-ICT-15-017. Illinois Center for Transportation, Rantoul, IL.
- Ali, H., and K. Grzybowski, 2012. Life Cycle of Hot In-Place Pavement Recycling. Transportation Research Record: Journal of the Transportation Research Board 2292: 29-35, Washington D.C.
- Ali, H., and Bonaquist, R, 2012. Evaluation of Binder Grade and Recycling Agent Blending for Hot In-Place Recycled Pavement. Transportation Research Board, 91st Annual Meeting Compendium 0768, Washington D.C.
- Alavi, S., LeCates, J. F., and Tavares, M. P. (2008). NCHRP Synthesis 381 Falling Weight Deflectometer Usage. Washington D.C.
- Ali, H., McCarthy, L. M., and Welker, A. (2013). Performance of hot in-place recycled Superpave mixtures in Florida. Construction and Building Materials, 49, 618–626. <http://doi.org/10.1016/j.conbuildmat.2013.08.043>
- Ali, H., and Sobhan, K. (2012). The road to sustainability, Properties of Hot In-Place Recycled Superpave Mix. Transportation Research Record: Journal of the Transportation Research Board, 2292(10), 88–93. <http://doi.org/10.3141/2292-11>
- Asli, H., Ahmadinia, E., Zargar, M., and Karim, M. R. (2012). Investigation on physical properties of waste cooking oil - Rejuvenated bitumen binder. Construction and Building Materials, 37, 398–405. <http://doi.org/10.1016/j.conbuildmat.2012.07.042>
- Asphalt Recycling and Reclaiming Association (ARRA), 2014. Basic Asphalt Recycling Manual, Asphalt Recycling and Reclaiming Association, Annapolis, MD.
- Brownlee, M. 2011. “Utilization of recycled and reclaimed materials in Illinois highway construction in 2010.” Report No 160. Illinois Department of Transportation Bureau of Materials and Physical Research, Springfield, IL.
- Button, J. W., Estakhri, C. K., and Little, D. N. (1992). Overview of Hot In-Place Recycling of. Transportation Research Record: Journal of the Transportation Research Board, 1684(99), 178–185.
- Chan, S., Lane, B., Kazmierowski, T., and Lee, W. (2011). Pavement Preservation. Transportation Research Record: Journal of the Transportation Research Board, 2235(-1), 36–42. <http://doi.org/10.3141/2235-05>
- Chappat M. and J. Bilal, 2003. The Environmental Road of the Future, COLAS SA, Paris 9, pp. 1-24.
- Chapter 13. Cold In-Place Recycling (Construction Methods and Equipment). (n.d.) (pp. 1–11).
- Chapter 53: PAVEMENT REHABILITATION, Bureau of Design and Environment Manual. (n.d.). Illinois.
- Chehovits, J., and Galehouse, L. (2010). Energy Usage and Green House Gas Emissions of Pavement Preservation Processes for Asphalt Conceter Pavements. Compendium of Papers from the First International Conferenceon Pavement Preservation, (pp 27-42). Newport Beach, California.
- Chen, D., and Bilyeu, J. (2001). Assessment of a Hot-in-Place Recycling Process. Tamkang Journal of Science and Engineering, 4(4), 265–276.

- Chen, D. H., and Scullion, T. (2008). Forensic Investigations of Roadway Pavement Failures. *Journal of Performance of Constructed Facilities*, 22(1), 35–44. [http://doi.org/10.1061/\(ASCE\)0887-3828\(2008\)22:1\(35\)](http://doi.org/10.1061/(ASCE)0887-3828(2008)22:1(35))
- Chen, M., Xiao, F., Putman, B., Leng, B., and Wu, S. (2014). High temperature properties of rejuvenating recovered binder with rejuvenator, waste cooking and cotton seed oils. *Construction and Building Materials*, 59, 10–16. <http://doi.org/10.1016/j.conbuildmat.2014.02.032>
- Crawley, A. (1999). Innovative Hot In-Place Recycling of Hot-Mix Asphalt Pavement in Mississippi. *Transportation Research Record*, 1654(1), 36–41. <http://doi.org/10.3141/1654-04>
- Cross, S. a., Chesner, W. H., Justus, H. G., and Kearney, E. R. (2011). Life-Cycle Environmental Analysis for Evaluation of Pavement Rehabilitation Options. *Transportation Research Record: Journal of the Transportation Research Board*, 2227(-1), 43–52. <http://doi.org/10.3141/2227-05>
- Dony, a., Colin, J., Bruneau, D., Drouadaine, I., and Navaro, J. (2013). Reclaimed asphalt concretes with high recycling rates: Changes in reclaimed binder properties according to rejuvenating agent. *Construction and Building Materials*, 41, 175–181. <http://doi.org/10.1016/j.conbuildmat.2012.11.031>
- Energy Conservation in Road Pavement Design (ECRPD), 2010. Energy Conservation in Road Pavement Design, Maintenance and Utilisation, Intelligent Energy – Europe.
- Finlayson, D., Nicoletti, C., Pilkington, I., Sharma, V., and B. Teufele, 2012. British Columbia's Success with Hot-In-Place Recycling - a 25 Year History, Proceedings of the Fifty-Sixth Annual Conference of the Canadian Technical Asphalt Association, Quebec City, Quebec, Canada.
- Hafeez, I., Ozer, H., and Al-Qadi, I. L. (2014). Performance Characterization of Hot In-Place Recycled Asphalt Mixtures. *Journal of Transportation Engineering*, 140(8), 04014029.
- Haider, S. W., and Baladi, G. Y. (2008). The effects of cracking type and location on the choice of asphalt pavement recycling method, 529–538.
- Heckel, L., and Ouyang, Y. (2007). Update Of Condition Rating Survey (Crs) Calculation / Prediction Models. Illinois Center for Transportation. Urbana Champaign.
- Horvath, A., 2004. A Life-cycle Analysis Model and Decision-Support Tool for Selecting Recycled Versus Virgin Materials for Highway Applications, University of California at Berkeley, CA.
- Hong, F., Chen, D.-H., and Mikhail, M. M. (2011). Long-Term Performance Evaluation of Recycled Asphalt Pavement Results from Texas. *Transportation Research Record: Journal of the Transportation Research Board*, 2180, 58–66. <http://doi.org/10.3141/2180-07>
- Horak, E. (1987). Aspects of Deflection Basin Parameters used in a Mechanistic Rehabilitation Design Procedure for Flexible Pavements in South Africa. Ph.D Thesis. University of Pretoria
- Horak, E., and Emery, S. (2006). Falling Weight Deflectometer Bowl Parameters as Analysis Tool for Pavement Structural Evaluations. 22nd ARRB Conference, 29th October - 2nd November 2006, Canberra
- International Organization for Standardization (ISO), 2006. “Environmental Management – Life-cycle Assessment – Principles and Framework.” ISO 14040:2006. Geneva, Switzerland.
- Im, S., Zhou, F., Lee, R., and Scullion, T., 2014. Impacts of Rejuvenators on Performance and Engineering Properties of Asphalt Mixtures Containing Recycled Materials. *Construction and Building Materials*, 53, 596–603.

- Jackson, N., Puccinelli, J., and Mahoney, J. (2014). *Using Existing Pavement in Place and Achieving Long Life*. Washington D.C.
- Kang, S., 2013. *The Development of a Regional Inventory Database for the Material Phase of the Pavement Life-Cycle with Updated Vehicle Emission Factors using MOVES*, Master's Thesis, Department of Civil and Environmental Engineering, University of Illinois at Urbana-Champaign.
- Karlsson, R., and Isacson, U. (2003). Application of FTIR-ATR to Characterization of Bitumen Rejuvenator Diffusion. *Journal of Materials in Civil Engineering*, 15(2), 157–165. [http://doi.org/10.1061/\(ASCE\)0899-1561\(2003\)15:2\(157\)](http://doi.org/10.1061/(ASCE)0899-1561(2003)15:2(157))
- Karlsson, R., Isacson, U., and Ekblad, J. (2007). Rheological characterisation of bitumen diffusion. *Journal of Materials Science*, 42(1), 101–108. <http://doi.org/10.1007/s10853-006-1047-y>
- Kazmierowski, T., Marks, P., and Lee, S. (1999). Ten-Year Performance Review of In Situ Hot-Mix Recycling in Ontario. *Transportation Research Record*, 1684(1), 194–202. <http://doi.org/10.3141/1684-23>
- Kuang, D., Feng, Z., Yu, J., Chen, X., and Zhou, B. (2011). A new approach for evaluating rejuvenator diffusing into aged bitumen. *Journal Wuhan University of Technology, Materials Science Edition*, 26(1), 43–46. <http://doi.org/10.1007/s11595-011-0164-x>
- Kuang, D., Yu, J., Chen, H., Feng, Z., Li, R., and Yang, H. (2014). Effect of rejuvenators on performance and microstructure of aged asphalt. *Journal of Wuhan University of Technology-Mater. Sci. Ed.*, 29(2), 341–345. <http://doi.org/10.1007/s11595-014-0918-3>
- Lee, J., Li, S., Kim, Y., and Lee, J. (2013). Effectiveness of Asphalt Rejuvenator. *Journal of Testing and Evaluation*, 41(3), 20120024. <http://doi.org/10.1520/JTE20120024>
- Lin, J., Guo, P., Wan, L., and Wu, S. (2012). Laboratory investigation of rejuvenator seal materials on performances of asphalt mixtures. *Construction and Building Materials*, 37, 41–45. <http://doi.org/10.1016/j.conbuildmat.2012.07.008>
- Lin, J., Guo, P., Xie, J., Wu, S., and Chen, M. (2012). Effect of Rejuvenator Sealer Materials on the Properties of Aged Asphalt Binder. *Journal of Materials in Civil Engineering*, (July), 121001063047003. [http://doi.org/10.1061/\(ASCE\)MT.1943-5533.0000702](http://doi.org/10.1061/(ASCE)MT.1943-5533.0000702)
- Lippert, D. L., Kang, S. G., and Ozer, H. (2015). *Illinois Highway Materials sustainability Efforts of 2014*. Urbana: Illinois Center for Transportation.
- Lytton, R. L. (2012). *Backcalculation of Pavement Layer Properties*. ASTM.
- Mahoney, J., Jackson, N., and Puccinelli, J. (2014). *Guide to Using Existing Pavement in Place and Achieving Long Life*. Transportation Research Record, SHRP-2 Report S2-R23-RW-2, Washington D.C., ISBN: 978-0-309-12965--7
- Mallick, R. B., Chen, B., Daniel, J. S., and Kandhal, P. S. (1997). Heating and its Effect on Hot In-Place Recycling of Asphalt Pavements with Rejuvenator, 5(6), 347–359.
- Manual, P. (2014). *Illinois highway information system, Roadway Information and Procedure Manual*.
- Miliutenko, S., Björklund, A., and Carlsson, A. (2013). Opportunities for environmentally improved asphalt recycling: The example of Sweden. *Journal of Cleaner Production*, 43, 156–165. <http://doi.org/10.1016/j.jclepro.2012.12.040>
- Mitchell, M. R., Link, R. E., Do Huh, J., and Park, J. Y. (2009). A New Technology of Recycling 100 % Reclaimed Asphalt Pavements. *Journal of Testing and Evaluation*. <http://doi.org/10.1520/JTE000144>

- O'Sullivan, K. (2010). 100 percent recycling—Sustainability in pavement construction. Report on 100 percent recycling of asphalt mixes. http://www.irfnews.org/files/pdfs/100_Percent_Recycling_%E2%80%93Sustainability_in_Pavement_Construction.pdf%20.
- Ozer, H., Al-Qadi, I. L., Lambros, J., El-Khatib, A., Singhvi, P., and Doll, B. (Accepted 2016). Development of a Fracture based Flexibility Index for Asphalt Concrete Cracking Potential using Modified Semi Circle Bending Test Parameters. *Construction and Building Materials*.
- Ozer, H., Singhvi, P., Khan, T., Perez, J. R., Al-Qadi, I. L., and El-Khatib, A. (Accepted 2016). Fracture Characterization of Asphalt Mixtures with RAP and RAS using Illinois Semi-Circular Bending Test Method and Flexibility Index. *Transportation Research Record. Journal of Transportation Research Board*.
- Park, T. (2007). Causes of bleeding in a hot-in-place asphalt pavement. *Construction and Building Materials*, 21(12), 2023–2030. <http://doi.org/10.1016/j.conbuildmat.2007.06.008>
- Pierce, L. M. (1996). Hot in- place recycling-SR-97 West Wapato road to lateral A road (SB). Washington.
- Peshkin, D., Smith, K.L., Wolters, A., Krstulovich, J., Moulthrop, J. and C. Alvarado, 2011. Guidelines for the Preservation of High-Traffic-Volume Roadways, SHRP 2 Report No. S2-R26-RR-2, Transportation Research Board of the National Academies, Washington D.C.
- Qureshi, N. A., Tran, N. H., Watson, D., and Jamil, S. M. (2013). Effects of rejuvenator seal and fog seal on performance of open-graded friction course pavement. *Journal of Science and Technology*, 7(02), 189–202.
- R.M. Anderson, G.N. King, D.I. Hanson, and P.B. Blankenship, King. Evaluation of the Relationship Between Asphalt Binder Properties and Non-Load Related Cracking. *Asphalt Paving Technology, Journal of the Association of Asphalt Paving Technologists*, Volume 80, Lancaster, PA (2011), 615-649.
- Robinette C. and J. Epps, 2010. Energy, Emissions, Material Conservation, and Prices Associated with Construction, Rehabilitation, and Material Alternatives for Flexible Pavement, *Transportation Research Record: Journal of the Transportation Research Board* 2179: 10-22, Washington, D.C.
- Rogge, D., Hislop, W., and Dominick, R. (1996). Hot In-Place Recycling of Asphalt Pavements: Oregon Experience. *Transportation Research Record*, 1545(1), 113–119. <http://doi.org/10.3141/1545-15>
- Sholar, G., Page, G., Musselman, J., and H. Moseley, 2004. Resurfacing of SR-471 Using the Hot-in-Place Recycling Process, Report FL/DOT/SMO/04-472, Prepared for Florida Dept. of Transportation.
- Singhvi, P., 2016. Field Investigation and Laboratory Performance Characterization of Hot In-place Recycled Asphalt Mixtures, Master's Thesis, Department of Civil and Environmental Engineering, University of Illinois at Urbana-Champaign.
- Skolnik, J., Brooks, M., and J. Oman, 2013. Fuel Usage Factors in Highway and Bridge Construction, National Cooperative Highway Research Program Report 744, Washington, D.C.
- Stroup-Gardiner, M., 2011. Recycling and Reclamation of Asphalt Pavements Using In-Place Methods, National Highway Cooperative Research Program Synthesis Report 421, Washington D.C.
- Sylvatic, 2013. US-Ecoinvent Database. Version 2.2., Prepared for Earth Shift, Huntington, VT.
- Sayers, M. W., and Karamihas, S. M. (1998). The little book of profiling. Basic Information about Measuring and Interpreting Road Profiles, (September), 100.

- Shen, J., Amirkhanian, S., and Lee, S.-J. (2005). The effects of rejuvenating agents on recycled aged CRM binders. *International Journal of Pavement Engineering*, 6(4), 273–279. <http://doi.org/10.1080/10298430500439319>
- Shen, J., Amirkhanian, S., and Tang, B. (2007). Effects of rejuvenator on performance-based properties of rejuvenated asphalt binder and mixtures. *Construction and Building Materials*, 21(5), 958–964. <http://doi.org/10.1016/j.conbuildmat.2006.03.006>
- Shen, J., Huang, B., and Hachiya, Y. (2004). Validation of Performance-based Method for Determining Rejuvenator Content in HMA. *International Journal of Pavement Engineering*, 5(2), 103–109. <http://doi.org/10.1080/10298430410001733509>
- Shen, J., and Ohne, Y. (2002). Determining Rejuvenator Content for Recycling Reclaimed Asphalt Pavement by SHRP Binder Specifications. *International Journal of Pavement Engineering*, 3(4), 261–268. <http://doi.org/10.1080/1029843021000083685>
- Shoenberger, J. E., and Vollar, T. W. (1990). Hot In-Place Recycling of Asphalt Pavements.
- Silva, H. M. R. D., Oliveira, J. R. M., and Jesus, C. M. G. (2012). Are totally recycled hot mix asphalts a sustainable alternative for road paving?. *Resources, Conservation and Recycling*, 60, 38–48. <http://doi.org/10.1016/j.resconrec.2011.11.013>
- Stroup-Gardiner, M. (2012). Selection Guidelines for In-Place Recycling Projects. *Transportation Research Record: Journal of the Transportation Research Board*, 2306(2306), 3–10. <http://doi.org/10.3141/2306-01>
- Su, J. F., Schlangen, E., and Qiu, J. (2013). Design and construction of microcapsules containing rejuvenator for asphalt. *Powder Technology*, 235, 563–571. <http://doi.org/10.1016/j.powtec.2012.11.013>
- Yang, R., Kang, S., Ozer, H. and I. L. Al-Qadi, 2015. Environmental and Economic Analyses of Recycled Asphalt Concrete Mixtures Based on Material Production and Potential Performance, *Resources, Conservation and Recycling* 104 p. 141-151.
- Yang, R., 2014. Development of a Pavement Life-Cycle Assessment Tool Utilizing Regional Data and Introducing an Asphalt Binder Model, Master's Thesis, Department of Civil and Environmental Engineering, University of Illinois at Urbana-Champaign.
- Zargar, M., Ahmadinia, E., Asli, H., and Karim, M. R. (2012). Investigation of the possibility of using waste cooking oil as a rejuvenating agent for aged bitumen. *Journal of Hazardous Materials*, 233-234, 254–258. <http://doi.org/10.1016/j.jhazmat.2012.06.021>
- Zaumanis, M., and Mallick, R. B. (2014). Review of very high-content reclaimed asphalt use in plant-produced pavements: state of the art. *International Journal of Pavement Engineering*, (June), 1–17. <http://doi.org/10.1080/10298436.2014.893331>
- Zaumanis, M., Mallick, R. B., and Frank, R. (2013). Evaluation of Rejuvenator's Effectiveness with Conventional Mix Testing for 100% RAP Mixtures. *TRB 2013 Annual Meeting*, (2370), 17–25. <http://doi.org/10.3141/2370-03>

APPENDIX A: Condition rating survey (CRS) calculation

1. Galesburg, IL - Before HIR (2014)

Distress Type and Range	Symbol	Distress Observed Yes/No	Severity Level VL/L/M/H/VH	Minimum Rating Given	Maximum Rating Given	Rating Range	Coefficients for AC/BBO
Severity rating of alligator cracking (0 to 4)	L	Yes	VL	1	2	0-4	0
Severity rating of block cracking (0 to 4)	M	Yes	M	1	2	0-4	-0.204
Severity rating of Rutting (0-3)	N	Yes	VL	0	0	0-3	
Severity rating of joint reflection/transverse cracks (0 to 5)	O	Yes	VH	4	5	0-5	-0.485
Severity rating of overlaid patch reflective cracking (0 to 5)	P	No	NA	0	0	0-5	
Severity rating of longitudinal/center of lane cracking (0 to 5)	Q	Yes	VH	3	4	0-5	-0.25
Severity rating of pavement widening crack (0 to 5)	R	Yes	H	2	3	0-5	-0.113
Severity rating of centerline deterioration (0 to 4)	S	Yes	H	2	3	0-4	-0.123
Severity rating of edge cracking (0 to 4)	T	Yes	VH	3	4	0-4	-0.182
Severity rating of permanent patch deterioration (0 to 4)	U	No	NA	0	0	0-4	
Severity rating of shoving, bumps, sags, and corrugation (0 to 3)	V	No	NA	0	0	0-3	
Severity rating of weathering/raveling/segregation/oxidation (0 to 4)	W	Yes	M	2	3	0-4	-0.283
Severity rating of reflective D-cracking (0 to 3)	X	No	NA	0	0	0-3	
Value of van sensor rut-depth measurement, inches.	RUT	No	NA	0.13	0.13	NA	-0.998
Average IRI	IRI	Yes	H	179	179	NA	-0.002

Pavement Type	AC-BBO
Minimum CRS (Without Rutting)	4.3
Maximum CRS (Without Rutting)	2.2
Minimum CRS (Including Rutting if Any)	4.2
Maximum CRS (Including Rutting if Any)	2.0

2. Galesburg, IL - Two years post overlay (2016)

Distress Type and Range	Symbol	Distress Observed Yes/No	Severity Level VL/L/M/H/VH	Minimum Rating Given	Maximum Rating Given	Rating Range	Coefficients for AC/BBO
Severity rating of alligator cracking (0 to 4)	L	No	VL	0	1	0-4	0
Severity rating of block cracking (0 to 4)	M	No	VL	0	1	0-4	-0.204
Severity rating of Rutting (0-3)	N	No	NA	0	0	0-3	
Severity rating of joint reflection/transverse cracks (0 to 5)	O	Yes	M	2	3	0-5	-0.485
Severity rating of overlaid patch reflective cracking (0 to 5)	P	No	NA	0	0	0-5	
Severity rating of longitudinal/center of lane cracking (0 to 5)	Q	Yes	L	1	2	0-5	-0.25
Severity rating of pavement widening crack (0 to 5)	R	Yes	L	1	2	0-5	-0.113
Severity rating of centerline deterioration (0 to 4)	S	Yes	L	1	1	0-4	-0.123
Severity rating of edge cracking (0 to 4)	T	Yes	L	1	2	0-4	-0.182
Severity rating of permanent patch deterioration (0 to 4)	U	No	NA	0	0	0-4	
Severity rating of shoving, bumps, sags, and corrugation (0 to 3)	V	No	NA	0	0	0-3	
Severity rating of weathering/raveling/segregation/oxidation (0 to 4)	W	No	NA	0	0	0-4	-0.283
Severity rating of reflective D-cracking (0 to 3)	X	No	NA	0	0	0-3	
Value of van sensor rut-depth measurement, inches.	RUT	No	VL	0.03	0.03	NA	-0.998
Average IRI	IRI	Yes	M	123	131	NA	-0.002

Pavement Type	AC-BBO
Minimum CRS (Without Rutting)	7.1
Maximum CRS (Without Rutting)	5.9
Minimum CRS (Including Rutting if Any)	7.1
Maximum CRS (Including Rutting if Any)	5.8

3. Machesney Park, IL - Before HIR (2014)

Distress Type and Range	Symbol	Distress Observed Yes/No	Severity Level VL/L/M/H/VH	Minimum Rating Given	Maximum Rating Given	Rating Range	Coefficients for ACP
Severity rating of alligator cracking (0 to 4)	L	Yes	H	2	3	0-4	-0.236
Severity rating of block cracking (0 to 4)	M	Yes	H	2	3	0-4	-0.271
Severity rating of Rutting (0-3)	N	No	NA	0	0	0-3	
Severity rating of joint reflection/transverse cracks (0 to 5)	O	Yes	M	2	3	0-5	-0.378
Severity rating of overlaid patch reflective cracking (0 to 5)	P	No	NA	0	0	0-5	
Severity rating of longitudinal/center of lane cracking (0 to 5)	Q	Yes	H	2	4	0-5	-0.199
Severity rating of pavement widening crack (0 to 5)	R	No	NA	0	0	0-5	-0.088
Severity rating of centerline deterioration (0 to 4)	S	Yes	H	2	3	0-4	-0.252
Severity rating of edge cracking (0 to 4)	T	Yes	M	2	3	0-4	-0.208
Severity rating of permanent patch deterioration (0 to 4)	U	Yes	H	3	4	0-4	-0.146
Severity rating of shoving, bumps, sags, and corrugation (0 to 3)	V	Yes	L	0	1	0-3	-0.253
Severity rating of weathering/raveling/segregation/oxidation (0 to 4)	W	Yes	VH	3	4	0-4	-0.311
Severity rating of reflective D-cracking (0 to 3)	X	No	NA	0	0	0-3	
Value of van sensor rut-depth measurement, inches.	RUT	No	NA	0.13	0.1	NA	-1.403
IRI	IRI	Yes	VH	314	413	NA	-0.002

Pavement Type	ACP
Minimum CRS (Without Rutting)	3.9
Maximum CRS (Without Rutting)	1.3
Minimum CRS (Including Rutting if Any)	3.7
Maximum CRS (Including Rutting if Any)	1.1

4. Machesney Park, IL - Two years post overlay (2016)

Distress Type and Range	Symbol	Distress Observed Yes/No	Severity Level VL/L/M/H/VH	Minimum Rating Given	Maximum Rating Given	Rating Range	Coefficients for ACP
Severity rating of alligator cracking (0 to 4)	L	No	NA	0	0	0-4	-0.236
Severity rating of block cracking (0 to 4)	M	No	NA	0	0	0-4	-0.271
Severity rating of Rutting (0-3)	N	No	NA	0	0	0-3	
Severity rating of joint reflection/transverse cracks (0 to 5)	O	No	NA	0	0	0-5	-0.378
Severity rating of overlaid patch reflective cracking (0 to 5)	P	No	NA	0	0	0-5	
Severity rating of longitudinal/center of lane cracking (0 to 5)	Q	No	NA	0	0	0-5	-0.199
Severity rating of pavement widening crack (0 to 5)	R	No	NA	0	0	0-5	-0.088
Severity rating of centerline deterioration (0 to 4)	S	No	NA	0	0	0-4	-0.252
Severity rating of edge cracking (0 to 4)	T	No	NA	0	0	0-4	-0.208
Severity rating of permanent patch deterioration (0 to 4)	U	No	NA	0	0	0-4	-0.146
Severity rating of shoving, bumps, sags, and corrugation (0 to 3)	V	No	NA	0	0	0-3	-0.253
Severity rating of weathering/raveling/segregation/oxidation (0 to 4)	W	No	NA	0	0	0-4	-0.311
Severity rating of reflective D-cracking (0 to 3)	X	No	NA	0	0	0-3	
Value of van sensor rut-depth measurement, inches.	RUT	No	VL	0.02	0.02	NA	-1.403
IRI	IRI	Yes	M	167	287	NA	-0.002

Pavement Type	ACP	Pavement Model
Minimum CRS (Without Rutting)	8.7	
Maximum CRS (Without Rutting)	8.4	
Minimum CRS (Including Rutting if Any)	8.6	
Maximum CRS (Including Rutting if Any)	8.4	

5. Dyer, IN - Before HIR (2014)

Distress Type and Range	Symbol	Distress Observed Yes/No	Severity Level VL/L/M/H/VH	Minimum Rating Given	Maximum Rating Given	Rating Range	Coefficients for ACP
Severity rating of alligator cracking (0 to 4)	L	Yes	VH	3	4	0-4	-0.236
Severity rating of block cracking (0 to 4)	M	Yes	VH	3	4	0-4	-0.271
Severity rating of Rutting (0-3)	N	No	VL	0	0	0-3	
Severity rating of joint reflection/transverse cracks (0 to 5)	O	Yes	H	2	3	0-5	-0.378
Severity rating of overlaid patch reflective cracking (0 to 5)	P	No	-	0	0	0-5	
Severity rating of longitudinal/center of lane cracking (0 to 5)	Q	Yes	VH	3	4	0-5	-0.199
Severity rating of pavement widening crack (0 to 5)	R	No	-	0	0	0-5	-0.088
Severity rating of centerline deterioration (0 to 4)	S	Yes	H	2	3	0-4	-0.252
Severity rating of edge cracking (0 to 4)	T	Yes	M	2	3	0-4	-0.208
Severity rating of permanent patch deterioration (0 to 4)	U	Yes	VH	4	4	0-4	-0.146
Severity rating of shoving, bumps, sags, and corrugation (0 to 3)	V	Yes	M	1	2	0-3	-0.253
Severity rating of weathering/raveling/segregation/oxidation (0 to 4)	W	Yes	H	2	3	0-4	-0.311
Severity rating of reflective D-cracking (0 to 3)	X	No	No	0	0	0-3	
Value of van sensor rut-depth measurement, inches.	RUT	-	-	NA	NA	NA	-1.403
IRI	IRI	-	-	NA	NA	NA	-0.002

Pavement Type	ACP
Minimum CRS (Without Rutting)	3.7
Maximum CRS (Without Rutting)	1.6
Minimum CRS (Including Rutting if Any)	3.7
Maximum CRS (Including Rutting if Any)	1.6

6. Dyer, IN - Two years post overlay (2016)

Distress Type and Range	Symbol	Distress Observed Yes/No	Severity Level VL/L/M/H/VH	Minimum Rating Given	Maximum Rating Given	Rating Range	Coefficients for ACP
Severity rating of alligator cracking (0 to 4)	L	Yes	L	1	2	0-4	-0.236
Severity rating of block cracking (0 to 4)	M	Yes	L	1	2	0-4	-0.271
Severity rating of Rutting (0-3)	N	No	NA	0	0	0-3	
Severity rating of joint reflection/transverse cracks (0 to 5)	O	Yes	M	2	3	0-5	-0.378
Severity rating of overlaid patch reflective cracking (0 to 5)	P	No	NA	0	0	0-5	
Severity rating of longitudinal/center of lane cracking (0 to 5)	Q	Yes	M	2	3	0-5	-0.199
Severity rating of pavement widening crack (0 to 5)	R	No	NA	0	0	0-5	-0.088
Severity rating of centerline deterioration (0 to 4)	S	Yes	L	1	2	0-4	-0.252
Severity rating of edge cracking (0 to 4)	T	Yes	VL	0	1	0-4	-0.208
Severity rating of permanent patch deterioration (0 to 4)	U	No	NA	0	0	0-4	-0.146
Severity rating of shoving, bumps, sags, and corrugation (0 to 3)	V	No	NA	0	0	0-3	-0.253
Severity rating of weathering/raveling/segregation/oxidation (0 to 4)	W	Yes	VL	0	1	0-4	-0.311
Severity rating of reflective D-cracking (0 to 3)	X	No	NA	0	0	0-3	
Value of van sensor rut-depth measurement, inches.	RUT	Yes	No	NA	NA	NA	-1.403
IRI	IRI	Yes	Yes	NA	NA	NA	-0.002

Pavement Type **ACP**

Minimum CRS (Without Rutting) 7.1

Maximum CRS (Without Rutting) 5.2

Minimum CRS (Including Rutting if Any) **7.1**

Maximum CRS (Including Rutting if Any) **5.2**

APPENDIX B: Falling weight deflectometer (FWD) deflection basin data

1. Galesburg, IL

FileName	Chainage (m)	Load (kN)	D1 (μmm)	D2 (μmm)	D3 (μmm)	D4 (μmm)	D5 (μmm)	D6 (μmm)	D7 (μmm)	Area A (mm)	RoC	Surface Curvature Index - SCI (mm)
HIR_GALESBURG_FWD_Existing EB	61.00	42.4	264.0	180.0	151.0	126.0	100.0	88.0	67.0	495.5	365.26	0.08
HIR_GALESBURG_FWD_Existing EB	122.00	42.2	353.0	241.0	183.0	147.0	123.0	90.0	69.0	470.4	274.31	0.11
HIR_GALESBURG_FWD_Existing EB	183.00	43.8	357.0	261.0	220.0	185.0	141.0	110.0	85.0	522.3	342.70	0.10
HIR_GALESBURG_FWD_Existing EB	244.00	42.4	351.0	251.0	206.0	165.0	133.0	106.0	83.0	503.8	321.79	0.10
HIR_GALESBURG_FWD_Existing EB	305.00	44.6	327.0	210.0	172.0	144.0	113.0	91.0	71.0	470.2	247.00	0.12
HIR_GALESBURG_FWD_Existing EB	366.00	41.9	435.0	285.0	213.0	167.0	122.0	96.0	69.0	452.8	196.55	0.15
HIR_GALESBURG_FWD_Existing EB	427.00	43.3	285.0	221.0	193.0	152.0	124.0	91.0	67.0	549.5	545.23	0.06
HIR_GALESBURG_FWD_Existing EB	488.00	45.3	80.0	65.0	61.0	54.0	46.0	39.0	31.0	601.9	2437.50	0.01
HIR_GALESBURG_FWD_Existing EB	542.29	43.3	75.0	64.0	54.0	46.0	33.0	31.0	26.0	586.0	3490.91	0.01
HIR_GALESBURG_FWD_Existing EB	612.14	44.8	233.0	192.0	168.0	148.0	129.0	105.0	84.0	585.2	904.43	0.04
HIR_GALESBURG_FWD_Existing EB	671.61	42.6	244.0	130.0	111.0	94.0	80.0	66.0	55.0	424.2	210.31	0.11
HIR_GALESBURG_FWD_Existing EB	732.00	42.4	211.0	116.0	97.0	80.0	62.0	50.0	39.0	427.3	260.41	0.09
HIR_GALESBURG_FWD_Existing EB	794.22	42.4	228.0	133.0	116.0	95.0	72.0	60.0	45.0	452.6	276.32	0.09
HIR_GALESBURG_FWD_Existing EB	856.14	42.1	346.0	225.0	171.0	132.0	93.0	70.0	53.0	453.0	241.84	0.12
HIR_GALESBURG_FWD_Existing EB	915.00	41.4	407.0	262.0	174.0	120.0	87.0	66.0	52.0	419.0	199.78	0.14
HIR_GALESBURG_FWD_Existing EB	976.61	42.4	416.0	322.0	248.0	194.0	139.0	106.0	81.0	514.9	370.55	0.09
HIR_GALESBURG_FWD_Existing EB	1038.22	40.6	777.0	579.0	378.0	251.0	178.0	126.0	96.0	456.2	169.36	0.20
HIR_GALESBURG_FWD_Existing EB	1098.31	41.4	419.0	319.0	234.0	174.0	129.0	95.0	74.0	494.0	342.60	0.10
HIR_GALESBURG_FWD_Existing EB	1159.61	42.0	315.0	205.0	162.0	128.0	98.0	74.0	54.0	462.9	266.23	0.11

HIR_GALESBURG_FWD_Existing EB	1220.61	41.1	544.0	344.0	233.0	167.0	123.0	93.0	71.0	419.4	142.28	0.20
HIR_GALESBURG_FWD_Existing EB	1282.53	41.5	528.0	415.0	301.0	211.0	150.0	113.0	84.0	498.9	313.00	0.11
HIR_GALESBURG_FWD_Existing EB	1342.31	41.5	502.0	374.0	276.0	201.0	144.0	111.0	81.0	486.8	261.92	0.13
HIR_GALESBURG_FWD_Existing EB	1406.36	41.3	519.0	382.0	262.0	177.0	124.0	88.0	71.0	463.0	241.76	0.14
HIR_GALESBURG_FWD_Existing WB	1406.36	40.8	661.0	480.0	320.0	214.0	150.0	105.0	74.0	452.7	180.54	0.18
HIR_GALESBURG_FWD_Existing WB	1343.22	41.6	426.0	321.0	258.0	195.0	146.0	112.0	84.0	513.4	322.94	0.10
HIR_GALESBURG_FWD_Existing WB	1281.00	41.6	396.0	303.0	234.0	177.0	140.0	106.0	83.0	509.1	370.23	0.09
HIR_GALESBURG_FWD_Existing WB	1219.70	41.3	400.0	268.0	207.0	154.0	110.0	83.0	63.0	463.5	228.41	0.13
HIR_GALESBURG_FWD_Existing WB	1158.09	41.9	310.0	203.0	167.0	126.0	98.0	77.0	61.0	470.8	275.40	0.11
HIR_GALESBURG_FWD_Existing WB	1097.39	41.9	324.0	257.0	209.0	160.0	112.0	84.0	64.0	536.6	532.75	0.07
HIR_GALESBURG_FWD_Existing WB	1037.00	41.0	646.0	493.0	352.0	250.0	181.0	127.0	90.0	486.0	224.46	0.15
HIR_GALESBURG_FWD_Existing WB	976.00	42.8	421.0	291.0	213.0	155.0	117.0	90.0	67.0	460.7	239.27	0.13
HIR_GALESBURG_FWD_Existing WB	914.09	41.6	296.0	178.0	143.0	113.0	88.0	71.0	57.0	442.4	229.33	0.12
HIR_GALESBURG_FWD_Existing WB	853.70	41.6	333.0	223.0	169.0	130.0	97.0	73.0	56.0	461.3	273.96	0.11
HIR_GALESBURG_FWD_Existing WB	793.00	42.4	223.0	114.0	97.0	78.0	69.0	54.0	44.0	409.6	211.05	0.11
HIR_GALESBURG_FWD_Existing WB	730.17	42.4	257.0	130.0	107.0	85.0	73.0	56.0	43.0	400.4	179.23	0.13
HIR_GALESBURG_FWD_Existing WB	670.70	41.8	275.0	140.0	116.0	101.0	78.0	67.0	52.0	408.0	169.70	0.13
HIR_GALESBURG_FWD_Existing WB	609.39	41.8	261.0	148.0	125.0	99.0	89.0	70.0	55.0	435.6	225.82	0.11
HIR_GALESBURG_FWD_Existing WB	549.00	40.7	865.0	605.0	344.0	184.0	105.0	80.0	63.0	406.1	121.05	0.26
HIR_GALESBURG_FWD_Existing WB	487.39	50.6	232.0	182.0	152.0	125.0	107.0	82.0	63.0	545.0	706.03	0.05
HIR_GALESBURG_FWD_Existing WB	426.39	42.2	281.0	190.0	153.0	126.0	98.0	79.0	61.0	482.0	334.36	0.09
HIR_GALESBURG_FWD_Existing WB	364.48	55.4	538.0	382.0	274.0	178.0	121.0	87.0	62.0	458.9	204.82	0.16
HIR_GALESBURG_FWD_Existing WB	304.70	52.3	450.0	299.0	245.0	200.0	155.0	122.0	88.0	479.7	198.01	0.15
HIR_GALESBURG_FWD_Existing WB	244.00	51.5	377.0	239.0	192.0	156.0	122.0	97.0	73.0	459.9	206.72	0.14
HIR_GALESBURG_FWD_Existing WB	182.70	50.2	540.0	398.0	299.0	224.0	171.0	123.0	83.0	488.9	233.57	0.14
HIR_GALESBURG_FWD_Existing WB	120.78	45.0	278.0	179.0	154.0	136.0	106.0	89.0	73.0	486.2	292.67	0.10
HIR_GALESBURG_FWD_Existing WB	58.87	42.7	293.0	210.0	163.0	131.0	106.0	85.0	61.0	491.5	388.59	0.08
HIR_GALESBURG_FWD_PostHIR EB	61.00	41.4	356.0	216.0	191.0	167.0	135.0	106.0	82.0	472.3	195.02	0.14
HIR_GALESBURG_FWD_PostHIR EB	122.00	41.9	419.0	249.0	208.0	162.0	124.0	96.0	75.0	446.1	157.31	0.17
HIR_GALESBURG_FWD_PostHIR EB	183.00	41.5	340.0	191.0	173.0	146.0	115.0	97.0	80.0	451.3	169.66	0.15

HIR_GALESBURG_FWD_PostHIR EB	244.00	42.1	284.0	192.0	172.0	140.0	110.0	93.0	73.0	507.0	330.68	0.09
HIR_GALESBURG_FWD_PostHIR EB	305.00	41.9	353.0	196.0	176.0	155.0	128.0	105.0	83.0	448.7	159.15	0.16
HIR_GALESBURG_FWD_PostHIR EB	366.00	41.7	392.0	253.0	199.0	155.0	121.0	92.0	74.0	458.4	208.95	0.14
HIR_GALESBURG_FWD_PostHIR EB	427.00	42.1	288.0	164.0	150.0	124.0	101.0	80.0	62.0	456.3	206.65	0.12
HIR_GALESBURG_FWD_PostHIR EB	488.61	42.1	174.0	135.0	120.0	90.0	64.0	41.0	26.0	550.9	895.23	0.04
HIR_GALESBURG_FWD_PostHIR EB	549.61	42.3	121.0	103.0	88.0	72.0	55.0	41.0	31.0	585.1	2128.10	0.02
HIR_GALESBURG_FWD_PostHIR EB	610.61	42.6	134.0	105.0	94.0	80.0	70.0	58.0	49.0	567.5	1215.90	0.03
HIR_GALESBURG_FWD_PostHIR EB	671.31	41.7	250.0	142.0	124.0	101.0	94.0	76.0	62.0	444.6	236.67	0.11
HIR_GALESBURG_FWD_PostHIR EB	732.61	41.9	333.0	111.0	102.0	93.0	73.0	64.0	53.0	333.8	67.57	0.22
HIR_GALESBURG_FWD_PostHIR EB	794.22	41.6	310.0	116.0	101.0	90.0	70.0	60.0	47.0	347.4	86.80	0.19
HIR_GALESBURG_FWD_PostHIR EB	855.22	43.4	425.0	255.0	212.0	160.0	117.0	77.0	56.0	446.1	158.82	0.17
HIR_GALESBURG_FWD_PostHIR EB	915.31	41.4	397.0	273.0	198.0	139.0	99.0	74.0	55.0	455.3	249.55	0.12
HIR_GALESBURG_FWD_PostHIR EB	976.61	41.5	627.0	468.0	306.0	197.0	147.0	108.0	80.0	455.5	211.25	0.16
HIR_GALESBURG_FWD_PostHIR EB	1037.31	41.5	482.0	421.0	316.0	222.0	152.0	107.0	78.0	546.8	644.34	0.06
HIR_GALESBURG_FWD_PostHIR EB	1098.31	41.4	544.0	367.0	264.0	203.0	165.0	123.0	92.0	452.8	171.52	0.18
HIR_GALESBURG_FWD_PostHIR EB	1159.61	42.1	407.0	300.0	235.0	181.0	137.0	104.0	78.0	500.5	310.00	0.11
HIR_GALESBURG_FWD_PostHIR EB	1228.24	41.2	596.0	422.0	271.0	175.0	118.0	89.0	71.0	436.7	183.12	0.17
HIR_GALESBURG_FWD_PostHIR EB	1281.31	41.1	574.0	422.0	313.0	229.0	161.0	115.0	85.0	483.7	217.66	0.15
HIR_GALESBURG_FWD_PostHIR EB	1342.00	41.4	547.0	420.0	306.0	217.0	149.0	105.0	81.0	492.5	272.06	0.13
HIR_GALESBURG_FWD_PostHIR EB	1403.31	41.2	537.0	388.0	295.0	226.0	169.0	128.0	97.0	486.3	218.21	0.15
HIR_GALESBURG_FWD_PostHIR WB	1403.31	41.5	524.0	398.0	307.0	219.0	155.0	113.0	82.0	502.4	271.26	0.13
HIR_GALESBURG_FWD_PostHIR WB	1341.70	41.6	351.0	252.0	209.0	159.0	125.0	91.0	71.0	504.3	326.34	0.10
HIR_GALESBURG_FWD_PostHIR WB	1281.00	41.6	374.0	248.0	206.0	164.0	130.0	98.0	72.0	480.5	236.82	0.13
HIR_GALESBURG_FWD_PostHIR WB	1210.85	41.7	415.0	280.0	226.0	174.0	132.0	99.0	74.0	477.5	224.90	0.14
HIR_GALESBURG_FWD_PostHIR WB	1159.00	41.9	275.0	170.0	143.0	120.0	94.0	76.0	59.0	464.2	264.94	0.11
HIR_GALESBURG_FWD_PostHIR WB	1097.70	41.0	655.0	462.0	307.0	204.0	131.0	93.0	74.0	443.1	164.46	0.19
HIR_GALESBURG_FWD_PostHIR WB	1037.00	41.5	424.0	340.0	269.0	204.0	146.0	107.0	80.0	532.8	429.58	0.08
HIR_GALESBURG_FWD_PostHIR WB	953.13	42.1	320.0	163.0	136.0	109.0	88.0	67.0	52.0	405.0	146.00	0.16
HIR_GALESBURG_FWD_PostHIR WB	915.00	41.3	456.0	261.0	182.0	130.0	93.0	69.0	51.0	398.4	132.09	0.20
HIR_GALESBURG_FWD_PostHIR WB	854.00	41.7	485.0	269.0	199.0	140.0	97.0	71.0	55.0	399.6	115.55	0.22

HIR_GALESBURG_FWD_PostHIR WB	793.00	41.7	319.0	105.0	91.0	86.0	61.0	53.0	44.0	325.4	69.21	0.21
HIR_GALESBURG_FWD_PostHIR WB	716.75	41.7	402.0	139.0	126.0	109.0	89.0	71.0	56.0	336.6	59.16	0.26
HIR_GALESBURG_FWD_PostHIR WB	669.17	41.9	337.0	116.0	107.0	88.0	74.0	62.0	50.0	336.1	70.09	0.22
HIR_GALESBURG_FWD_PostHIR WB	610.00	41.9	338.0	163.0	143.0	117.0	105.0	78.0	62.0	401.2	124.01	0.18
HIR_GALESBURG_FWD_PostHIR WB	548.70	41.5	277.0	155.0	151.0	132.0	106.0	89.0	73.0	469.0	206.40	0.12
HIR_GALESBURG_FWD_PostHIR WB	486.78	42.0	341.0	196.0	173.0	147.0	129.0	98.0	77.0	453.1	178.38	0.15
HIR_GALESBURG_FWD_PostHIR WB	426.39	41.8	331.0	169.0	149.0	126.0	95.0	74.0	57.0	418.7	141.83	0.16
HIR_GALESBURG_FWD_PostHIR WB	364.48	42.5	281.0	125.0	86.0	56.0	38.0	33.0	28.0	338.4	128.32	0.16
HIR_GALESBURG_FWD_PostHIR WB	305.00	42.1	400.0	221.0	197.0	166.0	140.0	104.0	78.0	442.9	138.90	0.18
HIR_GALESBURG_FWD_PostHIR WB	244.00	41.6	387.0	204.0	187.0	159.0	125.0	99.0	75.0	435.7	129.62	0.18
HIR_GALESBURG_FWD_PostHIR WB	183.00	41.6	484.0	309.0	256.0	206.0	162.0	128.0	97.0	468.3	164.17	0.18
HIR_GALESBURG_FWD_PostHIR WB	121.70	41.5	381.0	204.0	178.0	140.0	121.0	88.0	69.0	425.6	136.13	0.18
HIR_GALESBURG_FWD_PostHIR WB	60.70	41.8	291.0	148.0	133.0	115.0	92.0	78.0	64.0	422.7	160.05	0.14
HIR_GALESBURG_FWD_PostOverlay EB	61.61	44.0	208.3	174.2	156.2	140.2	106.2	86.6	68.8	601.5	1106.07	0.03
HIR_GALESBURG_FWD_PostOverlay EB	123.22	43.2	326.4	227.6	176.0	140.0	109.0	81.8	59.2	480.7	317.57	0.10
HIR_GALESBURG_FWD_PostOverlay EB	183.61	43.7	251.5	168.7	135.9	112.3	94.0	74.9	60.7	479.7	364.50	0.08
HIR_GALESBURG_FWD_PostOverlay EB	244.92	43.8	239.0	172.5	136.9	111.8	87.4	75.7	60.2	500.2	487.93	0.07
HIR_GALESBURG_FWD_PostOverlay EB	306.22	43.9	261.9	182.9	148.6	127.0	101.3	83.3	65.5	497.7	397.83	0.08
HIR_GALESBURG_FWD_PostOverlay EB	367.22	43.3	279.9	197.1	142.0	111.5	80.3	63.5	53.3	467.6	382.68	0.08
HIR_GALESBURG_FWD_PostOverlay EB	427.00	43.5	257.8	179.3	136.7	106.7	81.5	64.5	48.8	475.4	398.80	0.08
HIR_GALESBURG_FWD_PostOverlay EB	489.22	44.1	95.3	71.9	57.9	47.5	33.3	30.7	25.9	520.4	1453.27	0.02
HIR_GALESBURG_FWD_PostOverlay EB	549.31	43.1	160.3	145.3	130.0	106.2	78.5	58.7	36.3	628.8	2722.03	0.01
HIR_GALESBURG_FWD_PostOverlay EB	611.53	43.2	126.2	88.1	73.2	59.9	53.1	45.2	39.6	499.8	824.63	0.04
HIR_GALESBURG_FWD_PostOverlay EB	672.22	43.1	177.3	125.5	98.0	81.3	61.5	53.6	43.7	490.8	614.64	0.05
HIR_GALESBURG_FWD_PostOverlay EB	732.92	43.7	133.1	92.5	78.5	67.1	59.7	46.0	37.1	506.7	769.18	0.04
HIR_GALESBURG_FWD_PostOverlay EB	794.53	43.6	169.2	107.2	88.9	65.3	53.3	48.0	38.1	460.6	460.07	0.06
HIR_GALESBURG_FWD_PostOverlay EB	853.70	43.7	249.2	191.0	144.0	114.3	87.9	67.3	53.1	507.2	593.05	0.06
HIR_GALESBURG_FWD_PostOverlay EB	915.00	43.3	219.2	167.4	127.8	92.5	73.9	56.1	43.2	502.7	663.17	0.05
HIR_GALESBURG_FWD_PostOverlay EB	976.92	42.2	339.6	257.8	192.8	147.1	110.0	83.6	65.5	499.1	417.69	0.08
HIR_GALESBURG_FWD_PostOverlay EB	1038.22	43.2	377.7	294.4	215.4	156.7	119.9	89.4	68.3	500.2	421.00	0.08

HIR_GALESBURG_FWD_PostOverlay EB	1098.92	43.0	445.0	348.7	251.7	181.4	140.7	102.4	77.7	498.4	366.33	0.10
HIR_GALESBURG_FWD_PostOverlay EB	1159.61	44.2	213.6	170.2	137.9	112.3	83.3	74.2	60.7	542.0	825.39	0.04
HIR_GALESBURG_FWD_PostOverlay EB	1220.61	43.0	329.9	241.8	175.5	129.0	93.2	72.9	57.9	478.2	374.18	0.09
HIR_GALESBURG_FWD_PostOverlay EB	1281.61	43.0	420.9	315.2	224.8	161.8	124.2	95.0	74.9	480.2	318.96	0.11
HIR_GALESBURG_FWD_PostOverlay EB	1343.53	43.0	382.5	288.8	215.9	160.8	119.4	90.9	71.4	495.6	362.48	0.09
HIR_GALESBURG_FWD_PostOverlay EB	1405.14	43.1	349.0	268.2	207.0	160.8	130.8	105.2	78.7	512.3	428.18	0.08
HIR_GALESBURG_FWD_PostOverlay WB	1403.31	43.1	386.3	308.4	232.4	173.5	126.0	96.0	71.6	517.6	460.61	0.08
HIR_GALESBURG_FWD_PostOverlay WB	1280.70	43.4	295.7	235.2	175.3	132.6	102.9	78.2	61.5	514.4	592.19	0.06
HIR_GALESBURG_FWD_PostOverlay WB	1220.61	43.1	373.9	271.5	191.3	135.4	98.8	73.2	59.7	466.7	319.26	0.10
HIR_GALESBURG_FWD_PostOverlay WB	1159.00	43.7	241.0	187.2	148.6	116.8	87.4	75.7	59.7	524.1	649.00	0.05
HIR_GALESBURG_FWD_PostOverlay WB	1097.70	43.3	328.7	254.0	189.2	132.3	98.8	78.5	60.5	499.0	465.69	0.07
HIR_GALESBURG_FWD_PostOverlay WB	1035.78	42.8	433.6	334.8	242.3	174.0	125.2	94.5	70.9	493.7	351.65	0.10
HIR_GALESBURG_FWD_PostOverlay WB	974.78	43.4	274.6	209.6	164.1	127.8	95.3	75.7	59.2	513.6	528.16	0.07
HIR_GALESBURG_FWD_PostOverlay WB	913.48	42.2	197.1	138.4	108.0	82.8	72.9	53.8	42.4	482.7	538.64	0.06
HIR_GALESBURG_FWD_PostOverlay WB	854.00	43.8	183.1	147.3	117.1	89.9	71.1	59.2	47.0	536.1	1010.77	0.04
HIR_GALESBURG_FWD_PostOverlay WB	792.39	43.8	127.0	87.1	73.9	64.5	58.7	46.0	38.1	503.7	774.11	0.04
HIR_GALESBURG_FWD_PostOverlay WB	728.65	43.5	162.6	113.3	89.4	76.2	56.4	49.8	38.6	489.8	636.40	0.05
HIR_GALESBURG_FWD_PostOverlay WB	670.39	43.7	182.1	125.7	97.8	79.0	67.6	58.2	47.5	479.7	550.95	0.06
HIR_GALESBURG_FWD_PostOverlay WB	609.09	41.9	258.3	172.5	130.3	103.9	75.7	63.2	48.8	461.8	349.95	0.09
HIR_GALESBURG_FWD_PostOverlay WB	549.00	42.5	195.6	166.1	138.9	106.2	95.0	67.8	49.0	571.9	1297.20	0.03
HIR_GALESBURG_FWD_PostOverlay WB	488.31	44.0	205.7	142.2	118.9	105.9	81.8	68.3	53.8	504.3	489.94	0.06
HIR_GALESBURG_FWD_PostOverlay WB	424.87	43.4	229.4	176.0	151.4	138.2	112.8	93.5	73.7	553.5	647.45	0.05
HIR_GALESBURG_FWD_PostOverlay WB	366.31	43.5	283.0	209.6	167.9	134.6	104.9	80.5	61.7	510.5	453.99	0.07
HIR_GALESBURG_FWD_PostOverlay WB	304.09	42.3	409.4	295.4	214.1	156.7	112.0	87.9	67.8	472.5	284.67	0.11
HIR_GALESBURG_FWD_PostOverlay WB	244.00	43.1	286.0	219.7	174.8	132.3	106.4	82.6	63.2	517.9	521.45	0.07
HIR_GALESBURG_FWD_PostOverlay WB	181.78	43.5	341.9	277.6	226.3	182.1	144.0	106.4	69.9	550.3	568.63	0.06
HIR_GALESBURG_FWD_PostOverlay WB	120.78	43.7	214.9	159.8	135.6	113.0	95.5	74.4	59.9	529.8	607.01	0.06
HIR_GALESBURG_FWD_PostOverlay WB	56.43	43.4	237.7	170.7	143.3	117.9	96.5	77.5	62.0	512.8	481.80	0.07

2. Machesney, IL

FileName	Chainage (m)	Load (kN)	D1 (μmm)	D2 (μmm)	D3 (μmm)	D4 (μmm)	D5 (μmm)	D6 (μmm)	D7 (μmm)	Area A (mm)	Surface Curvature Index - SCI (mm)	RoC
Machesney 4567 HIR_FWD Existing EB	60.09	41.0	764	303	57	32	24	23	18	238.1	0.46	38.71
Machesney 4567 HIR_FWD Existing EB	124.75	41.6	810	328	71	29	43	35	31	242.4	0.48	37.79
Machesney 4567 HIR_FWD Existing EB	126.88	40.9	691	301	69	39	35	35	29	253.8	0.39	50.28
Machesney 4567 HIR_FWD Existing EB	186.05	40.6	980	426	89	30	37	32	27	247.0	0.55	35.31
Machesney 4567 HIR_FWD Existing EB	244.00	40.3	743	324	103	51	35	30	22	267.4	0.42	46.87
Machesney 4567 HIR_FWD Existing EB	305.00	40.4	1045	382	74	53	44	35	28	233.7	0.66	24.82
Machesney 4567 HIR_FWD Existing EB	369.05	40.2	1088	435	79	40	39	32	25	237.3	0.65	27.57
Machesney 4567 HIR_FWD Existing EB	427.61	41.1	829	348	84	42	36	32	26	251.0	0.48	39.26
Machesney 4567 HIR_FWD Existing EB	488.00	41.0	661	297	106	54	39	30	27	277.7	0.36	55.54
Machesney 4567 HIR_FWD Existing EB	489.53	40.8	659	289	87	40	36	28	23	264.6	0.37	53.38
Machesney 4567 HIR_FWD Existing EB	549.31	40.4	966	366	50	31	29	31	25	227.2	0.60	28.42
Machesney 4567 HIR_FWD Existing EB	610.92	40.2	1032	398	60	49	43	36	30	232.4	0.63	27.38
Machesney 4567 HIR_FWD Existing EB	671.61	39.7	1152	515	135	62	52	42	33	260.3	0.64	31.60
Machesney 4567 HIR_FWD Existing WB	671.61	40.2	1109	522	157	80	60	45	36	273.9	0.59	36.08
Machesney 4567 HIR_FWD Existing WB	605.73	41.0	832	503	217	102	67	52	37	337.3	0.33	82.62
Machesney 4567 HIR_FWD Existing WB	548.70	39.7	1274	421	42	47	41	35	29	215.0	0.85	17.42
Machesney 4567 HIR_FWD Existing WB	488.00	41.8	637	260	88	49	27	27	21	264.2	0.38	48.74
Machesney 4567 HIR_FWD Existing WB	427.00	40.6	837	349	68	31	26	28	24	242.5	0.49	38.46
Machesney 4567 HIR_FWD Existing WB	366.00	40.4	1001	453	132	55	44	35	27	265.7	0.55	37.14
Machesney 4567 HIR_FWD Existing WB	304.39	40.2	1025	429	90	45	39	31	25	245.7	0.60	31.61
Machesney 4567 HIR_FWD Existing WB	242.17	40.6	747	280	56	34	28	21	16	235.5	0.47	36.10

Machesney 4567 HIR_FWD Existing WB	182.70	44.7	1141	438	93	40	42	38	30	237.3	0.70	24.56
Machesney 4567 HIR_FWD Existing WB	121.70	40.5	921	427	125	54	54	46	37	269.1	0.49	42.23
Machesney 4567 HIR_FWD Existing WB	60.70	41.3	945	452	147	67	43	33	30	279.1	0.49	43.70
Machesney 4567 HIR_FWD PostHIR EB	76.25	39.9	1426	596	64	16	36	39	30	227.8	0.83	22.65
Machesney 4567 HIR_FWD PostHIR EB	122.00	40.9	916	489	163	80	62	55	41	296.6	0.43	56.26
Machesney 4567 HIR_FWD PostHIR EB	183.00	39.9	1284	426	78	55	43	29	20	224.4	0.86	17.40
Machesney 4567 HIR_FWD PostHIR EB	244.31	39.9	1436	582	137	61	39	31	20	245.7	0.85	21.35
Machesney 4567 HIR_FWD PostHIR EB	309.58	38.9	1668	709	166	90	59	49	44	251.7	0.96	19.94
Machesney 4567 HIR_FWD PostHIR EB	372.10	40.3	1395	493	81	24	39	34	28	223.0	0.90	17.63
Machesney 4567 HIR_FWD PostHIR EB	427.31	40.5	1322	464	61	37	42	37	31	220.7	0.86	18.41
Machesney 4567 HIR_FWD PostHIR EB	488.92	39.9	1054	440	137	77	54	47	37	262.5	0.61	30.58
Machesney 4567 HIR_FWD PostHIR EB	549.92	40.2	1149	414	79	44	36	27	19	230.4	0.74	22.06
Machesney 4567 HIR_FWD PostHIR EB	610.31	40.8	1069	410	82	45	39	32	27	236.8	0.66	26.18
Machesney 4567 HIR_FWD PostHIR WB	610.31	40.7	1241	514	91	42	30	27	23	239.2	0.73	25.64
Machesney 4567 HIR_FWD PostHIR WB	547.78	41.5	1092	436	78	29	37	27	23	235.3	0.66	27.40
Machesney 4567 HIR_FWD PostHIR WB	488.00	40.8	770	335	125	62	54	40	33	276.0	0.43	45.03
Machesney 4567 HIR_FWD PostHIR WB	426.70	40.5	1115	596	155	46	38	38	29	278.0	0.52	46.32
Machesney 4567 HIR_FWD PostHIR WB	358.38	40.2	1573	634	96	24	28	29	26	231.0	0.94	19.31
Machesney 4567 HIR_FWD PostHIR WB	305.00	39.0	1613	687	95	43	43	38	35	235.6	0.93	20.70
Machesney 4567 HIR_Post Overlay EB	61.61	43.7	516	329	154	64	34	25	20	353.4	0.19	152.87
Machesney 4567 HIR_Post Overlay EB	124.75	44.4	544	303	124	57	37	38	33	318.0	0.24	103.94
Machesney 4567 HIR_Post Overlay EB	183.00	43.7	500	318	160	82	57	40	31	366.0	0.18	157.71
Machesney 4567 HIR_Post Overlay EB	244.00	43.6	385	243	120	67	45	36	26	364.5	0.14	200.15
Machesney 4567 HIR_Post Overlay EB	305.00	43.1	691	357	125	54	40	32	26	293.6	0.33	69.62
Machesney 4567 HIR_Post Overlay EB	366.92	43.3	436	286	155	88	60	42	34	385.2	0.15	197.55
Machesney 4567 HIR_Post Overlay EB	427.31	43.5	433	272	126	60	37	29	24	352.5	0.16	175.85
Machesney 4567 HIR_Post Overlay EB	488.92	43.2	433	285	159	86	53	31	25	389.1	0.15	201.02
Machesney 4567 HIR_Post Overlay EB	549.31	44.0	515	277	99	40	30	30	26	300.1	0.24	101.88
Machesney 4567 HIR_Post Overlay EB	619.76	43.3	656	328	122	65	39	28	22	295.7	0.33	68.91
Machesney 4567 HIR_Post Overlay EB	672.83	43.6	614	342	138	68	44	35	30	317.5	0.27	92.03

Machesney 4567 HIR_Post Overlay WB	670.70	43.1	666	418	203	96	56	41	36	357.1	0.25	113.77
Machesney 4567 HIR_Post Overlay WB	623.12	43.3	490	309	140	67	43	33	25	351.0	0.18	156.38
Machesney 4567 HIR_Post Overlay WB	549.31	43.4	555	295	115	55	43	34	28	306.5	0.26	91.89
Machesney 4567 HIR_Post Overlay WB	488.31	43.2	453	272	126	60	31	25	22	343.1	0.18	148.19
Machesney 4567 HIR_Post Overlay WB	426.39	43.2	516	304	139	69	49	34	26	339.2	0.21	125.41
Machesney 4567 HIR_Post Overlay WB	366.00	43.2	560	320	126	50	34	24	22	316.4	0.24	106.89
Machesney 4567 HIR_Post Overlay WB	304.09	43.3	576	340	149	73	37	30	25	334.8	0.24	112.01
Machesney 4567 HIR_Post Overlay WB	243.09	43.5	436	244	93	39	24	19	15	311.3	0.19	131.47
Machesney 4567 HIR_Post Overlay WB	182.70	43.2	497	288	121	53	34	30	26	326.1	0.21	124.91
Machesney 4567 HIR_Post Overlay WB	119.87	43.3	476	299	137	60	37	32	27	349.5	0.18	160.01
Machesney 4567 HIR_Post Overlay WB	58.56	42.8	473	336	201	117	76	46	33	421.1	0.14	232.88
Machesney 89 HIR_Existing EB	76.25	42.2	530	285	127	71	42	36	26	322.6	0.24	98.77
Machesney 89 HIR_Existing EB	129.93	41.8	610	256	83	45	30	26	20	264.8	0.35	53.35
Machesney 89 HIR_Existing EB	194.59	42.0	633	295	94	49	31	26	18	276.1	0.34	62.05
Machesney 89 HIR_Existing EB	249.80	43.9	704	334	103	43	25	24	20	274.2	0.37	57.70
Machesney 89 HIR_Existing EB	305.31	44.4	714	279	61	25	28	16	17	239.5	0.43	40.42
Machesney 89 HIR_Existing WB	305.00	42.8	601	269	71	30	29	19	16	260.1	0.33	60.67
Machesney 89 HIR_Existing WB	236.38	41.8	689	323	100	50	41	28	22	274.7	0.37	57.64
Machesney 89 HIR_Existing WB	179.65	40.5	711	343	98	49	25	23	17	274.1	0.37	58.99
Machesney 89 HIR_Existing WB	121.70	42.3	566	315	153	77	45	27	20	335.0	0.25	99.78
Machesney 89 HIR_Existing WB	61.00	43.3	605	291	83	44	39	26	25	274.2	0.31	68.93
Machesney 89 HIR_PostHIR EB	62.22	41.0	683	374	170	84	51	33	25	325.2	0.31	79.69
Machesney 89 HIR_PostHIR EB	122.31	39.6	850	375	104	39	24	24	19	259.7	0.47	41.79
Machesney 89 HIR_PostHIR EB	183.31	40.9	846	327	86	47	36	26	20	246.8	0.52	33.49
Machesney 89 HIR_PostHIR EB	244.31	40.0	806	340	95	43	24	21	17	256.6	0.47	40.77
Machesney 89 HIR_PostHIR WB	242.48	40.1	747	332	94	42	31	20	16	262.8	0.42	48.18
Machesney 89 HIR_PostHIR WB	182.39	41.3	814	337	62	37	22	21	18	241.8	0.48	39.06
Machesney 89 HIR_PostHIR WB	122.00	42.9	700	220	115	53	36	26	22	257.8	0.48	29.45
Machesney 89 HIR_PostHIR WB	60.70	40.6	750	336	138	78	43	33	26	288.0	0.41	48.70
Machesney 89 HIR_Overlay EB	61.00	43.2	442	294	152	80	45	39	29	380.3	0.15	203.11

Machesney 89_HIR_Overlay EB	122.92	43.8	419	254	114	47	23	18	15	339.0	0.17	164.42
Machesney 89_HIR_Overlay EB	183.31	43.5	422	239	101	42	31	21	17	321.9	0.18	139.06
Machesney 89_HIR_Overlay EB	243.70	44.6	424	255	117	49	26	18	14	339.9	0.17	159.93
Machesney 89_HIR_Overlay EB	308.36	43.4	440	259	112	54	31	25	19	333.2	0.18	146.48
Machesney 89_HIR_Overlay WB	304.09	42.2	427	245	107	50	36	24	19	328.3	0.18	141.36
Machesney 89_HIR_Overlay WB	243.70	43.6	359	215	94	38	12	16	12	333.9	0.14	187.17
Machesney 89_HIR_Overlay WB	182.70	43.0	463	319	167	73	37	24	19	385.2	0.14	215.78
Machesney 89_HIR_Overlay WB	122.00	43.5	354	218	99	48	27	21	17	346.9	0.14	203.88
Machesney 89_HIR_Overlay WB	60.39	43.1	510	299	131	62	38	31	24	333.4	0.21	125.91
Machesney 15-18_FWD_Existing EB	122.61	41.6	586	298	142	78	54	38	29	318.9	0.29	79.46
Machesney 15-18_FWD_Existing EB	183.00	41.0	621	317	146	80	49	38	29	316.4	0.30	75.56
Machesney 15-18_FWD_Existing EB	244.92	41.4	525	227	100	67	49	41	29	291.1	0.30	65.29
Machesney 15-18_FWD_Existing EB	305.31	40.2	910	469	197	115	80	57	43	311.2	0.44	52.59
Machesney 15-18_FWD_Existing EB	370.58	40.5	859	489	285	135	77	57	45	358.5	0.37	69.24
Machesney 15-18_FWD_Existing EB	427.31	40.8	637	309	139	85	62	43	32	308.2	0.33	66.55
Machesney 15-18_FWD_Existing EB	488.61	41.0	535	257	126	91	70	55	43	318.2	0.28	77.76
Machesney 15-18_FWD_Existing EB	545.95	44.0	500	248	143	97	75	41	27	339.3	0.25	88.57
Machesney 15-18_FWD_Existing EB	610.31	40.4	686	372	169	101	66	50	41	327.3	0.31	77.71
Machesney 15-18_FWD_Existing EB	671.92	41.4	734	395	167	78	55	35	26	314.9	0.34	71.44
Machesney 15-18_FWD_Existing EB	732.00	41.8	655	306	116	68	43	35	27	288.8	0.35	60.24
Machesney 15-18_FWD_Existing EB	793.61	42.8	591	281	111	69	38	35	29	295.2	0.31	69.02
Machesney 15-18_FWD_Existing EB	854.00	41.8	625	267	111	66	46	37	29	283.2	0.36	53.70
Machesney 15-18_FWD_Existing EB	915.92	43.3	609	275	103	63	54	35	28	284.0	0.33	60.84
Machesney 15-18_FWD_Existing EB	976.61	42.2	595	277	111	66	41	31	22	292.4	0.32	65.88
Machesney 15-18_FWD_Existing EB	1046.15	40.4	697	356	144	86	57	47	40	307.1	0.34	67.40
Machesney 15-18_FWD_Existing EB	1098.31	41.8	870	415	176	89	65	44	36	297.6	0.45	47.18
Machesney 15-18_FWD_Existing WB	1098.00	41.4	1002	481	197	94	67	51	40	295.1	0.52	41.46
Machesney 15-18_FWD_Existing WB	1037.00	46.4	668	352	136	76	54	44	33	307.2	0.32	75.04
Machesney 15-18_FWD_Existing WB	1036.09	41.3	712	357	152	81	56	41	33	306.3	0.35	63.56
Machesney 15-18_FWD_Existing WB	975.70	40.7	607	294	128	74	51	37	27	304.2	0.31	69.63

Machesney 15-18_FWD_Existing WB	914.70	40.0	1017	477	169	95	57	46	37	284.2	0.54	39.09
Machesney 15-18_FWD_Existing WB	853.39	41.9	705	353	130	76	45	37	30	296.6	0.35	64.01
Machesney 15-18_FWD_Existing WB	792.09	42.7	688	360	103	54	36	32	26	285.2	0.33	71.79
Machesney 15-18_FWD_Existing WB	732.00	40.4	801	371	123	61	47	34	26	277.0	0.43	48.47
Machesney 15-18_FWD_Existing WB	671.00	41.1	713	369	164	97	58	44	33	317.0	0.34	67.70
Machesney 15-18_FWD_Existing WB	610.00	47.3	764	406	180	103	72	52	44	320.6	0.36	66.80
Machesney 15-18_FWD_Existing WB	547.17	41.3	575	278	127	75	62	44	34	308.3	0.30	73.25
Machesney 15-18_FWD_Existing WB	606.95	41.2	750	345	165	97	81	58	47	304.4	0.41	51.08
Machesney 15-18_FWD_PostHIR EB	668.26	41.0	1010	454	206	110	65	49	34	294.9	0.56	36.38
Machesney 15-18_FWD_PostHIR EB	729.56	40.1	813	331	123	71	44	34	25	269.5	0.48	38.00
Machesney 15-18_FWD_PostHIR EB	790.87	40.1	759	267	127	79	48	39	31	268.6	0.49	32.17
Machesney 15-18_FWD_PostHIR EB	912.56	42.5	768	321	118	73	47	39	31	273.1	0.45	42.08
Machesney 15-18_FWD_PostHIR EB	973.26	42.4	670	300	121	62	37	33	24	285.2	0.37	54.44
Machesney 15-18_FWD_PostHIR EB	1034.56	40.2	873	442	173	96	67	52	40	301.9	0.43	52.85
Machesney 15-18_FWD_PostHIR EB	1095.26	43.0	836	363	148	96	66	51	42	285.5	0.47	41.31
Machesney 15-18_FWD_PostHIR WB	1094.95	42.2	933	405	153	89	66	48	39	278.6	0.53	36.98
Machesney 15-18_FWD_PostHIR WB	1033.34	41.4	783	389	164	93	77	50	38	305.2	0.39	56.69
Machesney 15-18_FWD_PostHIR WB	971.73	40.2	665	298	122	67	56	40	30	287.3	0.37	54.93
Machesney 15-18_FWD_PostHIR WB	911.95	39.6	1274	645	220	107	73	55	42	290.3	0.63	36.20
Machesney 15-18_FWD_PostHIR WB	728.95	40.3	1049	501	167	84	61	45	34	281.4	0.55	39.20
Machesney 15-18_FWD_PostHIR WB	665.82	39.9	1029	500	218	119	84	61	44	303.8	0.53	41.36
Machesney 15-18_FWD_PostHIR WB	606.04	39.9	1002	454	174	94	65	55	44	284.1	0.55	37.19
Machesney 15-18_FWD_Overlay EB	502.03	43.0	396	263	145	85	67	49	37	391.9	0.13	225.11
Machesney 15-18_FWD_Overlay EB	545.95	43.1	486	298	154	83	57	40	30	362.2	0.19	146.58
Machesney 15-18_FWD_Overlay EB	606.65	43.1	399	278	162	95	68	48	37	412.2	0.12	261.64
Machesney 15-18_FWD_Overlay EB	667.95	42.8	415	253	127	76	47	37	29	361.3	0.16	170.07
Machesney 15-18_FWD_Overlay EB	728.95	43.1	428	269	134	61	42	27	21	359.6	0.16	178.78
Machesney 15-18_FWD_Overlay EB	789.95	43.9	340	201	96	44	26	24	20	343.1	0.14	192.17
Machesney 15-18_FWD_Overlay EB	850.95	43.1	373	240	125	64	41	31	24	372.7	0.13	215.66
Machesney 15-18_FWD_Overlay EB	911.95	42.9	484	310	153	81	48	37	30	366.1	0.17	165.73

Machesney 15-18_FWD_Overlay EB	973.26	43.1	413	235	100	50	36	26	21	326.4	0.18	143.41
Machesney 15-18_FWD_Overlay EB	1036.39	43.3	410	261	137	87	48	39	31	377.6	0.15	192.12
Machesney 15-18_FWD_Overlay EB	1095.26	43.0	468	284	136	76	43	38	30	352.7	0.18	148.52
Machesney 15-18_FWD_Overlay EB	1155.65	43.3	401	247	113	49	29	23	18	345.3	0.15	179.67
Machesney 15-18_FWD_Overlay WB	1155.65	43.0	390	239	111	56	30	24	19	348.9	0.15	182.26
Machesney 15-18_FWD_Overlay WB	1093.73	43.0	409	268	142	79	50	35	29	381.3	0.14	209.11
Machesney 15-18_FWD_Overlay WB	1033.34	43.2	357	251	151	92	58	41	30	420.3	0.11	295.91
Machesney 15-18_FWD_Overlay WB	970.21	42.9	467	290	144	76	44	31	25	359.7	0.18	158.21
Machesney 15-18_FWD_Overlay WB	911.34	42.5	504	295	136	61	40	30	23	336.8	0.21	126.71
Machesney 15-18_FWD_Overlay WB	850.04	43.3	456	283	131	60	45	29	23	349.2	0.17	161.51
Machesney 15-18_FWD_Overlay WB	788.12	42.3	499	307	145	64	33	25	21	348.6	0.19	144.71
Machesney 15-18_FWD_Overlay WB	727.73	42.7	454	267	117	52	34	23	19	332.4	0.19	141.36
Machesney 15-18_FWD_Overlay WB	667.65	43.0	393	249	131	71	45	33	27	372.9	0.14	199.53
Machesney 15-18_FWD_Overlay WB	605.43	43.0	449	270	140	73	47	37	31	358.4	0.18	151.69
Machesney 15-18_FWD_Overlay WB	545.04	43.0	401	239	126	75	56	45	34	362.1	0.16	166.22
Machesney 15-18_FWD_Overlay WB	502.34	42.8	425	268	144	81	56	47	39	374.6	0.16	179.92

3. Dyer, IN

FileName	Chainage (m)	Load (kN)	D1 (µmm)	D2 (µmm)	D3 (µmm)	D4 (µmm)	D5 (µmm)	D6 (µmm)	D7(µmm)	Area A (mm)	Surface Curvature Index - SCI (mm)	RoC
Dyer_HIR_FWD_Existing EB	366.00	41.14	354	257	185	141	117	96	82	475.4	0.10	336.8
Dyer_HIR_FWD_Existing EB	427.00	40.93	429	300	195	134	78	62	48	438.1	0.13	243.9
Dyer_HIR_FWD_Existing EB	488.92	40.86	500	338	214	141	95	78	61	422.1	0.16	187.8
Dyer_HIR_FWD_Existing EB	549.61	42.48	322	247	174	120	89	68	54	483.1	0.08	460.2
Dyer_HIR_FWD_Existing EB	610.61	41.56	397	295	197	128	96	62	48	458.7	0.10	327.8
Dyer_HIR_FWD_Existing EB	671.31	41.92	426	289	187	128	81	70	55	428.5	0.14	222.8
Dyer_HIR_FWD_Existing EB	732.00	41.85	400	285	177	110	76	56	44	430.9	0.12	278.8

Dyer_HIR_FWD_Existing EB	793.00	44.32	374	268	179	121	89	65	49	449.6	0.11	304.2
Dyer_HIR_FWD_Existing EB	856.75	42.06	363	243	151	100	69	53	42	416.5	0.12	251.0
Dyer_HIR_FWD_Existing EB	915.31	42.27	382	261	151	85	49	39	32	404.5	0.12	254.1
Dyer_HIR_FWD_Existing EB	973.87	42.34	269	195	128	88	64	47	37	450.6	0.07	440.8
Dyer_HIR_FWD_Existing EB	1047.98	50.33	360	270	186	126	89	64	50	470.0	0.09	375.0
Dyer_HIR_FWD_Existing EB	1098.31	42.13	407	302	210	153	113	91	77	472.5	0.11	318.0
Dyer_HIR_FWD_Existing EB	1160.22	41.28	478	367	251	172	126	103	86	476.7	0.11	311.3
Dyer_HIR_FWD_Existing EB	1220.31	41.85	257	193	135	103	76	68	56	480.4	0.06	528.0
Dyer_HIR_FWD_Existing EB	1281.92	41.35	375	247	154	93	61	45	35	409.2	0.13	231.6
Dyer_HIR_FWD_Existing EB	1341.09	43.12	295	205	132	86	58	42	32	432.2	0.09	347.5
Dyer_HIR_FWD_Existing EB	1405.14	42.84	283	199	138	89	60	45	34	448.9	0.08	376.7
Dyer_HIR_FWD_Existing EB	1464.61	41.92	286	200	129	87	57	47	36	435.8	0.09	365.9
Dyer_HIR_FWD_Existing EB	1528.36	43.12	351	234	157	105	80	58	46	429.1	0.12	256.4
Dyer_HIR_FWD_Existing EB	1586.61	42.27	391	353	174	98	55	33	26	456.5	0.04	1069.1
Dyer_HIR_FWD_Existing EB	1647.31	41.7	678	501	296	138	77	54	46	422.3	0.18	187.9
Dyer_HIR_FWD_Existing EB	1708.61	41.63	358	250	167	113	81	63	49	442.0	0.11	291.0
Dyer_HIR_FWD_Existing EB	1769.92	41.99	286	207	144	97	75	55	43	460.5	0.08	412.3
Dyer_HIR_FWD_Existing EB	1830.92	47.36	370	266	170	104	67	41	28	437.8	0.10	311.1
Dyer_HIR_FWD_Existing EB	1895.58	41.56	378	237	145	89	67	41	32	394.4	0.14	200.1
Dyer_HIR_FWD_Existing EB	1959.02	41.99	356	228	146	99	66	50	38	410.8	0.13	225.2
Dyer_HIR_FWD_Existing EB	2013.61	42.2	255	181	114	73	44	34	28	433.5	0.07	431.6
Dyer_HIR_FWD_Existing EB	2074.00	42.91	313	203	132	84	59	45	34	414.1	0.11	265.3
Dyer_HIR_FWD_Existing EB	2135.61	41.7	367	233	138	86	56	41	30	393.2	0.13	213.2
Dyer_HIR_FWD_Existing WB	2135.00	41.07	480	305	168	95	58	41	33	380.0	0.18	163.4
Dyer_HIR_FWD_Existing WB	2074.31	41.63	432	286	179	118	75	57	44	414.6	0.15	204.1
Dyer_HIR_FWD_Existing WB	2012.09	41.99	344	225	134	81	57	38	30	400.3	0.12	247.3
Dyer_HIR_FWD_Existing WB	1951.39	41.7	352	245	159	101	67	50	38	433.0	0.11	292.7
Dyer_HIR_FWD_Existing WB	1890.39	41.85	348	252	160	105	65	46	37	441.8	0.10	339.4
Dyer_HIR_FWD_Existing WB	1830.00	41.78	381	270	163	96	59	40	31	422.4	0.11	287.3
Dyer_HIR_FWD_Existing WB	1769.00	43.26	389	287	188	125	93	65	51	453.9	0.10	325.5

Dyer_HIR_FWD_Existing WB	1708.00	41.35	358	249	159	104	78	54	41	431.1	0.11	287.1
Dyer_HIR_FWD_Existing WB	1645.78	41.7	415	305	194	114	68	40	37	441.7	0.11	300.7
Dyer_HIR_FWD_Existing WB	1583.56	41.7	414	301	178	61	41	29	24	410.1	0.11	289.5
Dyer_HIR_FWD_Existing WB	1515.85	42.13	358	246	173	123	92	67	52	449.6	0.11	276.1
Dyer_HIR_FWD_Existing WB	1463.70	41.99	288	200	140	104	76	57	44	454.2	0.09	355.1
Dyer_HIR_FWD_Existing WB	1403.31	39.51	246	158	100	66	51	38	26	408.5	0.09	328.4
Dyer_HIR_FWD_Existing WB	1341.70	42.27	340	231	146	95	70	53	43	422.6	0.11	280.5
Dyer_HIR_FWD_Existing WB	1278.87	43.61	469	325	208	135	94	69	52	430.2	0.14	216.6
Dyer_HIR_FWD_Existing WB	1220.00	41.21	519	367	236	151	101	80	65	436.1	0.15	209.3
Dyer_HIR_FWD_Existing WB	1157.48	40.93	456	339	234	164	120	91	78	469.4	0.12	285.9
Dyer_HIR_FWD_Existing WB	1098.00	41.35	451	330	224	153	116	87	72	459.6	0.12	272.1
Dyer_HIR_FWD_Existing WB	1017.48	41.7	394	288	194	136	96	69	57	459.1	0.11	310.3
Dyer_HIR_FWD_Existing WB	975.39	41.78	417	314	204	131	92	68	50	456.8	0.10	329.0
Dyer_HIR_FWD_Existing WB	914.09	41.07	467	308	183	109	74	52	41	401.5	0.16	186.7
Dyer_HIR_FWD_Existing WB	854.00	41.7	267	202	140	100	75	54	45	477.0	0.07	523.8
Dyer_HIR_FWD_Existing WB	791.48	42.27	321	255	173	125	86	68	55	489.3	0.07	541.6
Dyer_HIR_FWD_Existing WB	729.26	41.7	379	254	157	100	77	56	45	414.4	0.13	241.3
Dyer_HIR_FWD_Existing WB	670.39	41.99	353	260	175	122	92	67	52	461.0	0.09	356.4
Dyer_HIR_FWD_Existing WB	610.61	41.42	437	296	171	98	57	42	35	402.6	0.14	216.2
Dyer_HIR_FWD_PostHIR EB	0.00	42.41	449	312	196	124	100	71	55	426.6	0.14	228.2
Dyer_HIR_FWD_PostHIR EB	61.00	42.48	405	293	177	110	76	57	46	430.4	0.11	290.7
Dyer_HIR_FWD_PostHIR EB	122.00	42.48	513	367	226	144	96	72	57	431.6	0.15	220.5
Dyer_HIR_FWD_PostHIR EB	183.00	43.12	360	245	151	102	65	55	44	420.4	0.12	266.3
Dyer_HIR_FWD_PostHIR EB	244.61	42.48	436	286	162	94	57	40	31	392.2	0.15	196.8
Dyer_HIR_FWD_PostHIR EB	305.00	42.48	331	233	150	105	65	50	38	439.1	0.10	323.2
Dyer_HIR_FWD_PostHIR EB	367.22	42.27	379	290	200	138	100	71	49	477.7	0.09	386.9
Dyer_HIR_FWD_PostHIR EB	428.83	42.06	478	358	242	168	122	99	82	466.9	0.12	280.9
Dyer_HIR_FWD_PostHIR EB	488.00	41.92	563	422	277	188	144	113	94	460.1	0.14	239.2
Dyer_HIR_FWD_PostHIR EB	550.53	42.13	367	260	176	129	96	83	68	452.9	0.11	297.9
Dyer_HIR_FWD_PostHIR EB	610.00	41.85	513	353	223	139	98	69	51	424.3	0.16	193.5

Dyer_HIR_FWD_PostHIR EB	675.88	42.48	350	240	154	97	76	54	40	426.4	0.11	280.5
Dyer_HIR_FWD_PostHIR EB	736.27	41.35	410	304	208	136	94	64	47	463.2	0.11	314.8
Dyer_HIR_FWD_PostHIR EB	915.92	41.85	848	557	270	102	32	26	30	362.1	0.29	101.6
Dyer_HIR_FWD_PostHIR EB	977.83	43.54	435	293	176	99	54	31	23	406.6	0.14	213.5
Dyer_HIR_FWD_PostHIR EB	1038.22	42.48	425	261	150	92	53	43	35	380.5	0.16	168.5
Dyer_HIR_FWD_PostHIR EB	1098.92	42.06	451	294	187	128	91	80	64	414.7	0.16	186.8
Dyer_HIR_FWD_PostHIR EB	1220.61	41.85	442	300	178	100	69	44	35	406.6	0.14	215.1
Dyer_HIR_FWD_PostHIR EB	1281.31	42.13	477	333	218	138	91	66	49	435.2	0.14	218.2
Dyer_HIR_FWD_PostHIR EB	1344.44	42.48	388	253	144	83	56	38	27	391.2	0.14	217.4
Dyer_HIR_FWD_PostHIR EB	1404.83	42.48	384	238	134	81	45	37	29	379.3	0.15	191.0
Dyer_HIR_FWD_PostHIR EB	1466.75	42.13	418	276	163	98	65	44	34	401.2	0.14	209.2
Dyer_HIR_FWD_PostHIR EB	1525.00	42.13	441	286	161	96	61	43	33	389.5	0.16	188.3
Dyer_HIR_FWD_PostHIR WB	1525.00	41.07	491	311	175	101	64	43	32	382.8	0.18	158.4
Dyer_HIR_FWD_PostHIR WB	1463.39	41.21	513	315	180	109	67	44	33	379.2	0.20	139.6
Dyer_HIR_FWD_PostHIR WB	1402.70	41.85	596	383	205	107	61	43	35	376.5	0.21	135.8
Dyer_HIR_FWD_PostHIR WB	1342.00	42.2	462	300	168	97	51	40	30	388.0	0.16	180.4
Dyer_HIR_FWD_PostHIR WB	1277.95	41.99	497	337	218	146	87	63	49	427.4	0.16	190.7
Dyer_HIR_FWD_PostHIR WB	1219.70	41.85	390	274	167	97	62	45	34	421.2	0.12	272.5
Dyer_HIR_FWD_PostHIR WB	1159.00	40.86	491	335	203	119	74	54	44	412.7	0.16	196.8
Dyer_HIR_FWD_PostHIR WB	1097.70	41.7	440	300	191	138	94	81	67	429.5	0.14	219.2
Dyer_HIR_FWD_PostHIR WB	1035.48	41.56	503	317	178	98	60	46	37	379.9	0.19	152.5
Dyer_HIR_FWD_PostHIR WB	975.70	41.14	426	284	173	96	49	31	24	405.6	0.14	211.3
Dyer_FWD_Post Overlay EB	610.31	43.68	306	246	181	130	95	69	50	511.8	0.06	602.9
Dyer_FWD_Post Overlay EB	672.83	44.11	298	237	171	109	85	58	46	496.3	0.06	586.7
Dyer_FWD_Post Overlay EB	732.92	43.61	240	185	133	95	71	52	41	491.3	0.06	630.7
Dyer_FWD_Post Overlay EB	793.31	43.68	229	187	139	103	76	56	43	522.1	0.04	874.9
Dyer_FWD_Post Overlay EB	854.31	43.9	257	203	154	123	96	79	65	520.0	0.05	658.2
Dyer_FWD_Post Overlay EB	916.22	43.68	272	199	134	91	58	45	37	457.7	0.07	451.0
Dyer_FWD_Post Overlay EB	976.61	43.54	288	196	125	80	52	39	29	424.0	0.09	332.9
Dyer_FWD_Post Overlay EB	1037.61	43.26	267	229	183	138	103	75	54	561.8	0.04	1015.7

Dyer_FWD_Post Overlay EB	1098.61	42.91	271	219	163	118	92	65	53	517.0	0.05	699.3
Dyer_FWD_Post Overlay EB	1160.53	43.47	239	173	128	97	80	61	47	480.1	0.07	493.5
Dyer_FWD_Post Overlay EB	1220.00	43.33	268	219	168	130	91	77	62	533.4	0.05	750.5
Dyer_FWD_Post Overlay EB	1283.75	43.68	266	208	155	112	85	70	57	505.3	0.06	606.7
Dyer_FWD_Post Overlay EB	1342.00	43.54	263	195	132	93	57	41	31	464.8	0.07	490.7
Dyer_FWD_Post Overlay EB	1404.83	43.9	185	144	103	70	54	37	29	490.5	0.04	854.3
Dyer_FWD_Post Overlay EB	1464.61	43.68	186	144	107	72	62	42	33	496.8	0.04	829.5
Dyer_FWD_Post Overlay EB	1525.31	43.75	194	141	105	73	55	45	35	477.8	0.05	617.1
Dyer_FWD_Post Overlay EB	1647.92	43.97	267	205	136	85	50	31	25	465.7	0.06	557.3
Dyer_FWD_Post Overlay EB	1708.31	42.76	504	355	224	136	82	58	44	429.5	0.15	212.7
Dyer_FWD_Post Overlay EB	1769.31	43.61	247	191	142	107	84	60	48	503.4	0.06	621.4
Dyer_FWD_Post Overlay EB	1833.36	43.47	175	138	106	79	58	44	34	517.7	0.04	959.1
Dyer_FWD_Post Overlay EB	1893.75	43.61	243	183	128	88	56	40	28	475.3	0.06	564.8
Dyer_FWD_Post Overlay EB	1952.61	43.68	239	178	121	81	56	40	30	464.4	0.06	549.4
Dyer_FWD_Post Overlay EB	2013.92	43.61	296	208	140	97	79	53	41	446.5	0.09	359.3
Dyer_FWD_Post Overlay EB	2075.83	43.68	220	152	104	71	49	35	28	443.9	0.07	457.2
Dyer_FWD_Post Overlay EB	2138.97	43.68	196	154	112	77	63	42	32	498.2	0.04	841.8
Dyer_FWD_Post Overlay WB	2135.00	44.67	361	266	180	120	78	56	40	460.0	0.10	349.0
Dyer_FWD_Post Overlay WB	2074.31	43.61	262	188	121	75	46	37	28	439.1	0.07	436.4
Dyer_FWD_Post Overlay WB	2012.09	43.54	221	168	121	91	58	45	35	490.0	0.05	645.4
Dyer_FWD_Post Overlay WB	1951.09	43.54	222	178	129	86	71	46	34	502.7	0.04	820.0
Dyer_FWD_Post Overlay WB	1890.39	44.04	228	180	125	83	57	38	28	487.5	0.05	740.1
Dyer_FWD_Post Overlay WB	1829.39	43.33	210	172	130	97	71	55	42	527.9	0.04	969.9
Dyer_FWD_Post Overlay WB	1768.39	43.54	279	213	150	108	75	55	43	483.9	0.07	520.5
Dyer_FWD_Post Overlay WB	1707.09	43.97	268	208	150	100	73	47	35	490.3	0.06	582.1
Dyer_FWD_Post Overlay WB	1525.61	43.54	219	166	118	86	63	50	39	484.2	0.05	643.6
Dyer_FWD_Post Overlay WB	1463.39	43.19	226	181	135	112	68	58	45	523.7	0.05	800.9
Dyer_FWD_Post Overlay WB	1402.39	43.47	262	206	148	103	77	55	42	496.4	0.06	631.8
Dyer_FWD_Post Overlay WB	1341.70	43.4	328	247	165	106	79	55	41	462.3	0.08	418.4
Dyer_FWD_Post Overlay WB	1280.39	43.12	269	211	153	106	71	66	54	497.4	0.06	608.6

Dyer_FWD_Post Overlay WB	1220.00	43.4	294	229	167	122	93	72	60	499.5	0.07	539.2
Dyer_FWD_Post Overlay WB	1158.39	43.33	296	232	172	124	97	74	58	504.7	0.06	551.1
Dyer_FWD_Post Overlay WB	1097.70	43.26	317	255	186	129	98	68	50	507.7	0.06	583.9
Dyer_FWD_Post Overlay WB	1037.00	43.19	306	246	185	135	101	76	57	518.1	0.06	602.9
Dyer_FWD_Post Overlay WB	975.39	43.33	357	248	162	102	74	47	37	433.2	0.11	286.8
Dyer_FWD_Post Overlay WB	915.31	43.26	266	219	168	122	102	69	52	531.8	0.05	788.3
Dyer_FWD_Post Overlay WB	852.78	43.75	225	189	149	116	85	65	51	552.0	0.04	1050.0
Dyer_FWD_Post Overlay WB	791.48	43.54	253	180	126	96	62	50	38	463.0	0.07	438.6
Dyer_FWD_Post Overlay WB	731.09	43.4	238	183	135	95	72	53	40	495.4	0.06	629.1
Dyer_FWD_Post Overlay WB	670.39	43.4	248	197	140	101	69	49	37	499.6	0.05	700.9
Dyer_FWD_Post Overlay WB	608.78	43.54	271	192	129	92	57	46	37	450.0	0.08	403.6

APPENDIX C: Extracted gradation of field collected samples

1. Galesburg, IL

Outer Lane

Project:		HIPR				Project:		HIPR			
Date Sampled (at ATREL):		6/13/2015				Date Sampled (at ATREL):		4/21/2015			
Date Tested:		6/13/2015				Date Tested:		4/22/2015			
Operator:		Punit				Operator:		Punit			
Material:		Gmm 1				Material:		Gmm 1			
Source:		Galesburg Outer Lane w/Rej				Source:		Galesburg Outer Lane w/Rej			
Date Sampled at Source:						Date Sampled at Source:					
Sample No:		1				Sample No:		2			

Sieve Size		Weight Retained	Cumulative Weight Retained	%Retained	%Passing	Sieve Size		Weight Retained	Cumulative Weight Retained	%Retained	%Passing
1"	25.0	0.0	0.0	0.0	100.0	1"	25.0	0.0	0.0	0.0	100.0
3/4"	19.0	0.0	0.0	0.0	100.0	3/4"	19.0	0.0	0.0	0.0	100.0
1/2"	12.5	9.5	9.5	0.6	99.4	1/2"	12.5	2.4	2.4	0.2	99.8
3/8"	9.5	128.8	138.3	8.7	91.3	3/8"	9.5	79.5	81.9	5.5	94.5
1/4"	6.25	0.0	138.3	8.7	91.3	1/4"	6.25	0.0	81.9	5.5	94.5
#4	4.75	547.2	685.5	43.0	57.0	#4	4.75	526.9	608.8	40.9	59.1
#8	2.36	349.6	1035.1	65.0	35.0	#8	2.36	353.7	962.5	64.6	35.4
#16	1.18	130.9	1166.0	73.2	26.8	#16	1.18	123.1	1085.6	72.9	27.1
#30	0.6	90.3	1256.3	78.9	21.1	#30	0.6	83.5	1169.1	78.5	21.5
#50	0.3	132.0	1388.3	87.2	12.8	#50	0.3	125.4	1294.5	86.9	13.1
#100	0.15	79.2	1467.5	92.1	7.9	#100	0.15	74.9	1369.4	92.0	8.0
#200	0.075	34.0	1501.5	94.3	5.7	#200	0.075	31.9	1401.3	94.1	5.9
Pan (Sieving)		31.3				Pan (Sieving)		30.0			
Pan (Cup Centrifuge)	Pan	59.7	1592.6			Pan (Cup Centrifuge)	Pan	57.5	1488.8		
Pan (Rotovap Filter)		0.1				Pan (Rotovap Filter)		0			
Initial Measurement before Extraction						Initial Measurement before Extraction					
Weight of Aggregates after Extraction	1592.6			Weight of Batch	1679.1	Weight of Aggregates after Extraction	1488.8			Weight of Batch	1570.7
Initial Weight of Evaporation Flask	205.7					Initial Weight of Evaporation Flask	205.7				
Final Weight of Evaporation Flask	289.3			Loss of Weight during Extraction	2.9	Final Weight of Evaporation Flask	284.6			Loss of Weight during Extraction	3.0
Binder Weight	83.6			% Loss	0.001727116	Binder Weight	78.9			% Loss	0.00191
Total Weight	1676.2			Binder Content (%)	4.98	Total Weight	1567.7			Binder Content (%)	5.02

Inner Lane

Project:	HIPR					Project:	HIPR				
Date Sampled (at ATREL):	5/28/2015					Date Sampled (at ATREL):	4/21/2015				
Date Tested:	5/28/2015					Date Tested:	4/22/2015				
Operator:	Punit					Operator:	Punit				
Material:	Gmm 1					Material:					
Source:	Galesburg Inner Lane w/Rej					Source:					
Date Sampled at Source:						Date Sampled at Source:					
Sample No:	1					Sample No:					

Sieve Size		Weight Retained	Cumulative Weight Retained	%Retained	%Passing	Sieve Size		Weight Retained	Cumulative Weight Retained	%Retained	%Passing	
1"	25.0	0.0	0.0	0.0	100.0	1"	25.0	0.0	0.0	0.0	100.0	
3/4"	19.0	0.0	0.0	0.0	100.0	3/4"	19.0	0.0	0.0	0.0	100.0	
1/2"	12.5	12.1	12.1	0.8	99.2	1/2"	12.5	13.4	13.4	0.9	99.1	
3/8"	9.5	127.0	139.1	9.0	91.0	3/8"	9.5	121.4	134.8	8.7	91.3	
1/4"	6.25	0.0	139.1	9.0	91.0	1/4"	6.25	0.0	134.8	8.7	91.3	
#4	4.75	521.1	660.2	42.5	57.5	#4	4.75	543.6	678.4	43.8	56.2	
#8	2.36	337.9	998.1	64.3	35.7	#8	2.36	333.1	1011.5	65.3	34.7	
#16	1.18	113.4	1111.5	71.6	28.4	#16	1.18	107.4	1118.9	72.2	27.8	
#30	0.6	77.7	1189.2	76.6	23.4	#30	0.6	74.6	1193.5	77.0	23.0	
#50	0.3	134.3	1323.5	85.3	14.7	#50	0.3	131.9	1325.4	85.5	14.5	
#100	0.15	86.6	1410.1	90.8	9.2	#100	0.15	85.5	1410.9	91.0	9.0	
#200	0.075	37.3	1447.4	93.2	6.8	#200	0.075	38.3	1449.2	93.5	6.5	
Pan (Sieving)	Pan	20.7	1552.3			Pan (Sieving)	Pan	36.1				
Pan (Cup Centrifuge)		83.8				Pan (Cup Centrifuge)		64.4	1549.7			
Pan (Rotovap Filter)		0.4				Pan (Rotovap Filter)						
Initial Measurement before Extraction						Initial Measurement before Extraction						
Weight of Aggregates after Extraction	1552.3	Weight of Batch			1641.3	Weight of Aggregates after Extraction	1549.7	Weight of Batch			1634.6	
Initial Weight of Evaporation Flask	205.4	Loss of Weight during Extraction			1.7	Initial Weight of Evaporation Flask	205.6	Loss of Weight during Extraction			1.4	
Final Weight of Evaporation Flask	292.7	% Loss			0.001035764	Final Weight of Evaporation Flask	289.1	% Loss			0.0008565	
Binder Weight	87.3	Binder Content (%)			5.32	Binder Weight	83.5	Binder Content (%)			5.11	
Total Weight	1639.6					Total Weight	1633.2					

2. Machesney, IL

Section 15-16

Project:		HIPR				Project:		HIPR			
Date Sampled (at ATREL):		4/23/2015				Date Sampled (at ATREL):		6/16/2015			
Date Tested:		4/23/2015				Date Tested:		6/16/2015			
Operator:		Punit				Operator:		Punit			
Material:		Gmm 1				Material:		Gmm 2			
Source:		Machesney Section 15-16 with Rejuvenator				Source:		Machesney Section 15-16 with Rejuvenator			
Date Sampled at Source:						Date Sampled at Source:					
Sample No:		1				Sample No:		2			

Sieve Size	Weight Retained	Cumulative Weight Retained	%Retained	%Passing	
1"	25.0	0.0	0.0	100.0	
3/4"	19.0	65.4	3.7	96.3	
1/2"	12.5	315.6	21.6	78.4	
3/8"	9.5	158.7	30.6	69.4	
1/4"	6.25	0.0	30.6	69.4	
#4	4.75	531.0	60.8	39.2	
#8	2.36	278.8	1349.5	76.6	23.4
#16	1.18	110.3	1459.8	82.9	17.1
#30	0.6	72.7	1532.5	87.0	13.0
#50	0.3	70.6	1603.1	91.0	9.0
#100	0.15	37.2	1640.3	93.1	6.9
#200	0.075	27.0	1667.3	94.7	5.3
Pan (Sieving)		28.2			
Pan (Cup Centrifuge)	Pan	66.0	1761.5		
Pan (Rotovap Filter)		0			

Sieve Size	Weight Retained	Cumulative Weight Retained	%Retained	%Passing	
1"	25.0	0.0	0.0	100.0	
3/4"	19.0	50.1	3.1	96.9	
1/2"	12.5	241.8	18.3	81.7	
3/8"	9.5	148.6	27.7	72.3	
1/4"	6.25	0.0	27.7	72.3	
#4	4.75	496.3	58.8	41.2	
#8	2.36	272.5	1209.3	75.9	24.1
#16	1.18	104.4	1313.7	82.5	17.5
#30	0.6	67.5	1381.2	86.7	13.3
#50	0.3	64.8	1446.0	90.8	9.2
#100	0.15	34.3	1480.3	92.9	7.1
#200	0.075	24.5	1504.8	94.5	5.5
Pan (Sieving)		32.6			
Pan (Cup Centrifuge)	Pan	55.6	1593.0		
Pan (Rotovap Filter)		0			

Initial Measurement before Extraction				Initial Measurement before Extraction			
Weight of Aggregates after Extraction	1761.5	Weight of Batch	1850.8	Weight of Aggregates after Extraction	1593.0	Weight of Batch	1674.7
Initial Weight of Evaporation Flask	205.7			Initial Weight of Evaporation Flask	205.7		
Final Weight of Evaporation Flask	293.9	Loss of Weight during Extraction	1.1	Final Weight of Evaporation Flask	286.1	Loss of Weight during Extraction	1.3
Binder Weight	88.2	% Loss	0.000594338	Binder Weight	80.4	% Loss	0.0007763
Total Weight	1849.7	Binder Content (%)	4.77	Total Weight	1673.4	Binder Content (%)	4.80

Section 17-18

Project:	HIPR
Date Sampled (at ATREL):	4/17/2015
Date Tested:	4/20/2015
Operator:	Punit
Material:	Gmm 1
Source:	Machesney Section 17-18 with Rejuvenator
Date Sampled at Source:	
Sample No:	1

Project:	HIPR
Date Sampled (at ATREL):	4/21/2015
Date Tested:	4/22/2015
Operator:	Punit
Material:	Gmm 2
Source:	Machesney Section 17-18 with Rejuvenator
Date Sampled at Source:	
Sample No:	2

Sieve Size		Weight Retained	Cumulative Weight Retained	%Retained	%Passing
1"	25.0	0.0	0.0	0.0	100.0
3/4"	19.0	162.2	162.2	11.0	89.0
1/2"	12.5	295.3	457.5	31.0	69.0
3/8"	9.5	140.8	598.3	40.6	59.4
1/4"	6.25	244.2	842.5	57.1	42.9
#4	4.75	130.2	972.7	66.0	34.0
#8	2.36	165.7	1138.4	77.2	22.8
#16	1.18	48.6	1187.0	80.5	19.5
#30	0.6	50.6	1237.6	83.9	16.1
#50	0.3	114.2	1351.8	91.7	8.3
#100	0.15	46.6	1398.4	94.8	5.2
#200	0.075	19.2	1417.6	96.1	3.9
Pan (Sieving)	Pan	19.9	1474.7		
Pan (Cup Centrifuge)		37.2			
Pan (Rotovap Filter)		0			

Sieve Size		Weight Retained	Cumulative Weight Retained	%Retained	%Passing
1"	25.0	0.0	0.0	0.0	100.0
3/4"	19.0	151.9	151.9	10.0	90.0
1/2"	12.5	216.8	368.7	24.3	75.7
3/8"	9.5	156.1	524.8	34.6	65.4
1/4"	6.25	279.3	804.1	53.1	46.9
#4	4.75	152.6	956.7	63.1	36.9
#8	2.36	195.7	1152.4	76.1	23.9
#16	1.18	54.7	1207.1	79.7	20.3
#30	0.6	55.3	1262.4	83.3	16.7
#50	0.3	122.8	1385.2	91.4	8.6
#100	0.15	49.6	1434.8	94.7	5.3
#200	0.075	20.3	1455.1	96.0	4.0
Pan (Sieving)	Pan	16.3	1515.2		
Pan (Cup Centrifuge)		43.8			
Pan (Rotovap Filter)		0			

Initial Measurement before Extraction				Initial Measurement before Extraction			
Weight of Aggregates after Extraction	1474.7	Weight of Batch	1536.4	Weight of Aggregates after Extraction	1515.2	Weight of Batch	1581.8
Initial Weight of Evaporation Flask	205.3			Initial Weight of Evaporation Flask	205.3		
Final Weight of Evaporation Flask	267.5	Loss of Weight during Extraction	-0.5	Final Weight of Evaporation Flask	272.5	Loss of Weight during Extraction	-0.6
Binder Weight	62.2	% Loss	-0.00032544	Binder Weight	67.2	% Loss	-0.000379
Total Weight	1536.9	Binder Content (%)	4.05	Total Weight	1582.4	Binder Content (%)	4.25

3. Dyer, IN

Project:			HIPR				
Date Sampled (at ATREL):			6/1/2015				
Date Tested:			6/1/2015				
Operator:			Punit				
Material:			Gmm 2				
Source:			Dyer w/Rej				
Date Sampled at Source:							
Sample No:			1				

Sieve Size		Weight Retained	Cumulative Weight Retained	%Retained	%Passing
1"	25.0	0.0	0.0	0.0	100.0
3/4"	19.0	0.0	0.0	0.0	100.0
1/2"	12.5	0.0	0.0	0.0	100.0
3/8"	9.5	81.9	81.9	4.9	95.1
1/4"	6.25	0.0	81.9	4.9	95.1
#4	4.75	618.2	700.1	41.7	58.3
#8	2.36	286.7	986.8	58.7	41.3
#16	1.18	141.7	1128.5	67.1	32.9
#30	0.6	113.1	1241.6	73.9	26.1
#50	0.3	162.9	1404.5	83.6	16.4
#100	0.15	102.2	1506.7	89.6	10.4
#200	0.075	50.7	1557.4	92.7	7.3
Pan (Sieving)	Pan	43.6	1680.8		
Pan (Cup Centrifuge)		71.9			
Pan (Rotovap Filter)		7.9			

Initial Measurement before Extraction			
Weight of Aggregates after Extraction	1680.8	Weight of Batch	1780.9
Initial Weight of Evaporation Flask	205.7		
Final Weight of Evaporation Flask	303.3	Loss of Weight during Extraction	2.5
Binder Weight	97.6	% Loss	0.001403785
Total Weight	1778.4	Binder Content (%)	5.48

APPENDIX D: Volumetric details of lab compacted samples

1. Galesburg, IL

Outer Lane

ID	Sample No.	Weight in Air	Weight in Water	SSD in Air	% Water Absorbed	Volume (cc)	Gmb (SSD Specific Gravity)	Voids (see below)	Gyrations	Height	Operator
GL-OL-R	1	7255.6	4207.5	7297.2	1.35	3089.7	2.348	6.9	12	179.54	P
GL-OL-R	1T	2089.8	1209.6	2095.8	0.68	886.2	2.358	6.5			
GL-OL-R	1B	2080	1202.6	2086.1	0.69	883.5	2.354	6.7			
GL-OL-R	H1	2500.6	1459.5	2519	1.74	1059.5	2.360	6.4	19	61.95	P
GL-OL-R	H2	2501.3	1458.4	2519.2	1.69	1060.8	2.358	6.5	18	61.94	P
GL-OL-R	H3	2499.9	1459.5	2520.3	1.92	1060.8	2.357	6.6	18	61.9	P
GL-OL-R	H4	2499.4	1457.8	2515.8	1.55	1058	2.362	6.3	20	61.97	P

Inner Lane

ID	Sample No.	Weight in Air	Weight in Water	SSD in Air	% Water Absorbed	Volume (cc)	Gmb (SSD Specific Gravity)	Voids (see below)	Gyrations	Height	Operator
GL-IL-R	1	6852	3976.4	6918.2	2.25	2941.8	2.329	7.0	10	169.9	P
GL-IL-R	1T	2078.6	1204.2	2086.3	0.87	882.1	2.356	5.9			
GL-IL-R	1B	2035.3	1173.8	2043.5	0.94	869.7	2.340	6.6			
GL-IL-R	H1	2498.6	1455.1	2521.5	2.15	1066.4	2.343	6.5	14	61.98	P
GL-IL-R	H2	2498.3	1459	2521.7	2.20	1062.7	2.351	6.1	16	61.93	P
GL-IL-R	H3	2498.5	1454.7	2521.9	2.19	1067.2	2.341	6.5	13	61.96	P
GL-IL-R	H4	2500.9	1458.6	2526.8	2.42	1068.2	2.341	6.5	16	61.95	P

2. Machesney, IL

Section 15-16

ID	Sample No.	Weight in Air	Weight in Water	SSD in Air	% Water Absorbed	Volume (cc)	Gmb (SSD Specific Gravity)	Voids (see below)	Gyrations	Height	Operator
M1516-R	1	7307.8	4263.9	7340.1	1.05	3076.2	2.376	7.1	53	179.97	P
M1516-R	1T	2109.7	1226.6	2115.8	0.69	889.2	2.373	7.2			
M1516-R	1B	2048.2	1194.8	2054.8	0.77	860	2.382	6.9			
M1516-R	H1	2515.9	1479.8	2529.1	1.26	1049.3	2.398	6.3	62	128	P
M1516-R	H2	2517.9	1481.2	2534	1.53	1052.8	2.392	6.5	61.99	110	P
M1516-R	H3	2516.2	1480.5	2529.9	1.31	1049.4	2.398	6.3	62	160	P
M1516-R	H4	2519.1	1483.3	2533.1	1.33	1049.8	2.400	6.2	62	201	P

Section 17-18

ID	Sample No.	Weight in Air	Weight in Water	SSD in Air	% Water Absorbed	Volume (cc)	Gmb (SSD Specific Gravity)	Voids (see below)	Gyrations	Height	Operator
M1718-R	1	7305.2	4311.6	7358	1.73	3046.4	2.398	5.8	69	179.96	P
M1718-R	1T	2124.8	1253.4	2132.1	0.83	878.7	2.418	5.1			
M1718-R	1B	2120.7	1255	2128.1	0.85	873.1	2.429	4.6			
M1718-R	H1	2497.1	1470.7	2513.5	1.57	1042.8	2.395	6.0	112	62	P
M1718-R	H2	2492.6	1464.8	2511.8	1.83	1047	2.381	6.5	98	62	P
M1718-R	H3	2498.5	1474.6	2518	1.87	1043.4	2.395	6.0	125	62	P
M1718-R	H4	2498.7	1472.3	2518	1.85	1045.7	2.389	6.2	135	62	P

3. Dyer, IN

ID	Sample No.	Weight in Air	Weight in Water	SSD in Air	% Water Absorbed	Volume (cc)	Gmb (SSD Specific Gravity)	Voids (see below)	Gyrations	Height	Operator
DY-R	1	7299	4240.9	7341.6	1.374	3100.7	2.354	6.4	31	179.87	P
DY-R	1T	2081.5	1210	2086.8	0.604	876.8	2.374	5.6			
DY-R	1B	2069.6	1203.6	2075.1	0.631	871.5	2.375	5.6			
DY-R	H1	2508.4	1468.8	2529.5	1.989	1060.7	2.365	6.0	78	61.99	P
DY-R	H2	2507.8	1466.7	2532.8	2.345	1066.1	2.352	6.5	67	62	P
DY-R	H3	2508.3	1467.9	2531.1	2.144	1063.2	2.359	6.2	71	61.99	P
DY-R	H4	2507.7	1468.8	2533.5	2.423	1064.7	2.355	6.4	73	62	P

APPENDIX E: Bending beam rheometer (BBR) summary

Section	Temperature (°C)	Sample ID	Stiffness (MPa)	Avg.	COV (%)	m value	Avg.	COV (%)
Galesburg Outer Lane	-36	S1	338	317	8.6	0.303	0.300	1.2
		S2	286			0.301		
		S3	327			0.296		
	-30	S1	162	169	10.2	0.349	0.337	3.1
		S2	157			0.331		
		S3	189			0.331		
Galesburg Inner Lane	-30	S1	248	258	4.1	0.301	0.290	4.0
		S2	325			0.272		
		S3	258			0.29		
		S4	269			0.278		
	-24	S1	134	132	3.1	0.33	0.335	1.6
		S2	127			0.341		
S3		134	0.335					
Machesney 15-16	-38	S1	268	255	4.7	0.317	0.315	3.1
		S2	245			0.304		
		S3	251			0.323		
	-36	S1	78.3	79	16.6	0.356	0.365	4.8
		S2	92			0.353		
		S3	65.9			0.385		
Machesney 17-18	-40	S1	304	185	0.4	0.289	0.216	1.0
		S2	184			0.214		
		S3	185			0.217		
	-36	S1	155	162	5.0	0.335	0.323	16.1
		S2	166			0.314		
		S3	156			0.385		
S4		172	0.259					
Dyer	-24	S1	259	259	NA	0.267	0.267	NA
	-18	S1	130	129	1.3	0.307	0.307	1.1
		S3	127			0.311		
		S4	130			0.304		


APPENDIX F.1: I-FIT parameter summary for lab compacted specimens using I-FIT tool



HIR Laboratory Compacted Mixtures Summary I-FIT Test under 50 mm/min loading application rate and 25°C

Mix ID	Mix Name	Specimen ID	Fracture Energy				Flexibility Index				Slope			
			Energy (LLD) (Gf) (J/m ²)	Avg. Fracture Energy	Std. Dev.	COV %	Flexibility Index	Avg. Flexibility Index	Std. Dev.	COV %	Slope	Avg. Slope	Std. Dev.	COV %
GAL-IL-R	Galesburg Inner Lane (with Rejuvenator)	R1B1	1024.85	1028.48	66.39	6.46	6.02	4.54	1.13	24.93	-1.70	-2.43	0.71	-29.12
		R1B2	1111.55				3.28				-3.39			
		R1T1	949.05				4.31				-2.20			
		R1T2	2060.54				9.65				-2.14			
GAL-OL-R	Galesburg Outer Lane (with Rejuvenator)	R1B1	610.96	811.36	120.11	14.80	4.66	8.15	0.66	8.07	-1.31	-0.99	0.10	-10.41
		R1B2	754.99				8.58				-0.88			
		R1T1	700.79				7.22				-0.97			
		R1T2	978.32				8.66				-1.13			
MACH 1516-R	Machesney 1516 (with Rejuvenator)	R1B1	791.10	360.60	31.68	8.79	12.02	4.08	0.32	7.74	-0.66	-0.88	0.03	-3.20
		R1B2	339.62				4.02				-0.84			
		R1T1	405.38				4.49				-0.90			
		R1T2	336.82				3.72				-0.90			
MACH 1718-R	Machesney 1718 (with Rejuvenator)	R1B1	985.33	960.05	202.83	21.13	0.65	0.59	0.11	18.62	-15.13	-16.13	0.90	-5.58
		R1B2	699.96				0.44				-15.95			
		R1T1	1194.85				0.69				-17.31			
		R1T2	1314.08				1.24				-10.59			
DYER-R	Dyer (with Rejuvenator)	R1B1	1067.33	1042.41	91.64	8.79	0.47	0.34	0.10	30.24	-22.72	-33.41	7.76	-23.22
		R1B2	1140.10				0.31				-36.61			
		R1T1	937.97				0.16				-58.51			
		R1T2	919.81				0.22				-40.90			

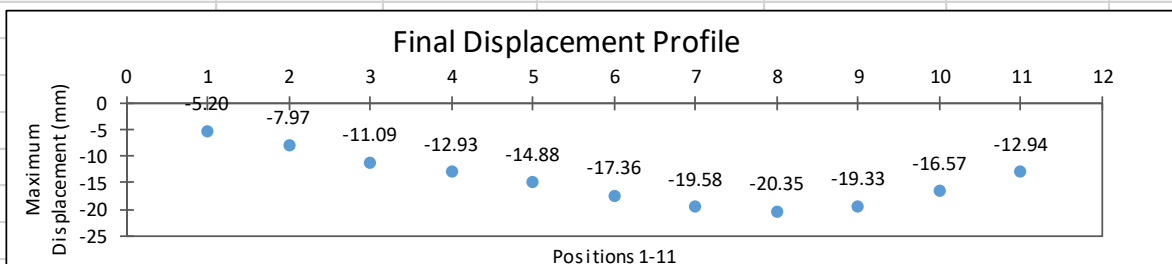
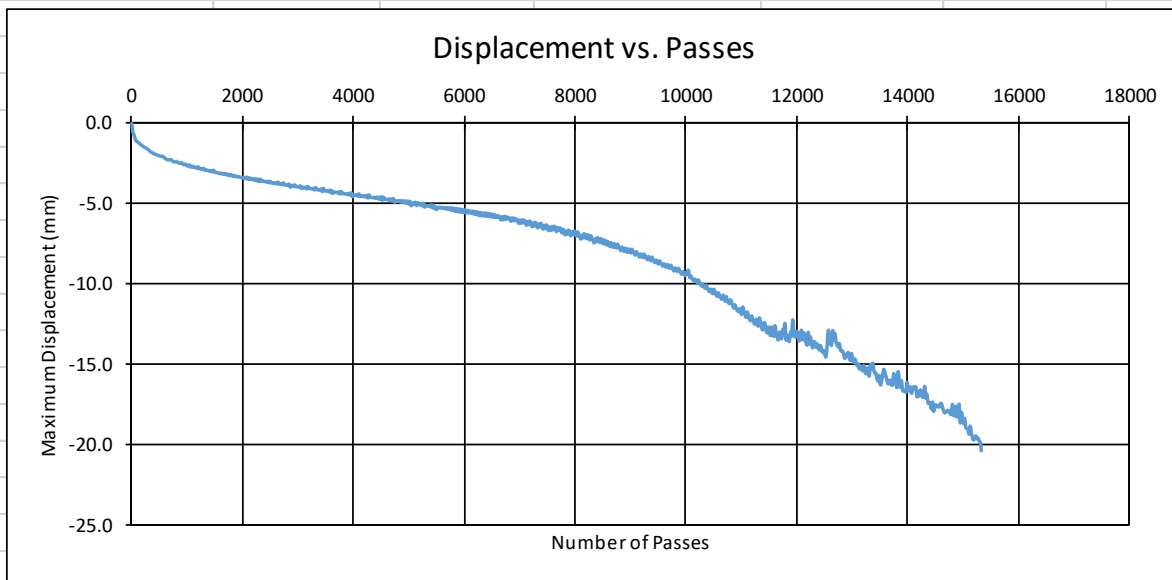
APPENDIX F.2: I-FIT parameter summary for field core specimens using I-FIT tool

	Sample Information		Fracture Energy (FE)			Flexibility Index (FI)					Slope				Thickness		Gmb	
	Mix Name	Specimen ID	FE (LLD) (Gf) (J/m ²)	Average FE	Std. Dev.	COV %	FI	Corrected FI	Average FI	Std. Dev.	COV %	Slope	Average of Slope	Std. Dev.	COV %	Thickness (mm)		Average Thickness (mm)
GW	Galesburg Inner Lane West bound	12R	2316.68	1912.10	406.33	21.25	18.99	6.09	5.68	2.09	36.86	-1.22	-1.61	0.36	-22.13	16.04	15.45	2.380
		12L	2245.27				14.12	4.20				-1.59				14.86		2.373
		36R	1304.92				5.99	3.96				-2.18				33.09		2.454
		36L	1781.53				12.37	8.48				-1.44				34.27		2.431
GE	Galesburg Inner Lane East bound	12R	1733.94	1449.86	228.98	15.79	27.09	9.16	4.27	3.52	82.47	-0.64	-3.03	2.15	-71.13	16.90	16.34	2.427
		12L	1614.10				14.41	4.55				-1.12				15.79		2.422
		36R	1197.96				2.32	1.66				-5.17				35.93		2.463
		36L	1253.42				2.42	1.72				-5.17				35.47		2.466
GWO	Galesburg Outer Lane West bound	12R	2754.86	2020.21	583.30	28.87	18.61	7.42	5.97	2.64	44.24	-1.48	-1.69	0.45	-26.72	19.94	19.77	2.415
		12L	2424.69				22.87	8.97				-1.06				19.60		2.402
		36R	1384.27				7.03	3.88				-1.97				27.61		2.439
		36L	1517.01				6.80	3.63				-2.23				26.66		2.465
GEO	Galesburg Outer Lane East bound	12R	2089.56	1611.80	277.94	17.24	9.86	4.46	4.51	0.26	5.84	-2.12	-1.99	0.34	-17.03	22.62	22.13	2.347
		12L	1407.50				9.98	4.32				-1.41				21.64		2.344
		36R	1446.60				6.34	4.36				-2.28				34.36		2.483
		36L	1503.55				7.06	4.89				-2.13				34.66		2.484
M1516	Machesney 1516	1R	892.39	1608.24	559.46	34.79	0.98	0.71	2.24	2.41	107.30	-9.14	-7.31	2.64	-36.10	36.26	35.77	2.341
		1L	2462.57				8.26	5.83				-2.98				35.27		2.339
		3R	1533.05				1.58	1.08				-9.71				34.12		2.404
		3L	1544.95				2.08	1.35				-7.42				32.52		2.377
M1718	Machesney 1718	1R	1872.41	1735.94	300.30	17.30	6.26	4.81	4.56	3.86	84.71	-2.99	-4.93	3.05	-61.87	38.42	38.51	2.398
		1L	1477.28				2.10	1.62				-7.03				38.61		2.398
		2R	2162.91				2.50	1.87				-8.66				37.45		2.400
		2L	1431.15				13.76	9.93				-1.04				36.07		2.396
DW	Dyer West Bound	28R	1223.49	1188.93	116.52	9.80	5.82	3.82	4.20	1.14	27.10	-2.102	-1.93	0.46	-24.00	32.78	32.72	2.291
		28L	1150.61				9.01	5.88				-1.277				32.66		2.283
		52R	1351.49				5.31	3.42				-2.543				32.15		2.335
		52L	1030.13				5.79	3.67				-1.78				31.71		2.338
DE	Dyer East Bound	28R	1497.10	1307.35	289.45	22.14	1.57	0.95	1.82	1.66	90.96	-9.54	-6.52	2.63	-40.42	30.19	30.48	2.162
		28L	1152.12				2.09	1.29				-5.51				30.78		2.176
		52R	919.67				1.11	0.77				-8.303				34.64		2.309
		52L	1660.53				6.10	4.29				-2.72				35.12		2.306

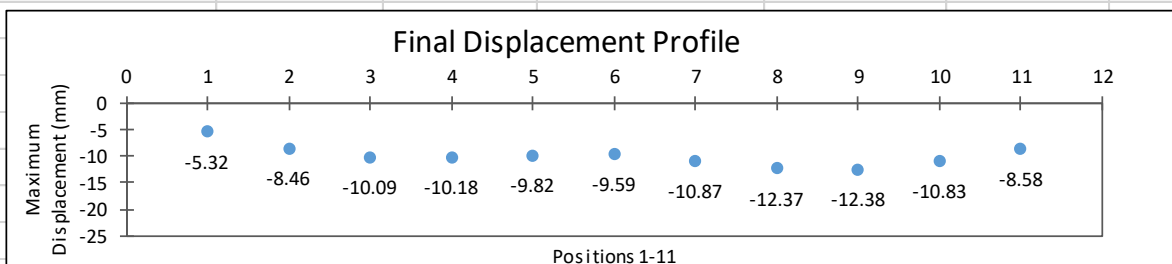
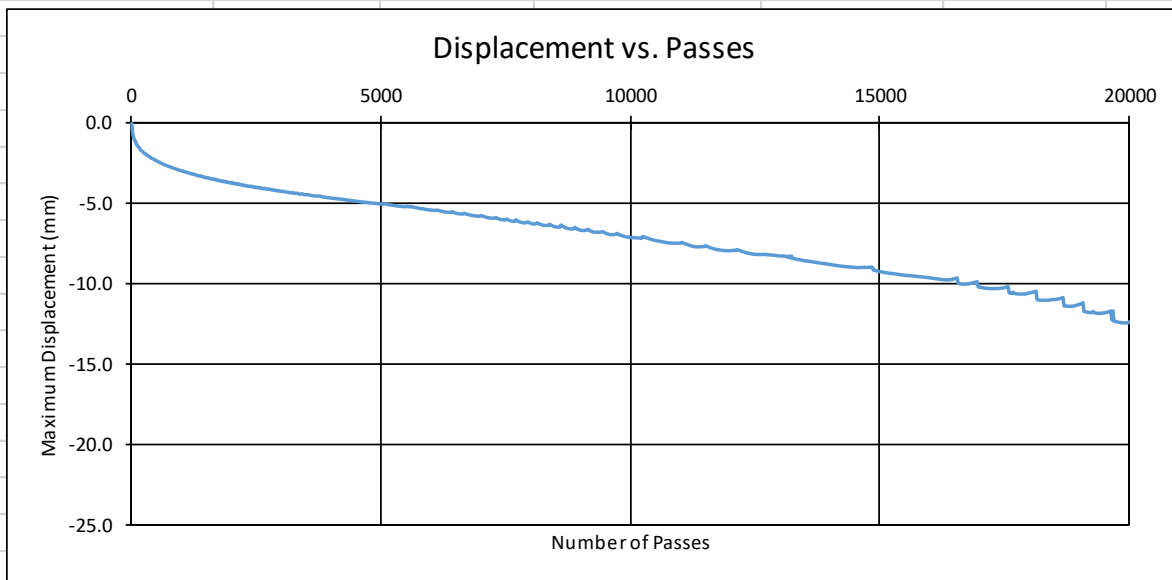
APPENDIX G: Hamburg wheel track test (HWTT) summary

Project Name:	HIR	Project Number:	CHPP	Date Tested:	05/01/15																								
Mix Type:	Gal-OL-R	Sampling:	Field Sampling																										
Binder:		Specimen Prep:	Lab compacted																										
Ndesign:		Compaction Type:	SGC																										
Specimen Information:																													
	Compacted Thickness:	62 mm																											
	Fabrication:	Saw cut mating faces																											
	Air Voids (%):	H1 = 6.4																											
		H2 = 6.5																											
Test Temperature:	50°C																												
Test Results:																													
Maximum Displacement	8.6	mm, at	10,000	passes																									
End Maximum Displacement	20.1	mm, at	20,000	passes																									
<p style="text-align: center;">Displacement vs. Passes</p>																													
<p style="text-align: center;">Final Displacement Profile</p> <table border="1" style="margin-left: auto; margin-right: auto;"> <thead> <tr> <th>Position</th> <th>Maximum Displacement (mm)</th> </tr> </thead> <tbody> <tr><td>1</td><td>-4.92</td></tr> <tr><td>2</td><td>-8.76</td></tr> <tr><td>3</td><td>-13.98</td></tr> <tr><td>4</td><td>-17.18</td></tr> <tr><td>5</td><td>-19.08</td></tr> <tr><td>6</td><td>-20.06</td></tr> <tr><td>7</td><td>-19.82</td></tr> <tr><td>8</td><td>-17.73</td></tr> <tr><td>9</td><td>-16.06</td></tr> <tr><td>10</td><td>-13.98</td></tr> <tr><td>11</td><td>-11.90</td></tr> </tbody> </table>						Position	Maximum Displacement (mm)	1	-4.92	2	-8.76	3	-13.98	4	-17.18	5	-19.08	6	-20.06	7	-19.82	8	-17.73	9	-16.06	10	-13.98	11	-11.90
Position	Maximum Displacement (mm)																												
1	-4.92																												
2	-8.76																												
3	-13.98																												
4	-17.18																												
5	-19.08																												
6	-20.06																												
7	-19.82																												
8	-17.73																												
9	-16.06																												
10	-13.98																												
11	-11.90																												

Project Name:	HIR	Project Number:	CHPP	Date Tested:	05/01/15
Mix Type:	Gal-OL-R	Sampling:	Field Sampling		
Binder:		Specimen Prep:	Lab compacted		
Ndesign:		Compaction Type:	SGC		
Specimen Information:					
	Compacted Thickness:	62 mm			
	Fabrication:	Saw cut mating faces			
	Air Voids (%):	H3 = 6.6			
		H4 = 6.3			
Test Temperature:	50°C				
Test Results:					
Maximum Displacement	9.3	mm,	at	10,000	passes
End Maximum Displacement	20.4	mm,	at	20,000	passes



Project Name:	HIR	Project Number:	CHPP	Date Tested:	05/05/15
Mix Type:	Gal-IL-R	Sampling:	Field Sampling		
Binder:		Specimen Prep:	Lab compacted		
Ndesign:		Compaction Type:	SGC		
Specimen Information:					
	Compacted Thickness:	62 mm			
	Fabrication:	Saw cut mating faces			
	Air Voids (%):	H1 = 6.5			
		H2 = 6.1			
Test Temperature:	50°C				
Test Results:					
Maximum Displacement	7.1	mm,	at	10,000	passes
End Maximum Displacement	12.4	mm,	at	20,000	passes



Project Name:	HIR	Project Number:	CHPP	Date Tested:	05/05/15
Mix Type:	Gal-IL-R	Sampling:	Field Sampling		
Binder:		Specimen Prep:	Lab compacted		
Ndesign:		Compaction Type:	SGC		

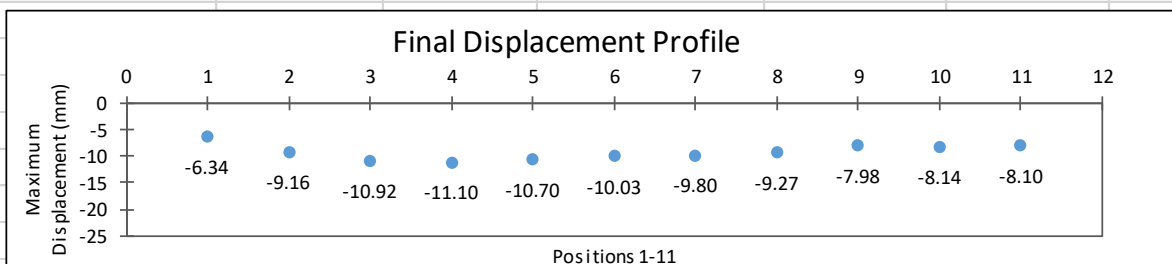
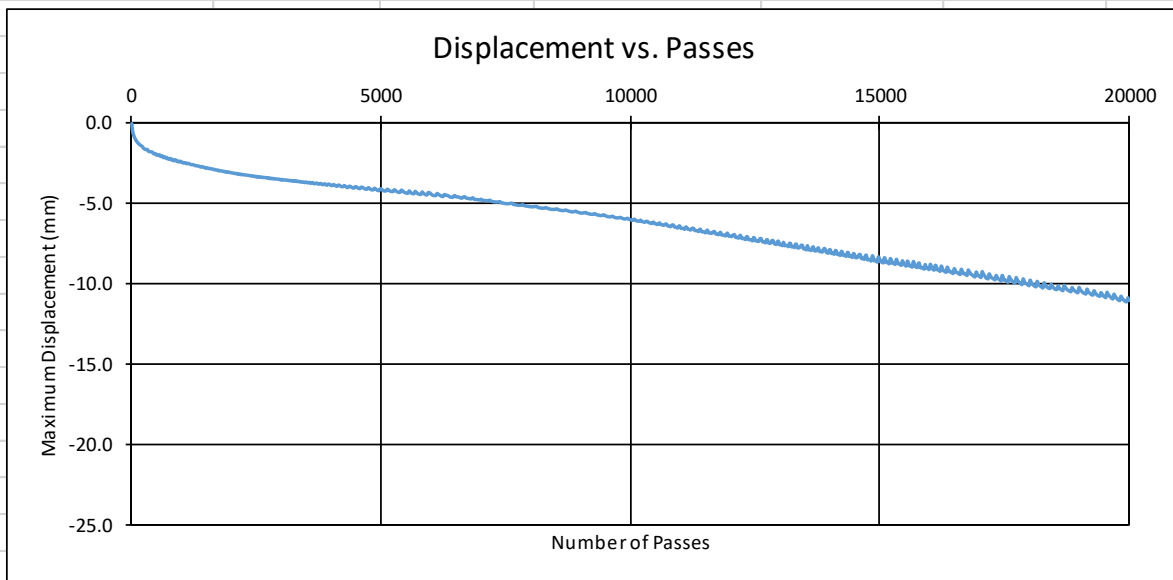
Specimen Information:

Compacted Thickness:	62 mm
Fabrication:	Saw cut mating faces
Air Voids (%):	H3 = 6.5 H4 = 6.5

Test Temperature: 50°C

Test Results:

Maximum Displacement	6.0	mm, at	10,000	passes
End Maximum Displacement	11.1	mm, at	20,000	passes



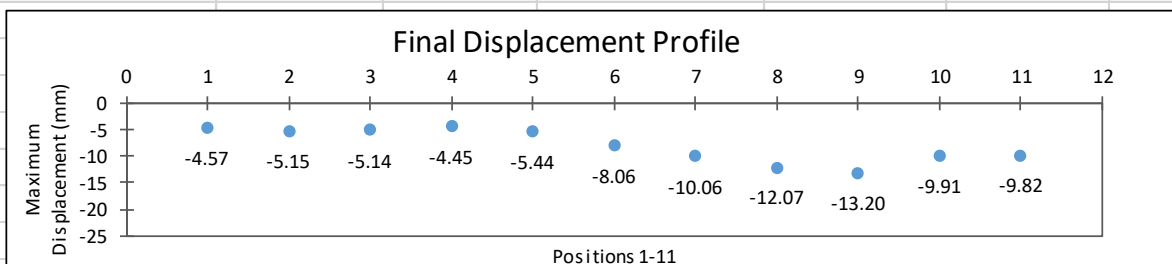
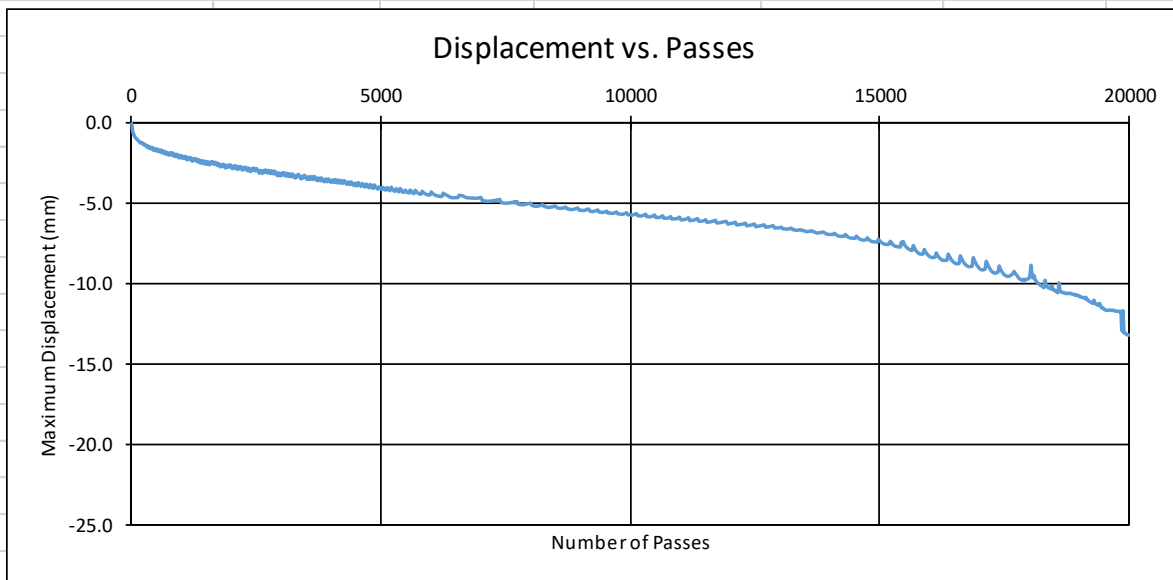
Project Name:	HIR	Project Number:	CHPP	Date Tested:	04/24/15
Mix Type:	Mach 15-16-R	Sampling:	Field Sampling		
Binder:		Specimen Prep:	Lab compacted		
Ndesign:		Compaction Type:	SGC		

Specimen Information:

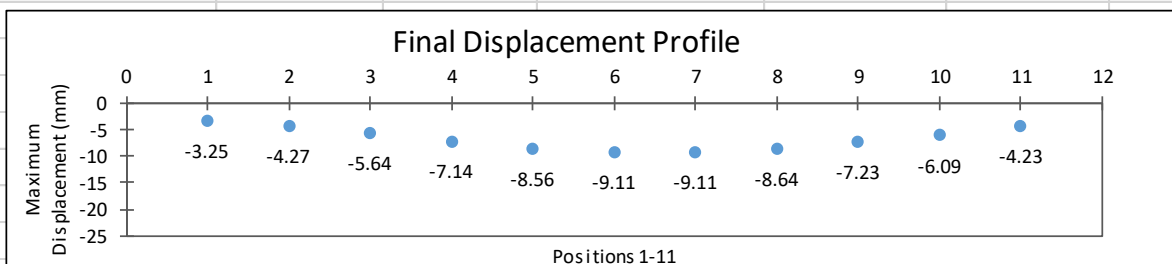
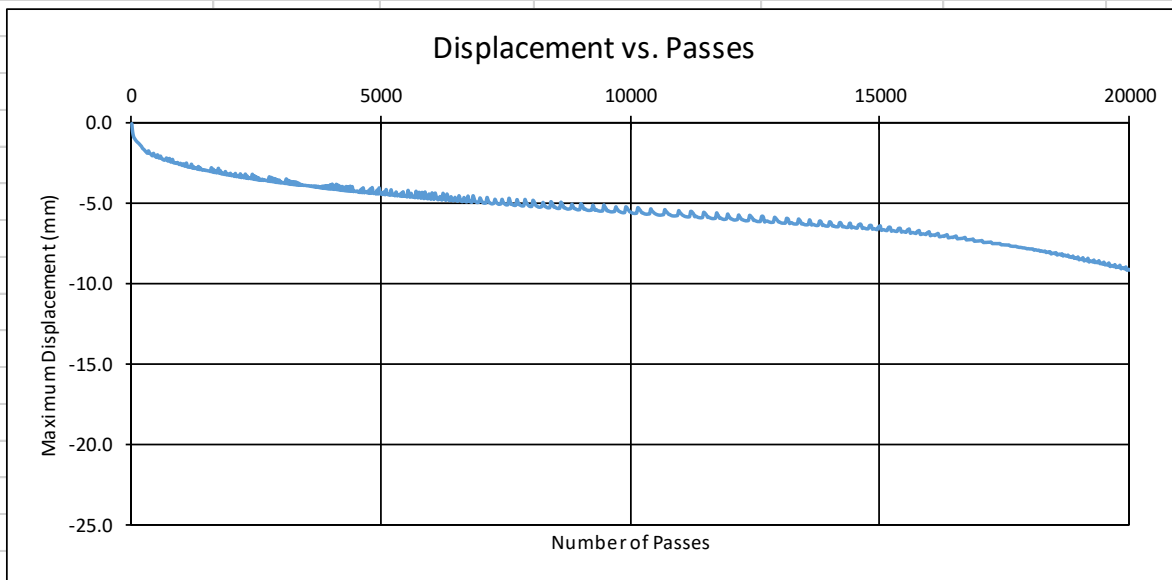
Compacted Thickness:	62 mm
Fabrication:	Saw cut mating faces
Air Voids (%):	H1 = 6.3 H2 = 6.5
Test Temperature:	50°C

Test Results:

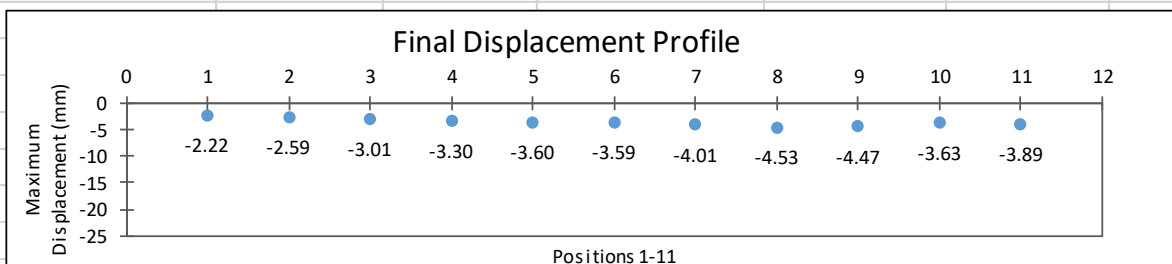
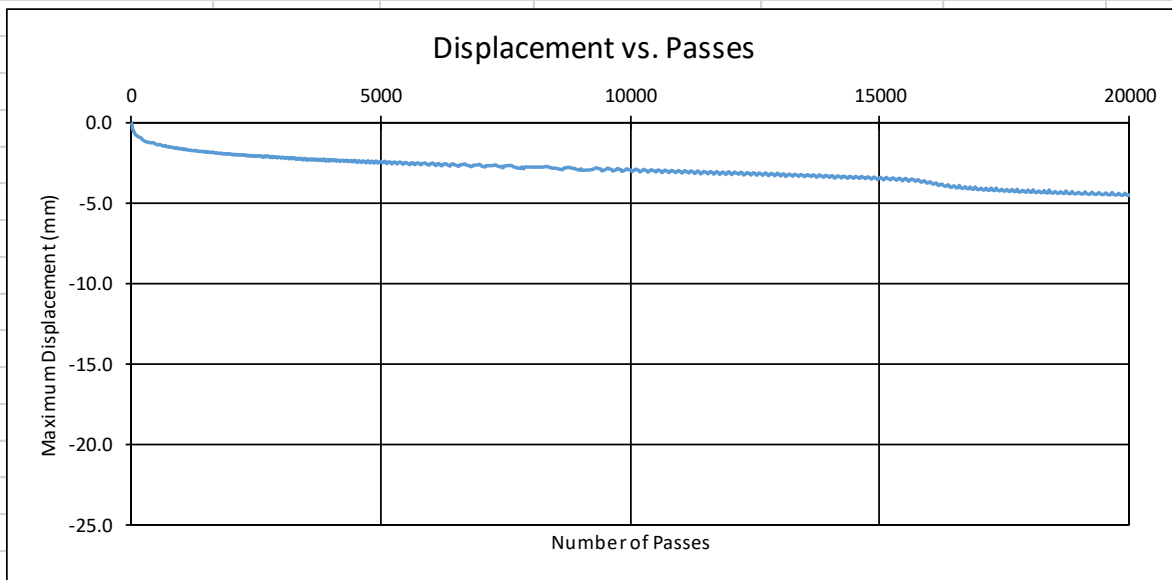
Maximum Displacement	5.7	mm, at	10,000	passes
End Maximum Displacement	13.2	mm, at	20,000	passes



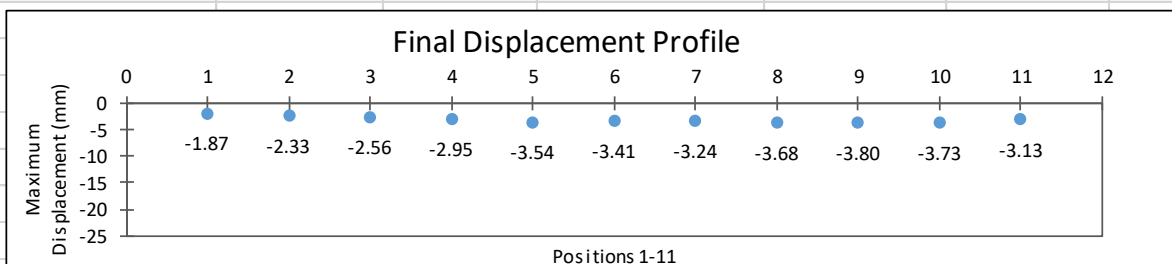
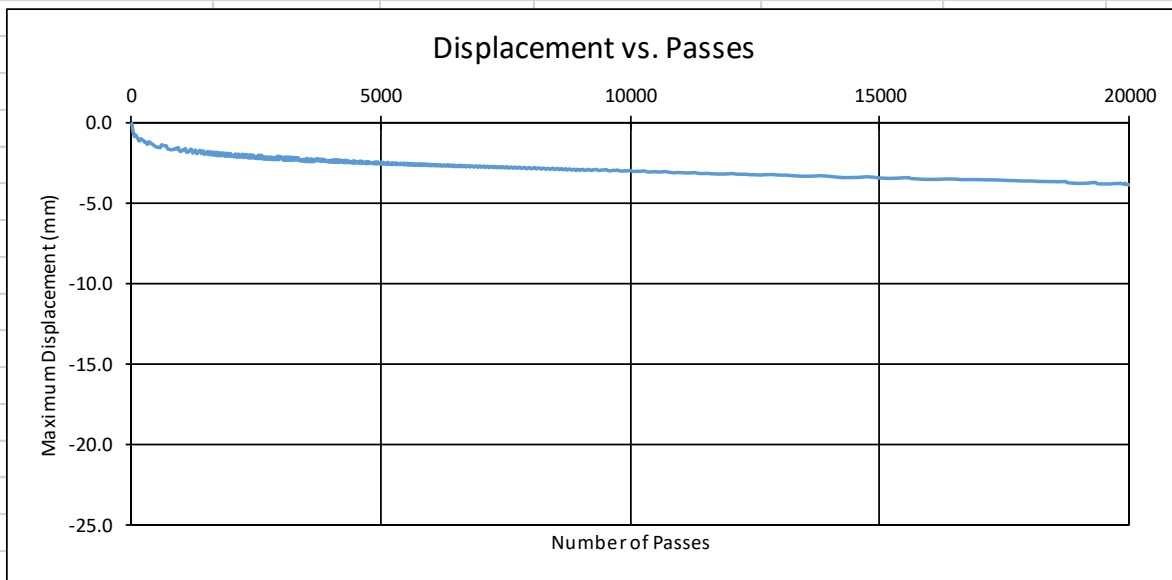
Project Name:	HIR	Project Number:	CHPP	Date Tested:	04/24/15
Mix Type:	Mach 15-16-R	Sampling:	Field Sampling		
Binder:		Specimen Prep:	Lab compacted		
Ndesign:		Compaction Type:	SGC		
Specimen Information:					
	Compacted Thickness:	62 mm			
	Fabrication:	Saw cut mating faces			
	Air Voids (%):	H3 = 6.3			
		H4 = 6.2			
Test Temperature:	50°C				
Test Results:					
Maximum Displacement	5.5	mm,	at	10,000	passes
End Maximum Displacement	9.1	mm,	at	20,000	passes



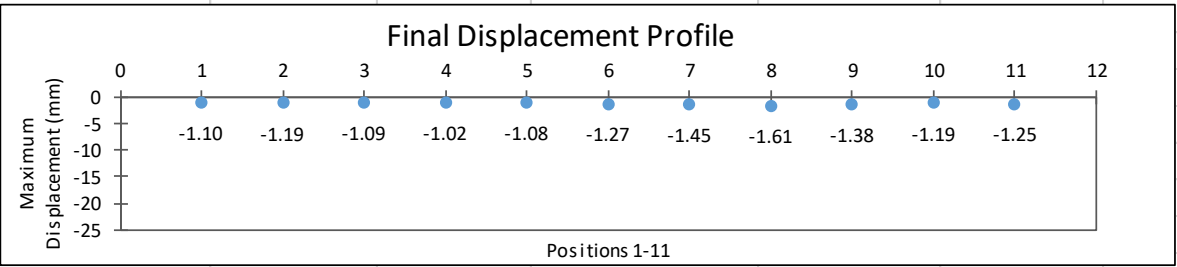
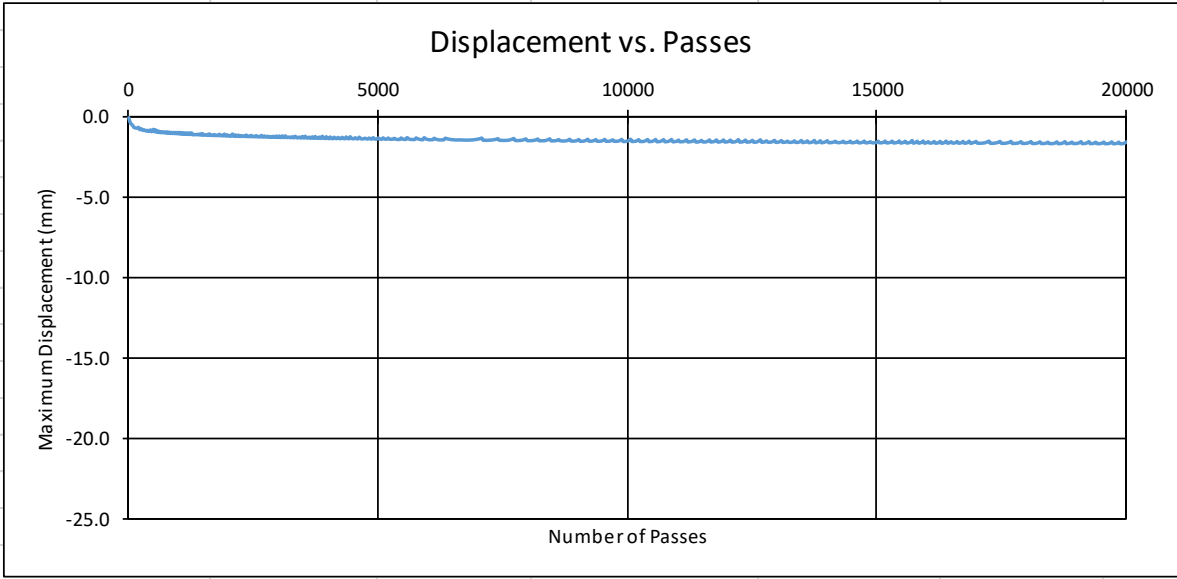
Project Name:	HIR	Project Number:	CHPP	Date Tested:	04/23/15
Mix Type:	Mach 17-18-R	Sampling:	Field Sampling		
Binder:		Specimen Prep:	Lab compacted		
Ndesign:		Compaction Type:	SGC		
Specimen Information:					
	Compacted Thickness:	62 mm			
	Fabrication:	Saw cut mating faces			
	Air Voids (%):	H1 = 6.0			
		H2 = 6.5			
Test Temperature:	50°C				
Test Results:					
Maximum Displacement	2.9	mm,	at	10,000	passes
End Maximum Displacement	4.5	mm,	at	20,000	passes



Project Name:	HIR	Project Number:	CHPP	Date Tested:	04/23/15
Mix Type:	Mach 17-18-R	Sampling:	Field Sampling		
Binder:		Specimen Prep:	Lab compacted		
Ndesign:		Compaction Type:	SGC		
Specimen Information:					
	Compacted Thickness:	62 mm			
	Fabrication:	Saw cut mating faces			
	Air Voids (%):	H3 = 6.0			
		H4 = 6.2			
Test Temperature:	50°C				
Test Results:					
Maximum Displacement	2.9	mm,	at	10,000	passes
End Maximum Displacement	3.8	mm,	at	20,000	passes



Project Name:	HIR	Project Number:	CHPP	Date Tested:	04/30/15
Mix Type:	Dyer-R	Sampling:	Field Sampling		
Binder:		Specimen Prep:	Lab compacted		
Ndesign:		Compaction Type:	SGC		
Specimen Information:					
	Compacted Thickness:	62 mm			
	Fabrication:	Saw cut mating faces			
	Air Voids (%):	H1 = 6.0			
		H2 = 6.5			
Test Temperature:	50°C				
Test Results:					
Maximum Displacement	1.4	mm,	at	10,000	passes
End Maximum Displacement	1.6	mm,	at	20,000	passes



Project Name:	HIR	Project Number:	CHPP	Date Tested:	04/30/15
Mix Type:	Dyer-R	Sampling:	Field Sampling		
Binder:		Specimen Prep:	Lab compacted		
Ndesign:		Compaction Type:	SGC		
Specimen Information:					
	Compacted Thickness:	62 mm			
	Fabrication:	Saw cut mating faces			
	Air Voids (%):	H3 = 6.2			
		H4 = 6.4			
Test Temperature:	50°C				
Test Results:					
Maximum Displacement	1.5	mm,	at	10,000	passes
End Maximum Displacement	1.8	mm,	at	20,000	passes

